

Feedback Optimization for Restorative Brain-Computer Interfaces

by

Sam Darvishi

B. Eng. (Electrical and Electronic Engineering),
University of Urmia, Iran, 1997

M. Eng. (Automation, with *Merit*),
The University of Sydney, Australia, 2007

Thesis submitted for the degree of

Doctor of Philosophy

in

Electrical and Electronic Engineering,
Faculty of Engineering, Computer and Mathematical Sciences
The University of Adelaide, Australia

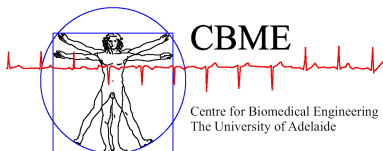
2016

Supervisors:

Associate Professor Mathias Baumert, School of Electrical & Electronic Engineering

Professor Michael Charles Ridding, School of Medicine

Professor Derek Abbott, School of Electrical & Electronic Engineering



© 2016
Sam Darvishi
All Rights Reserved



*To my dearest Dad who taught me to think big,
to my beloved Mum who loves me unconditionally,
and to my sweethearts: Sara and Ryan, who give me motivation for life.*

Contents

Contents	v
Abstract	xiii
Statement of Originality	xv
Acknowledgments	xvii
Thesis Conventions	xxi
Awards and Scholarships	xxiii
Publications and Talks	xxv
List of Figures	xxvii
List of Tables	xxix
Chapter 1. Introduction	1
1.1 Introduction	2
1.1.1 The origin of brain-computer interfaces	2
1.1.2 BCI for motor rehabilitation after stroke	2
1.1.3 Research motivations and thesis objectives	3
1.2 Summary of original contributions	4
1.2.1 Signal processing	4
1.2.2 Feedback optimization	4
1.3 Overview of the thesis	5
Chapter 2. Neurophysiological Background	9
2.1 Sensorimotor system	10
2.1.1 Motor cortex	10

Contents

2.1.2	Corticospinal tract	11
2.1.3	Somatosensory cortex	11
2.2	Stroke: its types and motor aftermaths	12
2.3	Underpinning mechanisms for stroke rehabilitation	13
2.4	New modalities for stroke rehabilitation	14
2.5	Overt and covert movements	14
2.5.1	Movement execution	15
2.5.2	Motor observation	15
2.5.3	Motor imagery	15
2.5.4	Motor intention	16
2.6	Signature of motor functions in EEG signals	16
2.6.1	Movement-related cortical potentials	16
2.6.2	Event related oscillatory activity within the sensorimotor cortex	17
2.7	How stroke affects ERD modulation	18
2.8	Operant conditioning and neurofeedback training	18
2.9	Hebbian learning and BCI research	20
2.10	Synergistic neurofeedback training for motor rehabilitation following stroke	21
2.10.1	Operant conditioning	21
2.10.2	Activity dependent Hebbian plasticity	22
2.10.3	Synergistic learning for therapeutic BCIs	22

Chapter 3. Brain-Computer Interfaces Components and Applications **27**

3.1	Introduction	28
3.2	BCI signal acquisition	28
3.2.1	Signals that reflect electrical activity of the brain	28
3.2.2	Signals that reflect magnetic activity of the brain	29
3.2.3	Signals that reflect the brain metabolism	29
3.3	EEG signal processing	30
3.3.1	Pre-processing	31
3.3.2	Feature extraction	32

3.3.3	Post-processing	33
3.3.4	Feature translation	34
3.4	Different BCI paradigms	39
3.4.1	P300-based BCIs	39
3.4.2	Steady-state evoked potential-based BCIs	39
3.4.3	Slow cortical potential-based BCIs	40
3.4.4	Motor imagery-based BCIs	40
3.5	BCI applications	41
3.6	Feedback optimization for restorative BCIs	41
3.7	The state of the art in restorative BCIs	43
3.8	Chapter summary	46
 Chapter 4. Optimizing Parameters for Restorative Brain-Computer Interfaces		47
4.1	Introduction	48
4.2	Analysis setup	49
4.2.1	Dataset	49
4.2.2	Feature extraction	50
4.2.3	Classification	52
4.3	Trade-off results	52
4.4	A feasible trade-off	55
4.5	Conclusion	57
 Chapter 5. Feedback Modality Impact on Restorative Brain-Computer Interfaces		59
5.1	Introduction	60
5.2	Experimental design	61
5.2.1	Ethics	62
5.2.2	Participants	62
5.2.3	Brain-interface system	62
5.2.4	Study design	63
5.2.5	Screening session	64

Contents

5.2.6	Participants' optimum features	65
5.2.7	Neurofeedback training session	66
5.2.8	Signal processing	67
5.2.9	MI+BCI	68
5.2.10	MI+BRI	68
5.2.11	Offline spectral analysis	69
5.2.12	Performance measures	70
5.2.13	Statistical analysis	70
5.3	Comparing visual and proprioceptive feedback effects	71
5.3.1	Spectral analysis of MI with feedback	71
5.3.2	Spectral analysis of MI without feedback	74
5.3.3	Accuracy and ERD duration for individual frequencies	74
5.3.4	Accuracy and ERD duration for the α and β bands	75
5.4	Feedback modality impact on modulation level and operant learning	76
5.4.1	Feedback modality and oscillatory modulation level	76
5.4.2	Feedback modality and operant learning	77
5.4.3	β band and the sensorimotor loop	78
5.5	Limitations of the study	80
5.6	Conclusion	80
Chapter 6. Feedback Update Interval Impact on Brain-Computer Interfaces		81
6.1	Introduction	82
6.2	Experimental setup	83
6.2.1	Participants	83
6.2.2	BCI system	83
6.2.3	Study design	84
6.2.4	Screening session	85
6.2.5	Online training session	86
6.2.6	Online signal processing	87
6.2.7	BCI performance measures	89
6.2.8	SRT measurement	89

6.2.9	Offline analysis	90
6.2.10	Statistical analysis	91
6.3	Feedback customization effect	92
6.4	Reaction time and feedback update rate	95
6.5	Limitations of the study	99
6.6	Conclusion	99
 Chapter 7. Feedback Optimization May Promote Restorative BCIs		101
7.1	Introduction	102
7.2	Methods	102
7.2.1	Ethics, subjects, and inclusion criteria	102
7.2.2	Study design	104
7.2.3	Neurofeedback training setup	104
7.2.4	Performance measures	105
7.3	Results	109
7.3.1	ARAT scores	109
7.3.2	Maximum voluntary contraction	109
7.3.3	Rest MEP	111
7.3.4	Active MEP	111
7.4	Discussion	111
7.5	Limitation of the study	113
7.6	Conclusion	113
 Chapter 8. Conclusion and Future Work		115
8.1	Introduction	116
8.2	Thesis summary	116
8.3	Summary of author’s original contributions	117
8.4	Potential future directions	118
8.5	In closing	119
 Appendices		121

Contents

Appendix A. PSO Application for ANFIS Training	123
A.1 Introduction	124
A.2 Feature extraction and classification	124
A.3 Results and discussion	126
Appendix B. A Novel Restorative BCI Setup	129
B.1 Introduction	130
B.2 Methods	130
B.2.1 The proposed design specification	131
B.3 Discussion	132
Appendix C. Feedback modality affects brain-computer interfaces	133
C.1 Introduction	134
C.2 Methods	135
C.2.1 Subjects	135
C.2.2 BCI Setup	136
C.2.3 Study design	137
C.2.4 Screening session setup	137
C.2.5 Subjects' optimum features	138
C.2.6 Feedback provision	138
C.2.7 Online training session	138
C.2.8 Power spectrum estimation	139
C.2.9 Classification	139
C.2.10 Performance measures	139
C.2.11 Statistical analysis	140
C.3 Results and discussion	140
C.4 Conclusion	141
Appendix D. Reaction Time Test Predicts Brain-Computer Interface Performance	143
D.1 Introduction	144
D.2 Methods	145

D.2.1	Subjects	145
D.2.2	Hardware and software	146
D.2.3	Screening session	146
D.2.4	Online training session	146
D.2.5	SRT Measurement	148
D.2.6	Performance measures	148
D.3	Results	149
D.4	Discussion	150
D.5	Conclusion and further development	151
Appendix E. Specification of the orthosis		153
E.1	Introduction	154
E.2	Mechanical design	154
E.3	Electrical design - servomotors and controllers	155
E.4	How the orthoses work	155
E.5	Software	156
Bibliography		161
List of Acronyms		179
Biography		183

Abstract

A brain-computer interface (BCI) provides an alternative communication channel for the human brain to directly interact with computers or machines. This technology has enabled patients with locked-in-syndrome to communicate with the outside world that otherwise would be impossible. It also promises recovery to stroke patients by supplying a platform to practice motor imagery of their impaired motor functions and receive feedback. The latter application is called motor imagery based BCI (MI-BCI) and has already provided promising results for stroke rehabilitation. However, its widespread application necessitates optimization.

This thesis investigates enhancement of MI-BCIs for stroke rehabilitation through feedback optimization, exploring the feedback modality (proprioceptive and visual) effect on BCI performance. It suggests that proprioceptive feedback is the superior choice for therapeutic BCIs. Next, it compares the effect of a short and a long proprioceptive feedback update interval (FUI) on BCI performance. It concludes that people with short reaction time benefit more from a short FUI whereas their slower counterparts show improved performance with motor imagery practice using a long FUI. In another study, which was run as a proof-of-principle study, we find a significant improvement in one stroke patient hand movement, after attending MI-BCI training sessions optimised through our findings on FUI length and proprioceptive feedback.

Overall, the research outcomes in this thesis highlight the effects of feedback modality and feedback update interval on MI-BCI performance. Furthermore, the single case study on a stroke patient provides primary evidence and motif for larger studies on the efficacy of the proposed strategies to enhance MI-BCI performance in stroke rehabilitation.

Statement of Originality

I certify that this work contains no material, which has been accepted for the award of any other degree or diploma in my name, in any university or other tertiary institution and, to the best of my knowledge and belief, contains no material previously published or written by another person, except where due reference has been made in the text. In addition, I certify that no part of this work will, in the future, be used in a submission in my name, for any other degree or diploma in any university or other tertiary institution without the prior approval of the University of Adelaide and where applicable, any partner institution responsible for the joint-award of this degree.

I give consent to this copy of my thesis when deposited in the University Library, being made available for loan and photocopying, subject to the provisions of the Copyright Act 1968.

I also give permission for the digital version of my thesis to be made available on the web, via the University's digital research repository, the Library Search and also through web search engines, unless permission has been granted by the University to restrict access for a period of time.

Signed

04/08/2016

Date

Acknowledgments

First and foremost, I would like to convey my deepest gratitude to my supervisors **A/Prof. Mathias Baumert**, **Prof. Michael C. Ridding** and **Prof. Derek Abbott** for their guidance and support throughout my candidature. My principal supervisor, A/Prof. Baumert advised me with his open view and broad knowledge in the field of biomedical engineering and statistics. His critical and thoughtful comments were always constructive and fruitful to improve the quality of my research. In addition, my co-supervisor Prof. Ridding also provided me with his solid knowledge in the field of neuroscience and neurophysiology. He has significantly helped me to embark in the field of neurophysiology and find my direction in implementing research for unexplored sensory feedback attributes. Further, I would like to express my gratitude to my other co-supervisor, Prof. Abbott, who has been of great help, support and advice, when it counted most. With his enthusiastic supervision, he always encouraged me to conduct high quality research and publications.

Another key person whom I am strongly indebted to is **Prof. Alireza Gharabaghi**. He invited me to visit his Neuroprosthetics Laboratory at the Center for Integrative Neuroscience of the University of Tuebingen, Germany. Prof. Gharabaghi's broad theoretical and experimental knowledge in the field of restorative BCIs was of great importance towards my PhD research. I would also like to thank his continuing support and encouragement throughout the course of last two years. I am also fully indebted to Dr Chadwick Boulay, who I had the chance to be with in Asilomar Conference Centre while we stayed there during the 5th BCI Meeting, for teaching me how to use *EEGLAB* software.

I would like to thank Dr Gervin Schalk and the other organizers of 10th *BCI2000* workshop in Asilomar Conference Centre in 2013, that gave me the opportunity to learn *BCI2000* software well enough to customize it for our BCI research. I also would like to thank Prof. Benjamin Blankertz and his group from Berlin BCI for organizing the 2014 Winter School on Neurotechnology by which I became exposed to the state of the art of the BCI and its challenges.

I would like to express my deepest gratitude to Dr Ann-Maree Vallence, Dr Brenton Hordacre, Dr Luke Schneider, and Dr Mitchell Goldsworthy from the Neuromotor

Acknowledgments

Plasticity and Development (NeuroPAD) laboratory who were always there for me in the lab and without their continuous assistance and support this work would not be possible. I also would like to especially thank Dr Michelle McDonnell from the University of South Australia who helped me with the proof-of-principle study design, ethics application and recruitment of stroke patients. Another key person who I am really indebted to, is Prof. Simon Koblar, the director of Stroke Research Programme (SRP) for his continuous support and persuasion throughout my candidature.

Within the school of Electrical & Electronic Engineering, I am indebted to Mr Ian Linke and Mr Brandon Pullen, for their valuable help in fabrication of the hardware required for my research. I also would like to thank the members of our Thursday Lunch Group whose friendly spirit and company made me feel at home.

I also like to thank the office & support staff of the school including Danny Di Giacomo for the logistical supply of required tools and items, IT officers, David Bowler, and the administrative staff, Stephen Guest, Greg Pullman, Ivana Rebellato, Rose-Marie Descalzi, Deborah Koch, and Jodie Schluter and Daphne Zammit for their kindness and assistance. I would also like to thank the head of school, Associate Prof. Cheng-Chew Lim, for his support regarding my research travel, supplying hardware required for my PhD, and provision of a friendly atmosphere at the School.

I am also thankful to my friends and colleagues within the University. I sincerely thank my friends and colleagues Dr Amir Ebrahimi, Dr Mostafa Rahimi, Ms Maryam Ebrahimpour, Dr Ali Karami, Dr Zahra Shaterian, Dr Ben Ng, Mr Nicolas Lawrence, Dr Muammar Kabir, Dr Azhar Iqbal, Ms Soulmaz Kahouzade, Mr Mehdi Kasaei, Dr Sarah Immanuel, Ms Yik Ling Lim, Mr Lachlan Gunn, Mr Vichet Duk, and Mr Yansong (Garrison) Gao, for making such a friendly research environment.

Also, my wife and I cordially appreciate help and support of our family friends in Adelaide: Ebi and Darwissa Mousavi, Arman and Gelareh Niknam, Fatemeh Soleimani and Javid Saeidi, Edward and Dena Khammash, Ali Gholampour and Hadis Afshar, Dr Amin Mahmoudi, Dr Meisam Valizadeh, and Ms Ayda Rajabnia whose company made our life in Adelaide so rich and abundant.

My endless gratitude goes to my dearest father who passed away just days before finalizing my thesis. My thoughts and prayers will be always with him who taught me pursuing my dreams no matter how hard they may seem. I also would like to thank my beloved mother for bestowing me her unconditional and genuine love. I also would

like to thank my dearest sibling, nieces, and nephews whose love and support gives my heart warmth and strength.

I honestly do not know how to thank my wife Sara and my son Ryan as words fail to express my gratitude. My darling Sara, thank you for your love, support, kindness, and standing by me throughout my candidature. I appreciate their values and they do mean a lot to me. My dear Ryan, you were born just weeks after I started this PhD journey, and soon you will become four years old. Thank you for giving me the blessing of fatherhood, even though I was not able to be with you as much as you wanted.

Sam Darvishi,
August 2016,
Adelaide, Australia.

Thesis Conventions

The following conventions have been adopted in this thesis:

Typesetting

This document was compiled using L^AT_EX2_ε. TeXstudio was used as text editor interfaced to L^AT_EX2_ε. Inkscape, Graphpad Prism 6 and Matlab R2014a were used to produce schematic diagrams and other drawings.

Referencing

The Harvard style has been adopted for referencing.

System of units

The units comply with the international system of units recommended in an Australian Standard: AS ISO 1000–1998 (Standards Australia Committee ME/71, Quantities, Units and Conversions 1998).

Spelling

Australian English spelling conventions have been used, as defined in the Macquarie English Dictionary (A. Delbridge (Ed.), Macquarie Library, North Ryde, NSW, Australia, 2001).

Awards and Scholarships

2015

- Endeavour Fellowship, Tuebingen, Germany (to be started following PhD conferral in 2016)

2014

- Invitation by Berlin BCI group to attend a Winter School on Neurotechnology, Berlin, 2014
- Interdisciplinary Research Fund (IRF), the University of Adelaide

2013

- IEEE-SA travel award to attend IEEE EMBS 2013, Osaka, Japan
- Walter and Dorothy Duncan Trust award to attend BCI Meeting 2013
- National Science Foundation (NSF) award to attend 10th BCI2000 Workshop, 2013

2012

- Travel reimbursement and free BMBSI Workshop registration, awarded by IEEE EMBS
- Faculty of Engineering, Computer and Mathematical Sciences Scholarship, The University of Adelaide

Publications and Talks

Publications

- **DARVISHI-S.**, GHARABAGHI-A., BOULAY-C. B., RIDDING-M. C., ABBOTT-D., AND BAUMERT-M. (2015c). Proprioceptive feedback facilitates motor imagery-related operant learning of sensorimotor beta-band modulation *Submitted to Frontiers in Neuroscience*.
- **DARVISHI-S.**, ABBOTT-D., AND BAUMERT-M. (2015a). Prediction of motor imagery based brain computer interface performance using a reaction time test, *37th Annual International Conference of the IEEE EMBS*, 2015, pp. 2880–2883.
- **DARVISHI-S.**, RIDDING-M. C., ABBOTT-D., AND BAUMERT-M. (2015b). Does feedback modality affect performance of brain computer interfaces?, *7th International IEEE EMBS Conference on Neural Engineering*, 2015, pp. 232–235.
- **DARVISHI-S.**, RIDDING-M. C., ABBOTT-D., AND BAUMERT-M. (2013). Proposing a novel feedback provision paradigm for restorative brain-computer interfaces, *Proceedings of the Fifth International Brain-Computer Interface Meeting*, 2013, pp. 146–147.
- **DARVISHI-S.**, MORADI-M. H., BAUMERT-M. AND ABBOTT-D. (2012). Classification of motor imagery EEG signals using adaptive neuro-fuzzy inference system trained by particle swarm optimization, *34th International IEEE EMBS Conference, EMB-CAS-SMCS Workshop on Brain-Machine-Body Interfaces*, 2012, P4.
- **DARVISHI-S.**, AND AL-ANI-A. (2007). Brain-computer interface analysis using continuous wavelet transform and adaptive neuro-fuzzy classifier, *29th Annual International Conference of the IEEE EMBS*, 2007, pp. 3220–3223.

Talks

- Oral presentation at the 35th International IEEE EMBS Conference, Osaka, Japan, 2013.

Publications and Talks

- Oral presentation at the 7th Neural Engineering Conference, Montpellier, France, 2015.
- Presenting research on restorative BCIs in a video for Scope TV of Channel 11, Australia. <https://www.youtube.com/watch?v=iFwWFGG5Htk>

List of Figures

1.1	Thesis outline and original contributions	6
<hr/>		
<hr/>		
3.1	BCI main components and its application	42
<hr/>		
4.1	Feature extraction steps	51
4.2	Classification accuracy results for different time window lengths	53
4.3	Mean and standard deviation of accuracies for different time windows	53
4.4	Comparison of accuracies for subject-dependent and subject-independent training methods	54
<hr/>		
5.1	Orthoses	63
5.2	Time course of the neurofeedback training sessions	67
5.3	Spectral analysis of imagery and relaxation with feedback	72
5.4	Spectral analysis of imagery and relaxation without feedback	73
5.5	Accuracy and ERD duration with and without feedback	75
<hr/>		
6.1	Time course of neurofeedback training sessions	88
6.2	Illustration of the relationship between SRT and BCI accuracy	93
6.3	Accuracy and ITR comparison	95
6.4	Power spectral density in 3–45 Hz with different feedback update intervals	96
<hr/>		
7.1	Illustration of the setup of the neurofeedback training session	106
7.2	Time course of the neurofeedback training sessions	107

List of Figures

7.3	The trend of performance measures across the study	110
<hr/>		
A.1	Feature extraction procedure	125
A.2	Procedure for training ANFIS with PSO	126
A.3	Comparing the accuracy of classifiers for training and testing data	127
<hr/>		
B.1	Illustration of the novel feedback provision paradigm	131
<hr/>		
C.1	Accuracy and information transfer rate (ITR) comparison for visual and proprioceptive feedback	141
<hr/>		
D.1	Screening session time course	146
D.2	Relationship between classification accuracies with visual and proprioceptive feedback and the SRT	150
<hr/>		
E.1	Application specific orthosis	154
E.2	Servomotors and the Micro Maestro controller	155

List of Tables

4.1	Dataset specifications	50
4.2	Classification statistics for different window lengths	54
5.1	Screening session results	66
5.2	Accuracy and ERD duration comparison	74
6.1	Screening session results	86
6.2	Summarizing SRT, ITR and accuracy results	93
7.1	Screening session results	103
7.2	Time course of the study design	105
D.1	BCI accuracies and reaction time results	149

Chapter 1

Introduction

THIS chapter provides an introductory background to the brain-computer interface (BCI) and its application for stroke rehabilitation. It also explains the objectives and motivations behind the presented research. Furthermore, the original contributions in this thesis are highlighted followed by an outline of the structural organisation of the thesis.

1.1 Introduction

1.1.1 The origin of brain-computer interfaces

Science fiction writers Larry and Andy Wachowsky, who wrote the *Matrix*, presented the story of cybernetically enslaved humans whose brains were connected to machines. While the readers of the novel or watchers of the *Matrix* film might consider these as complete science fiction, there is nevertheless a real basis that may make it plausible to some extent in the future. German psychiatrist Hans Berger published his seminal work (Berger 1929) on application of electroencephalogram (EEG) for monitoring the brain activity and turned what used to be purely fantasy into a scientific phenomenon. That phenomenon, which is now referred to as the *brain-computer interface* (BCI), measures brain activity and translates it into a format readable by computers or machines (Vidal 1973). However, the emergence of BCIs occurred few decades after the emergence of EEG, when the technology became advanced enough to provide real time recording and processing of multichannel EEG signals. During the last 30 years, BCI has attracted much attention from many research laboratories all around the globe. Since then, different types of brain signals and a myriad of BCI paradigms have been exploited to enable patients with locked-in-syndrome to communicate directly with the outside world through their brain signals (Donchin *et al.* 2000). In addition, there has been a growing interest in BCI applications for healthy populations such as gaming (Finke *et al.* 2009) and monitoring car drivers' vigilance (Lin *et al.* 2008).

1.1.2 BCI for motor rehabilitation after stroke

According to World Health Organization, 15 million people suffer stroke each year, where almost one third thereof do not adequately recover after stroke (Mackay *et al.* 2004). One of the major stroke aftermaths is hemiparesis of the upper limbs and impairment of the arm motor functions. Rehabilitation of the hand motor functions following stroke is a key element to properly performing daily life activities (Kaiser *et al.* 2011). However, traditional stroke rehabilitation techniques such as physiotherapy do not provide sufficient improvement to at least 30% of stroke victims who are not able to move their affected arms (Kwakkel *et al.* 1999). To address this gap, application of motor imagery (MI) has been proposed (Sharma *et al.* 2006, De Vries and Mulder 2007). Motor imagery activates the brain in a similar manner to actual movement. These

similar phenomena are associated with a decrease in the spectral power of sensorimotor rhythms that occur within 8–30 Hz frequency band (Pfurtscheller *et al.* 1997). This decrement in spectral power of EEG signals recorded over the motor cortex is referred as event related desynchronization (ERD) and is followed by a spectral power rebound effect referred to as event related synchronization (ERS) (Pfurtscheller *et al.* 1997). Further discussion on movement related potentials will appear in Chapters 2 and 3. These phenomena mainly occur within the hemisphere contralateral to the performed or imagined hand movement. Thus it appears that motor imagery offers a unique opportunity to activate the perilesional brain areas of the damaged hemisphere for those 30% of stroke patients with no residual hand movement. This brain activation if properly coupled with real time sensory feedback closes the sensorimotor loop (Gomez-Rodriguez *et al.* 2011), and thus may promote Hebbian-like neuroplasticity following stroke (Murphy and Corbett 2009). Therefore, brain-computer interfaces have been employed to enhance stroke rehabilitation through harnessing the power of neuroplasticity by i) monitoring MI occurrence through screening movement related potentials and, ii) providing sensory feedback to close the sensorimotor loop. For simplicity we will use phrases “BCI application for stroke rehabilitation” and “restorative BCI” interchangeably throughout this thesis.

1.1.3 Research motivations and thesis objectives

Previous applications of BCI for stroke rehabilitation offer promising results (Pichiorri *et al.* 2015, Ang and Guan 2013, Buch *et al.* 2008, Gomez-Rodriguez *et al.* 2011, Shindo *et al.* 2011, Prasad *et al.* 2010, Ramos-Murguialday *et al.* 2013). However, widespread application and dissemination of BCI for stroke rehabilitation necessitates its optimization to provide clinically significant outcomes in a timely fashion. This lack of efficacy in application of BCI to restore impaired motor functions after stroke may at least partly be caused by sub-optimal feedback provision.

In light of the above background, this thesis investigates whether feedback optimization impacts the efficacy of BCI application for stroke rehabilitation. This potential performance enhancement has been pursued through investigating a pivotal hypothesis stating that efficacious stroke rehabilitation requires optimal feedback at the right time. More specifically, it necessitates the feedback provision in restorative BCIs to be

1.2 Summary of original contributions

optimal both modality-wise and temporally. To study these two key aspects of feedback, three phases of experimental studies were carried out: In phase one, the effect of feedback modality was investigated where the impact of visual and proprioceptive feedback on brain activation patterns were compared. In the second phase, the interplay between feedback update rate and ERD modulation was examined. In the third phase the findings of the last two phases were tested on a stroke patient as a proof-of-principle study.

In addition to the studies on feedback provision, some studies on machine learning and signal processing aspects of restorative BCIs were also performed. These studies on signal processing methods were performed using offline analysis of publicly available EEG databases to fine-tune BCI parameters for restorative applications.

1.2 Summary of original contributions

This thesis provides a number of contributions in the area of BCI optimization. These contributions can be categorized into two main topics: The first part of the thesis encompasses studies on signal processing for BCIs. The second part, however, is focused mainly on the neurophysiological side of BCI through a series of studies on feedback optimization.

1.2.1 Signal processing

This section outlines the contributions in the first part of this thesis that investigates a practical trade off between feedback update rate, time window length, and accuracy.

1.2.2 Feedback optimization

This part, which can be considered as the major contribution of this thesis, explores how feedback modality and update rate impacts the performance within a restorative BCI framework. The outcomes of the initial studies on the effect of feedback modality and feedback update rate on BCI performance of healthy participants, were then verified in a proof-of-principle study on one stroke patient. The study employed a number of clinical and neurophysiological measures to study the effect of feedback optimization on stroke recovery where the results corroborate with our initial observations with healthy population. The key outcomes are:

- The effect of feedback modality on performance of restorative BCIs has been investigated by comparing proprioceptive and visual feedback. To compare their effect, modulation of sensorimotor oscillations and BCI accuracy in BCI setups that were only different in their feedback modality were studied. It was observed that proprioceptive feedback outperforms visual feedback in both accuracy and the strength of ERD modulation. The outcome of this research is currently under review with the *Frontiers in Neuroscience*.
- In the next step, the impact of feedback update rate on sensorimotor rhythm desynchronization and BCI accuracy was studied. It was found that modification of feedback update rate significantly affects BCI performance where the direction of the impact depends on the user's BCI aptitude. The outcome of this research is under final pre-submission preparation.
- The outcomes of the two studies on the effect of feedback modality and feedback update rate on BCI performance, were verified in a proof-of-principle study design on one stroke patient. The study employed a number of clinical and neurophysiological measures to study the effect of feedback optimization on stroke recovery where the results corroborate with the findings of the initial phases. This study is under preparation for submission as a journal paper.

1.3 Overview of the thesis

As illustrated in Fig. 1.1, this thesis encompasses four parts including the background, two main parts containing original contributions, and the conclusion. The detailed explanations for each part of the thesis are presented as follows:

Background section that includes Chapter 1, 2, and 3 comprises the current introductory chapter and Chapters 2&3 that provide neurophysiological background and explain required concepts and provides background information for the rest of the thesis chapters.

Signal processing section (Chapter 4) simulates the interplay of a number of combinations for time window length, accuracy and feedback update rate to find a practical trade off among them that fulfils real time constraints of restorative BCIs.

1.3 Overview of the thesis

Background	Chapter 1-3	Introduction ----- Neurophysiological Background ----- Brain-Computer Interfaces; Components and Applications -----
Signal Processing	Chapter 4	Signal Processing Parameters for Restorative Brain-Computer Interfaces -----
Feedback Modality	Chapter 5	Feedback Modality Impact on Restorative Brain-Computer Interfaces -----
Feedback Update Interval	Chapter 6	Feedback Update Interval Effect on Brain-Computer Interfaces -----
Stroke Rehabilitation	Chapter 7	Feedback Optimization Enhances Stroke Rehabilitation -----
Conclusion	Chapter 8	Conclusion Future Research Directions

Figure 1.1. Thesis outline and original contributions. This dissertation is composed of eight chapters in total, divided in four main parts and five appendices. The original contributions are distributed in two parts: signal processing and feedback optimization.

Feedback optimization part (Chapters 5, 6, and 7) elaborates on our studies regarding the effect of feedback modality and update rate on both healthy BCI users and

stroke patients. Chapter 5 focuses on comparison between visual and proprioceptive feedback with eight healthy participants. Chapter 6 presents our work on the impact of feedback update rate modification on BCI performance where ten healthy participants were tested. Chapter 7 investigates whether findings of the previous studies on healthy subjects were applicable to stroke patients in a single-case proof-of-principle study.

Conclusion (Chapter 8) summarizes the findings and contributions of the aforementioned studies and highlights their significance towards further developments and future research on optimizing restorative BCIs.

Appendix section that includes four appendices that have been published as conference papers related to either signal processing (Appendix A) or feedback optimization for BCIs (Appendices B, C, and D). The appendix section ends with Appendix E that describes the details of the fabricated orthoses for the implemented studies.

Chapter 2

Neurophysiological Background

SINCE the ultimate goal of the studies reported in this thesis involves motor rehabilitation following stroke, this chapter provides a brief overview on the structure of the sensorimotor system in humans followed by the effects of stroke on the sensorimotor system. Next, different types of movements including overt and covert movements are briefly explained. Then, different signatures of movement observable in electroencephalography (EEG) signals and the effect of stroke on them are discussed. Finally, different learning paradigms for neurofeedback training and their hypothesized synergy for stroke rehabilitation are discussed.

2.1 Sensorimotor system

Stroke impairs volitional motor control. This thesis involves feedback optimization for restorative BCIs aimed at stroke rehabilitation. Therefore, to provide the necessary neurophysiological background the following sections describe the sensorimotor pathways involved with control of voluntary movement.

2.1.1 Motor cortex

The motor cortex is comprised of a number of cortical regions including the primary motor cortex (M1), and premotor areas that encompass premotor cortex (PMC), supplementary motor area (SMA), and cingulate motor area (CMA).

The M1 is topographically organized, i.e. each segment of the body has a specific representation in the M1, where the medial parts represent foot and leg and the lateral parts represent face and head. Within the M1, each neuron maps its outputs to a specific movement pattern rather than a specific muscle and neuronal cells are organized in six layers (layers I-IV). The most direct pathway for motor execution is originated from large pyramidal neurons that belong to layers III, V, and VI. Pyramidal cells long axons travel through the corticospinal tract and synapse with alpha motor neurons in the spinal cord. Also, dendrites of pyramidal cells synapse with all cortical layers and provide the basis for plasticity of the brain. Instead, the stellate cells, which contain 20–25% of M1 cells, produce axonal and dendritic projections excluded to the cortex. Stellate cells are responsible for interneuronal excitatory and inhibitory connections and are important for maintaining normal cortical representations.

The premotor areas (PMC, SMA, and CMA) are extensively projected to M1 and also project directly to the spinal cord. In addition, the premotor areas demonstrate a high degree of topographic organization with distinct projections to proximal and distal muscle groups within arms and legs. The PMC is activated during movement preparation and is also involved with delayed movement cued by sensory stimuli. However, the SMA is active during movement preparation only when movement is self-paced. The CMA has a critical role in motivational and cognitive aspects of volitional movement. Altogether, the topographic organization of premotor areas, their connections to the periphery and their projections to M1 suggest that premotor areas influences preparation and execution of volitional motor functions both indirectly (through M1) and directly.

2.1.2 Corticospinal tract

The corticospinal tracts receive axons from M1, premotor, parietal and somatosensory areas where almost 60% of them originate in layer V of the M1. The efferent routes within the corticospinal tract travel via the internal capsule and then 75% of them decussate in the lower medulla. Next, the crossed pathways move through the spinal cord as the lateral corticospinal tract. However, the ventral corticospinal tract is formed by a small portion of the uncrossed pathways. Finally, the remainder of uncrossed fibres continue to project ipsilaterally and join the fibres in the lateral corticospinal tract.

At the spinal cord, the cortical motor (CM) system is shaped where corticospinal tracts make mono-synaptic excitatory connection with spinal motor neurons and each spinal motor neuron receives several CM inputs. The CM control plays an important role for implementation of precise motor skills such as precise gripping and also for acquisition of new motor skills. In addition, corticospinal tracts project to spinal interneurons in the ventral intermediate layers of the spinal cord that create indirect pathways to coordinate large and proximal muscles involved in reaching and lifting.

2.1.3 Somatosensory cortex

The primary motor cortex, premotor areas and corticospinal tracts are key components of the motor output system for volitional motor functions. However, in addition to these motor outputs, sensory feedback is also required to perform dexterous motor functions.

The sensory information to the motor system is provided via the somatosensory cortex and the afferent spinothalamic pathways. The somatosensory cortex receives cutaneous and proprioceptive sensory information and similar to the M1 is somatotopically organized, i.e. it contains a representation for each segment of the human body. Sensory information from the skin, muscles and joints travel upward to the dorsal horn of the spinal cord and then axons either synapse locally (for spinal reflex circuits) or ascend to reach the medulla.

Modulation of the sensory information for motor control starts at the spinal cord. Many motor inputs are projected to the dorsal horn of the spine that receives also somatosensory information. Therefore, these motor projections are considered important for control, selection and/or interruption of the afferent sensory information. The

2.2 Stroke: its types and motor aftermaths

afferent pathways that carry sensory information from the body and posterior head decussate in the medulla and then terminate in the ventral posterior lateral nucleus of the thalamus. However, those that carry cutaneous information from the face enter the ventral posterior medial nucleus of the thalamus after decussating in the medulla.

The projected cutaneous and proprioceptive information to nuclei of the thalamus are mainly transferred to the layer IV of the somatosensory cortex. However, some afferent pathways carrying sensory information are directly projected to pyramidal cells of the M1 area. Therefore, motor outputs are modulated by sensory information both via thalamocortical projections to M1 and through axonal connections to the somatosensory cortex.

For further details on neurophysiology of sensorimotor systems refer to Miller and Hatsopoulos (2012).

2.2 Stroke: its types and motor aftermaths

Stroke is an abrupt loss in brain function caused by lack of or severe decrease in blood supply (ischemic stroke) or leakage of blood in the brain (hemorrhagic stroke). Stroke covers a diverse range of vascular diseases that are related to the blood vessels that supply blood for the brain.

Depending on the type of stroke and particular blood vessels, stroke can affect the brain differently and in turn results in different symptoms. In the most common type of stroke, called ischemia, which consists of about 85% of stroke cases, a blockage in blood vessel(s) occurs within the brain. The other 15% of stroke cases, in a condition called hemorrhage, are caused by a rupture in these blood vessels. In the case of a hemorrhage, a large quantity of blood gathers in the brain leading to higher pressure in the brain tissues. If this pressure does not discharge promptly, it causes permanent damage to the brain. Ischemia occurs in three categories: (i) thrombosis, which occurs when a local blockage appears in a blood vessel due to diseases that narrow the artery, (ii) embolism, when a blockage occurs due to loose clots that may originate from a distant area such as the aorta, and (iii) hypoperfusion, when ischemia occurs due to insufficient pumping of blood by the heart or low volume of blood in the body.

Depending on the part of the brain that suffers from the lack of blood supply, and for the amount of time that the blockage occurs in the blood vessel, the symptoms and

damage to the brain can be very different. There are three main arteries that supply the blood for the brain: anterior cerebral artery (ACA), medial cerebral artery (MCA), and posterior cerebral artery (PCA). For instance, if the blockage occurs in the MCA that supplies the sensorimotor cortices, the sensory and/or motor abilities of the subject in the ipsilateral part of the subject's body will be impaired. Other motor impairments following such a stroke may include difficulty with swallowing, problems with keeping balance, fatigue, spasticity, and foot drop.

2.3 Underpinning mechanisms for stroke rehabilitation

There is evidence that recovery after stroke involves neuroplasticity (Murphy and Corbett 2009). Several forms of plasticity are thought to be involved in the recovery after stroke including homeostatic (Turrigiano and Nelson 2004) and Hebbian (Hebb 2005) plasticity (Murphy and Corbett 2009).

Homeostatic plasticity: According to homeostatic plasticity, reduced activity in neuronal populations affected by the stroke leads to compensatory changes including greater transmitter release in the pre-synaptic neurons and also larger responses to the neurotransmitters in post-synaptic neurons. These adjustments are viewed as an attempt within the CNS to restore activity at a set point (Turrigiano and Nelson 2004) responding to lower level of activity in the brain following stroke. In addition to up-regulation of existing synaptic connections, homeostatic plasticity also causes formation of new synaptic connections manifested as axonal sprouting (Carmichael 2003), and increase of dendritic spine production following stroke (Brown *et al.* 2009).

Hebbian plasticity: This plasticity rule that is discussed further in the context of its role in BCI training in Sections 2.9 and, 2.10, enhances the synaptic efficacy when pre- and post-synaptic neurons are coincidentally activated. In this thesis we investigate the occurrence of Hebbian plasticity during neurofeedback training.

2.4 New modalities for stroke rehabilitation

The gold-standard for motor stroke rehabilitation still involves application of task-specific training and aerobic exercise (Dimyan and Cohen 2011). However, even after intensive task-specific training, almost one third of stroke survivors remain disabled (Lloyd-Jones *et al.* 2009). Therefore, novel methods that promote neuroplasticity following stroke are sought to allow rehabilitation of those portion of stroke survivors who do not recover with traditional therapies.

One novel technique known as constraint induced movement therapy (CIMT) (Taub *et al.* 1993) relies on constricting the movement of the intact side of the body to force the use of the stroke affected side to drive recovery following stroke. In another intervention, even though very experimental at this stage, stem cell therapy (Lichtenwalner and Parent 2006) has been shown to provide some level of recovery for stroke survivors. Also, electrophysiological approaches including excitation of the damaged hemisphere or inhibition of the intact hemisphere through application of repetitive transcranial magnetic stimulation (rTMS) have been proposed to promote neuroplasticity after stroke (Ridding and Rothwell 2007). In addition paired associative stimulation (PAS) (Stefan *et al.* 2000) in which cortical activation is temporally conditioned with a peripheral stimulation (such as median nerve stimulation) have been suggested for motor recovery following stroke (Castel-Lacanal *et al.* 2009, Jayaram and Stinear 2008, Rizzo *et al.* 2009). Another novel approach for enhancement of plasticity after stroke is covert movement. Covert or simulated movement encompasses motor imagery, motor observation and motor attempt (De Vries and Mulder 2007, Szameitat *et al.* 2012). The following section describes the attributes of each movement category.

2.5 Overt and covert movements

In humans, overt movements is associated with activation of several areas of the sensorimotor system and causes observable movements in the intended body limbs/muscles. Covert activities such as motor imagery are associated with similar activations of the motor cortex as seen during overt movement (Jeannerod 2001, Hiremath *et al.* 2015). This thesis report studies that involve motor imagery that is categorized as a specific type of covert movements. Thus, in the following sections a brief overview on different types of movements and their correlations and distinctions is provided.

2.5.1 Movement execution

Motor execution or overt movement is associated with activations in various parts of the sensorimotor system. However, the problem with application of overt movement for motor stroke recovery is that it is not applicable for those who have no residual motor functions in their limbs following stroke.

2.5.2 Motor observation

There is evidence that observing another person's movements activates the brain of observers correlated with the brain activation patterns during motor execution of the same action (Gallese and Goldman 1998). It is believed that the underpinning mechanism that activates the brain during motor observation is a specific type of neurons referred as mirror neurons (Gallese and Goldman 1998).

Not only watching other humans' action triggers mirror neurons in the observer, some researchers maintain that even observing robotic manipulators' movement activates mirror neurons (Gazzola *et al.* 2007). However, others reject this argument and maintain that activation of motor neurons in humans is excluded to observing biological movements (Tai *et al.* 2004). However, even Gazzola *et al.* (2007) who maintain that observing movements of the robotic objects activates the mirror neurons, have shown that observing *repetitive* robotic actions results in habituation and thereby fails to activate the mirror neurons.

2.5.3 Motor imagery

According to the literature (Decety *et al.* 1989, Frak *et al.* 2001, Szameitat *et al.* 2012), motor imagery and motor execution of a specific task are temporally correlated, activate the sensorimotor system similarly, and are under same constraints such as Fitts law (Sirigu *et al.* 1995). Therefore, motor imagery has been one of the first types of covert movements that was proposed to have correlated neural mechanisms with those of overt movements (Jeannerod 1997, Jeannerod 1994).

Not surprisingly, it has been shown that practicing motor imagery may benefit those stroke survivors who have no residual motor functions following

2.6 Signature of motor functions in EEG signals

stroke (Zimmermann-Schlatter *et al.* 2008). However, motor imagery performance cannot be naturally monitored, and therefore BCIs have been used to support correct performance of motor imagery by provision of feedback.

2.5.4 Motor intention

Severe damage to the nervous system such as spinal cord injury may lead to deafferentation and therefore may limit such patients's abilities for motor imagery performance (Lopez-Larraz *et al.* 2012). Therefore, motor intention (motor attempt) has been tested with such patients and found to provide a better substrate for neurofeedback training with spinal cord injury patients (Lopez-Larraz *et al.* 2012). However, motor intention is only applicable to those stroke survivors who have no residual motor functions, whereas motor imagery is applicable for both healthy populations and most stroke survivors. Moreover, several studies (Ang *et al.* 2011, De Vries and Mulder 2007, Dijkerman *et al.* 2004) have demonstrated that the quality of motor imagery in such populations is sufficient for neurofeedback training. Therefore, motor imagery has been chosen as the covert type of movement for the studies reported in this thesis.

While the brain activation patterns during the reviewed movement types have close similarities, each movement type have their own specific signatures that make them distinct from others types. For a detailed review see (Jeannerod 2001, Hiremath *et al.* 2015).

2.6 Signature of motor functions in EEG signals

2.6.1 Movement-related cortical potentials

Movement-related cortical potentials (MRCP) are extracted by averaging EEG signals recorded over the sensorimotor cortex before and after a voluntary movement (Hallett 1993). The MRCP begin with a slowly increasing negativity, referred to as readiness potential or Bereitschaftspotential (BP). Next, they continue with a larger negativity starting about 400 ms prior to the start of movement or motor imagery, named as negativity slope (NS). The initial slope of the motor potential occurs just before the onset of electromyographic (EMG) activity and is topographically focal over

the primary motor cortex (M1) that may reflex the activation of M1. The mentioned focal negativity lasts for 30–50 ms following the onset of EMG activity. Next, the peak negativity moves toward the anterior contralateral area, where it reaches its largest negativity, known as the frontal peak of motor potential (Hallett 1993). There is evidence that motor imagery evokes similar MRCPs to those of motor actions (Mrachacz-Kersting *et al.* 2012, Niazi *et al.* 2012, Sano and Bakardjian 2009, Xu *et al.* 2014). However, evoked potentials in imagery exhibits lower and delayed peaks compared to MRCP with actual movement. Nonetheless, MRCP related responses in the primary and supplementary motor areas are similar for motor imagery and motor actions (Sano and Bakardjian 2009).

2.6.2 Event related oscillatory activity within the sensorimotor cortex

Prior to, during, and after motor actions and motor imagery the oscillatory patterns of the EEG signals recorded over the sensorimotor cortex change. These alterations in the oscillatory activity of the sensorimotor cortex are divided into two main subcategories:

Event related desynchronization

Processing motor and cognitive tasks prior to and during motor actions and motor imagery poses a high demand on these cortical areas. Also, receiving sensory information during motor execution is an additional processing task for the sensorimotor cortex. As a result different neuronal ensembles within the sensorimotor cortex attend to different tasks and consequently, a desynchronization occurs among them that is manifested as lower amplitude in the oscillatory activity of this region. This phenomenon is known as event related desynchronization (ERD) (Pfurtscheller and Aranibar 1979, Pfurtscheller and Lopes da Silva 1999). Therefore, ERD is considered as a signature of the cortical activation for motor action and motor imagery (Pfurtscheller and Lopes da Silva 1999).

Event related synchronization

After the offset of motor action or imagery, activated neuronal networks have no more processing task and thereby return to their baseline (idling) status. Subsequently, a synchronization occurs that is known as event related synchronization (ERS) (Pfurtscheller

2.7 How stroke affects ERD modulation

and Aranibar 1979, Pfurtscheller and Lopes da Silva 1999). The ERS is used as a signature of baseline activity (idling status) for the EEG signals recorded over the sensorimotor cortex.

The ERD/ERS phenomena are thought to occur as a result of thalamo-cortical and cortico-cortical feedback loops (Pfurtscheller and Lopes da Silva 1999). They are time locked but not phase-locked, i.e. they have different manifestations for different frequencies. The frequency band of interest that is usually used for ERD/ERS analysis of EEG signals lies within 0–50 Hz in which few specific frequency bands exist: i) Delta band (0–4 Hz); ii) Theta band (4–8 Hz); iii) Alpha band (8–13 Hz); iv) Beta band (16–30 Hz); v) lower Gamma band (30–50 Hz). Among the mentioned frequency bands, Alpha and Beta bands are more explored within the MI-BCI studies and are also the selected frequency bands in the studies reported in this thesis.

This thesis explores a potential synergy between Hebbian and operant learning (see below for further details on Hebbian and operant learning), and therefore MRCP cannot be chosen as it only occurs prior to motor imagery/execution. Accordingly, ERD has been chosen as the signal of interest because it occurs both prior to and during motor imagery performance.

2.7 How stroke affects ERD modulation

A number of studies have demonstrated that the occurrence of stroke in different cortical and subcortical areas of the brain may disrupt movement preparation and motor imagery (Battaglia *et al.* 2006) and weaken the ERD to different extents (Leocani and Comi 2006, Platz *et al.* 2000, Stepien *et al.* 2011). However, even these weaker ERDs of stroke survivors have been shown to be sufficient for taking part in neurofeedback training session (Ang *et al.* 2011). Also some other techniques such as transcranial direct current stimulation (tDCS) have been shown to enhance the ability of stroke survivors to elicit stronger ERDs (Kasashima *et al.* 2012, Tohyama *et al.* 2011). Nonetheless, novel approaches to elicit stronger ERDs for stroke patients are highly desirable.

2.8 Operant conditioning and neurofeedback training

In operant (instrumental) conditioning, implementing a specific behaviour of an animal is rewarded (reinforced) through provision of food or drinks. Here, there is no

verbal instructions and the animals are expected to find by themselves what strategy to do to receive rewards or avoid punishments. However, operant learning with humans is usually associated with clear verbal/visual instructions and they are explicitly instructed to follow specific strategies to be rewarded (Dayan and Abbott 2001).

Fetz (1969) employed conditional learning with monkeys and had them elicit a specific brain activation pattern so as to be rewarded with food or drinks and then it was successfully repeated in their following studies (Engelhard *et al.* 2013, Ganguly and Carmena 2009, Hiremath *et al.* 2015). Also in humans, operant conditioning has been used in neurofeedback paradigms to achieve a specific oscillatory pattern and receive feedback (Pfurtscheller and Aranibar 1979, Pfurtscheller and Lopes da Silva 1999, Boe *et al.* 2014, Florin *et al.* 2013, Kaiser *et al.* 2014).

The most common paradigm for BCI training is the cue-based paradigm in which participants receive clear instructions and even specific strategies to establish the required oscillatory patterns. However, a number of studies have shown that the occurrence of operant learning within a neurofeedback setting does not necessitate conscious control and can be achieved implicitly (Birbaumer *et al.* 2013, Kaplan *et al.* 2005, Kober *et al.* 2013). It has also been found that participants who were instructed to follow a specific strategy and elicit desired activation patterns, presented poorer results compared with those who did it implicitly (Kober *et al.* 2013). Therefore, it appears that, it might be beneficial to allow participants 'go on their own journey' (Gruzelier 2014) instead of providing explicit strategies.

It is also worth mentioning that in a recent review on the learning strategies adopted for neurofeedback training (Strehl 2014), while operant learning was highlighted as a key player for BCI training, it was mentioned that there are other major factors involved. These factors have to be derived from classical conditioning, two-process-theory and in particular from skill learning and research into motivational aspects of BCI training (Strehl 2014).

Considering the adaptation medium that is selected for the occurrence of learning during neurofeedback training, it appears that there are three main regimes that choose man, machine, or both for learning: i) operant conditioning regime such as the approach of Gert Pfurtscheller and colleagues at the University of Graz, Austria, who allow the training to occur in the user along a number of training sessions; ii) machine learning approach such as the method of Benjamin Blankertz and his colleagues from Berlin BCI (BBCI) group that invest on machine learning techniques so as the user can

2.9 Hebbian learning and BCI research

control the BCI within a single session; iii) the combined regime such as the approach taken by Jon Wolpaw and colleagues in Wadsworth, Albany where they consider BCI training as a co-adaptive procedure to occur mutually between man (such as operant learning) and machine (machine learning).

2.9 Hebbian learning and BCI research

In 1949, Donald Hebb (Hebb 2005) postulated if input from neuron A, contributes to activation of neuron B, the synaptic connection from neuron A to neuron B will be strengthened. This form of synaptic plasticity that is based on the correlation between neurons' activity is referred as activity-dependent Hebbian plasticity (Dayan and Abbott 2001). Using this learning rule, both enhancement and weakening of the synaptic connections between neurons can be explained. More specifically, if the activity of two neurons (or group of neurons) are correlated, then long term potentiation (LTP) occurs and manifest itself by strengthening the synaptic efficacy between co-activated neurons. However, if activity between two neurons (or ensemble of neurons) is dissociated, then long term depression (LTD) occurs that weakens the synaptic connection between dissociated neurons (Dayan and Abbott 2001).

In the realm of BCI application for motor rehabilitation following stroke, the activity dependent plasticity has been exploited by a number of laboratories including a research group from the Alborg University, Denmark that have run a series of studies (Jochumsen 2015, Mrachacz-Kersting *et al.* 2012, Niazi *et al.* 2012, Xu *et al.* 2014). They investigated the effect of this learning rule through accurately coupling MRCP elicited from imagination of a simple dorsiflexion movement with afferent feedback using peripheral electrical stimulation to the common peroneal nerve. They reported that significant plasticity was induced only when the afferent volley was timed to arrive during the peak negativity of the MRCP generated during the imagined task. In this paradigm, appropriately timed afferent input activates corticocortical projections from sensory cortex to M1 (Lemon 1979) at a time that M1 is active (through imagery), results in strengthening of the sensorimotor pathways. This may explain why they recorded stronger motor evoked potentials, that reflect the corticospinal excitability, following the neurofeedback training sessions, compared to the control values.

Also recently, another group at the University of Tuebingen, Germany (Naros *et al.* 2016) have shown that learning sensorimotor desynchronization leads to behavioural

gains after neurofeedback training using a brain-robot interface. They reported that the acquired skill for sustained Beta-ERD was correlated significantly with subsequent motor improvement. In another study of the same group (Kraus *et al.* 2016), they reported that the robotic feedback to motor-imagery related sensorimotor Beta-ERD induced robust and muscle-specific changes of corticospinal excitability.

Therefore, it appears that a growing body of evidence suggesting a potential role for activity-dependent Hebbian plasticity within therapeutic BCI paradigms.

2.10 Synergistic neurofeedback training for motor rehabilitation following stroke

There are two main paradigms that are used for the occurrence of BCI training in the user's brain for motor rehabilitation following stroke:

2.10.1 Operant conditioning

A myriad of techniques have been employed to capitalize on operant learning for promoting stroke recovery following stroke: i) in the most common method a cursor position update on a monitor is used as visual feedback to reward down-regulation of sensorimotor rhythms (Buch *et al.* 2008); ii) in another method that largely capitalizes on activation of the mirror neurons system (MNS), movement of a virtual arm is given to reward ERD modulation (Pichiorri *et al.* 2011, Pichiorri *et al.* 2015); iii) proprioceptive feedback provision via an orthosis, a robot, or by FES has also been used to reward self-regulation of the brain oscillatory patterns for stroke rehabilitation (Gomez-Rodriguez *et al.* 2011, Ramos-Murguialday *et al.* 2013, Daly *et al.* 2009). Note that using robots, FES and orthosis in tandem with BCI, can also provide a direct visual feedback (in contrast to the indirect visual feedback such as cursor update on a monitor). If this visual feedback exploited besides the proprioceptive feedback, may provide a more similar feedback to what is perceived during motor skill learning.

However, operant learning of sensorimotor rhythms regulation is usually a long and time consuming procedure even with healthy populations. Thus, this length of training time may be an important barrier for administering neurofeedback training with stroke patients who may lose motivation if they do not gain the sense of autonomy in a

2.10 Synergistic neurofeedback training for motor rehabilitation following stroke

timely manner. Moreover even when stroke patients learned ERD modulation through operant learning, no behavioural gain was reported.

2.10.2 Activity dependent Hebbian plasticity

As it was discussed in Section 2.9, this method has been adopted by some researchers (Mrachacz-Kersting *et al.* 2012, Niazi *et al.* 2012, Sano and Bakardjian 2009, Xu *et al.* 2014), to co-activate the periphery and the motor cortical areas so as to capitalize on Hebbian learning for promoting synaptic plasticity and thereby achieving motor rehabilitation. Also in a recent study by Reynolds *et al.* (2015), they examined the optimal timing between the onset of motor imagery and functional electrical stimulation (FES) and found that performing motor imagery during FES application resulted in stronger ERDs compared with other scenarios in which motor imagery preceded or succeeded FES application. This finding may be interpreted by activity dependent Hebbian plasticity that emphasize the correlated activation of cortical and peripheral systems.

2.10.3 Synergistic learning for therapeutic BCIs

While the mentioned paradigms for application of BCI for motor rehabilitation following stroke have shown to be efficient to some extent, it appears that some aspects of neurofeedback training such as the efficacy of training and the long training time may require optimization. Therefore, within the studies reported in this thesis I have examined whether it is possible to make a BCI setup that benefits from a potential synergy between Hebbian learning and operant conditioning.

Since the specific BCI design that was used in this thesis capitalizes on some of neurophysiological mechanisms underpinning PAS that was introduced in Section 2.4 as a novel method for stroke recovery, prior to explaining the rationale for our hypothesized BCI design, this method is further described as follows: Stefan *et al.* (2000) demonstrated that electrical stimulation of the median nerve if follows by a TMS application over the hand representation of the contralateral primary motor cortex, results in larger motor evoked potentials (MEPs). The larger MEPs that reflect higher cortical excitability only occurs when the TMS application is applied 25 ms after the median nerve stimulation. The transfer time for a median nerve stimulation to reach the primary sensory cortex is almost 20 ms (Samii *et al.* 1998). Also, there

is evidence that afferent stimulation disinhibits the motor cortex for few milliseconds (Hess *et al.* 1999, Ridding and Rothwell 1999). Therefore, they concluded that the recorded larger and longer lasting increase in MEP amplitude (i.e. plastic effect) was caused by the occurrence of LTP-like plasticity in the motor cortex as a result of co-activation of the primary motor and sensory cortices. Likewise, this thesis will explore co-activation of the primary motor and sensory cortices via a specific BCI design that follows.

To design such a BCI system this thesis considers the following facts and their rational consequences:

- Takemi *et al.* (2013a) reported that ERD is a biomarker for cortico-spinal excitability and M1 activation. Also, Kilavik *et al.* (2013) showed that ERD magnitude in the sensorimotor cortex represents cortico-muscular communication during motor imagery performance. Furthermore, Rossiter *et al.* (2014) demonstrated that ERD magnitude is negatively correlated with functional impairment following stroke. Therefore, enhancement of ERD modulation was adopted as the key measure for the studies reported within this thesis.
- Motor imagery performance of stroke survivors can activate the peri-lesional area within the damaged motor cortex, however, it elicits weaker ERDs with low signal-to-noise ratio compared to healthy populations (Leocani and Comi 2006, Platz *et al.* 2000, Stepien *et al.* 2011).
- There is evidence (Brouwer and Schryburt-Brown 2006) that subthreshold and high frequency (50 Hz) cortical stimulation delivered concurrently with intensive rehabilitation therapy resulted in behavioural gains for patients with chronic hemiparetic stroke. Also PAS administration causes LTP-like neuroplasticity in the motor cortex (Stefan *et al.* 2000).
- Sensory afferent signals caused by finger flexion/extension via an orthosis are transferred through thalamo-cortical tracts to the sensory cortex and then in almost 10 ms are diffused to some neurons in the motor cortex (Dell'Acqua *et al.* 2010) and disinhibits M1 neurons for few milliseconds (Lemon 1979, Hess *et al.* 1999, Ridding and Rothwell 1999). Therefore, it appears that provision of recurrent sensory feedback during motor imagery performance leads to recurrent afferent sensory signals that activate sensory and thereby motor cortices.

2.10 Synergistic neurofeedback training for motor rehabilitation following stroke

- An afferent volley from stimulation of the hand arrives in the sensorimotor cortex after about 20 ms. This can be recorded as an evoked potential (N20), later processing events can also be recorded in the form of later components e.g. the P300 (Allison *et al.* 2012).
- If afferent input is precisely planned to arrive in the motor cortex at a time that its activity is increased via motor imagery, it can lead to strengthening in sensorimotor synapses and thereby may translate into improved motor function after stroke. Specifically, according to Hebbian plasticity, it may cause LTP-like plasticity and enhance connectivity in the motor cortex that may elicit stronger ERDs during motor imagery, which would ease neurofeedback training for stroke patients. Enhancement of the connectivity may also contribute to reorganization of the damaged neuronal ensembles within the peri-lesional area of the motor cortex and therefore may cause behavioural gains for stroke patients.
- In addition, perception of the late phases of the sensory feedback (or the visual feedback through observation of the hand movement) as reward to ERD modulation may provide the basis for the occurrence of operant learning.

To summarize, we hypothesized that using a specific BCI design that provides appropriately timed and recurrent sensory feedback provides the basis for the occurrence of i) Hebbian plasticity that not only increases ERD, which eases BCI training, may also results in behavioural gains for stroke survivors; ii) operant learning through perception of late responses to the sensory stimuli. The hypothesized synergy between the Hebbian plasticity and operant conditioning may not only shorten the training time for ERD modulation, also may enhance the efficacy of restorative BCIs.

This thesis will study how and to what extent further activation of the motor cortex during motor imagery through provision of rapid and recurrent sensory feedback enhances ERD modulation (for healthy populations) and behavioural gains (for stroke survivors).

Note that visual feedback does not close the sensorimotor loop during neurofeedback training. Thus, it is unlikely that Hebbian learning occurs during neurofeedback training with pure visual feedback. Accordingly, in this thesis the occurrence of Hebbian learning has been investigated only for the BRI setup (with proprioceptive feedback) and not the BCI setup (with visual feedback).

Next Chapter provides a brief overview on the fundamental elements of a BCI system followed by a literature review on the BCI application for motor stroke rehabilitation.

Chapter 3

Brain-Computer Interfaces Components and Applications

THIS chapter is designed to briefly overview the main aspects of a BCI system including, signal acquisition, signal processing, and BCI applications and feedback. Numerous references have been provided for readers to delve deeper into each specific sub-discipline. Next, BCI application for stroke rehabilitation is further explained and motivated. Finally, a literature review on restorative BCIs and their state of the art is presented highlighting the current challenges and open questions.

3.1 Introduction

According to John Wolpaw brain-computer interfaces (BCIs) are determined as follows: *'A BCI is a system that measures central nervous system (CNS) activity and converts it into artificial output that replaces, restores, enhances, supplements or improves natural CNS output thereby changes the ongoing interactions between CNS and its external or internal environment'* (Wolpaw and Wolpaw 2012a). The activity of CNS can be measured via sensors mounted on the scalp, on the brain's surface or within the brain. Note that a BCI measures the signals arising from CNS activity, extracts their related features, and then translates them into commands readable by computers/machines.

This chapter is aimed at providing a brief overview of the main aspects of any BCI system, including signal acquisition, signal processing (mainly excluded to the applied techniques within the thesis), and major BCI applications followed by the state of the art in therapeutic BCIs for motor recovery after stroke. Note that the different aspects and paradigms are briefly reviewed to motivate the area and understand the chosen study in this context. For further exploration, numerous reference papers are provided for all sections.

3.2 BCI signal acquisition

Signals from a BCI reflect either electrical/magnetic activity of the brain or the brain metabolism. This section describes different electromagnetic or brain metabolism signals that are used for BCIs.

3.2.1 Signals that reflect electrical activity of the brain

Local field potentials: Local field potentials (LFP) that are recorded within the brain's cortex, mainly represent the cortical activity within 0.1–1 mm of the recording electrode(s). This signal provides high quality and signal-to-noise ratio, however it requires surgery to mount the electrodes within the brain.

Electrocorticogram: Electrocorticogram (ECoG) signals are recorded from the surface of the brain cortical tissues and are known to reflect the cortical activity within 2–5 mm around the recording electrodes. Here, ECoG electrodes are mounted on the surface of the brain through small holes made in the skull and thus are less

invasive than LFPs. The ECoG also provides a reasonable quality and signal-to-noise ratio signal.

Electroencephalogram: Electroencephalogram (EEG) signals are obtained from the scalp where each electrode represents the neural activity of 10–40 cm² of the cortical sheet centred around the electrode. The biggest drawback of EEG is its low signal-to-noise ratio that renders it prone to environmental and biological artefacts. However, as the only non-invasive signal that measures the brain electrical activity, it is the most commonly used signal in the realm of BCI research (Srinivasan 2012).

3.2.2 Signals that reflect magnetic activity of the brain

The magnetoencephalogram (MEG) records the brain's very small magnetic fields. This technology that was introduced in 1980s, is more sensitive than EEG to cortical activities oriented parallel to MEG sensors (Srinivasan 2012). Another advantage of MEG over EEG originates from transparency of the skull and other tissues circumscribing the brain to the magnetic field. However, in practice, EEG electrodes are placed much closer to the neural sources than MEG sensors. Note that MEG equipment is significantly more costly than EEG hardware, requiring a magnetically shielded chamber, and its sensors need to be cooled using liquid helium. Therefore, MEG has been used as a supportive, rather than a primary method for BCI development (Srinivasan 2012).

3.2.3 Signals that reflect the brain metabolism

Measuring the brain activity through its electromagnetic activity has a number of inherent limitations such as reflecting the activity only in the immediate vicinity of the sensors. The brain's metabolic processes, however, provide an overall picture of the whole brain via its energy consumption that is correlated with neuronal firing rate. Increased brain metabolism is reflected by greater consumption of required resources such as sugar and oxygen that necessitate increased blood flow in the brain. The blood flow in the brain is locally controlled and thus can be employed as a biomarker for neural activity. Four main technologies to monitor the brain metabolism are summarized as follows.

3.3 EEG signal processing

Functional transcranial Doppler: Functional transcranial Doppler (fTCD) is another method that measures the brain metabolism via monitoring changes in blood flow through the brain's main arteries (Stroobant and Vingerhoets 2000). Its advantages comprise affordability and mobility of the equipment. However, it only measures differences between the right and left hemispheres activity that renders it suboptimal for BCI studies.

Positron emission tomography: Positron emission tomography (PET) tracks the blood flow through tracing injected radioactive compounds (Fox *et al.* 1984). Similar to fTCD, PET is not an attractive option for BCI research as it is relatively slow and radioactive compound injection is an invasive technique.

Functional near infrared spectroscopy: Functional near infrared spectroscopy (fNIRS) monitors the blood flow in the brain through screening modification in different types of the haemoglobin cells (Villringer *et al.* 1993, Boas *et al.* 2004). These changes in haemoglobin types are referred to as blood oxygen level dependent (BOLD) response (Ogawa *et al.* 1990). It measures the response of haemoglobin cells exposed to a near infrared radiation to calculate the blood flow accordingly. Its spatial resolution is on the order of centimetres and has a temporal resolution on the order of several seconds. It is easy and convenient to apply and thus an appealing method for BCI research (Ramsey 2012).

Functional magnetic resonance imaging: (fMRI) is another technique that like fNIRS also monitors the BOLD response to measure the brain metabolism (Ogawa *et al.* 1990). It screens the response of different haemoglobin cells to a magnetic field to determine oxygen consumption and blood flow. It is very high-cost, but is presently the most sensitive technique for monitoring the brain metabolism with high resolution and thus it is commonly used for BCI research (Ramsey 2012).

3.3 EEG signal processing

All reported studies in the thesis were performed by recording EEG signals. Consequently, in the following review of signal processing techniques only methods relevant to EEG signals, which are most relevant to the techniques used in this thesis, will be described.

3.3.1 Pre-processing

This step involves artefact removal and enhancement of spatial, temporal and/or spectral characteristics of the EEG signals using *a priori* knowledge. The following section describes the typical steps performed during pre-processing:

Pre-filtering: Frequency range pre-filtering removes unwanted frequencies while retaining desired frequencies. For instance, in motor imagery based BCIs (MI-BCI) sensorimotor rhythms (8–30 Hz) are explored to extract spectral features and therefore, frequency range pre-filtering for MI-BCI involves band-pass filtering of EEG signals to eliminate spectral features outside 8–30 Hz frequency band.

Down sampling: To enhance computational efficiency, the data are down sampled following the primary filtering by a suitable factor. The adjusted sampling rate must remain at least two times greater than the largest frequency of interest in the signal. This approach guarantees preservation of all relevant information in the signal through keeping the sampling frequency greater than Nyquist frequency and thereby prevent signal distortion.

Spatial filtering: EEG signals reflect the activity of a fairly large area of the brain. Furthermore, the recorded signals of the channels close to each other are largely correlated. To enhance the spatial resolution of EEG electrodes and to render them more representative of independent cortical activities a myriad of spatial filtering techniques have been proposed. Data dependent spatial filtering encompasses principal component analysis (PCA), independent component analysis (ICA), and common spatial patterns (CSP). It increases the spatial resolution while considering the covariance between all available channels. However, data independent spatial filtering such as with the Laplacian filter and common average reference (CAR) do not deal with the relationship among different electrodes (Krusienski *et al.* 2012).

Artefact removal-environmental noise: Environmental artefact removal involves removing electrical and magnetic interference originated from the environment out of EEG signals. For instance, the power-line noise (50 Hz in Europe, Asia and Australia or 60 Hz in America) interfere with EEG signals. Power-line noise is produced when the electromagnetic fields of the equipment working at 50/60 Hz affect the human body that produces strong noise in their respected frequencies. To remove this artefact a band-stop (notch filter) is applied to EEG signals.

3.3 EEG signal processing

Artefact removal-biological noise: Biological noise that affects EEG signals mainly manifests as muscular contraction potentials, i.e. electromyogram (EMG), and eye movement potentials, i.e. electrooculogram (EOG) and eye blinks. Since these signals affect the neighbour electrodes similarly, spatial filtering techniques such as Laplacian filtering remove a large portion of them.

3.3.2 Feature extraction

Following pre-processing that suppresses the noise and enhances desired aspects of the signals, the next step is to extract relevant features using *a priori* knowledge of the recorded signal. Notably, for motor imagery-based BCIs, the desired features are amplitude modulation of EEG signals within 8–30 Hz frequency band. To extract these features mainly one of the following methods is adopted:

Fast Fourier transform: The fast Fourier transform (FFT) is a computationally efficient method used to calculate the spectral power of a signal within an individual frequency or a frequency band. The FFT takes an N sample signal and produces N frequency samples uniformly spaced over $-f/2$ to $+f/2$ range where f represents the sampling frequency. Note that FFT values are complex values that have magnitude and phase. To calculate the spectral power, we square the magnitude of FFT values. To reduce artefacts introduced by abruptly changing edges that occur through segmentation of the EEG signals, tapering windows such as Hamming and Hanning window functions are multiplied by the finite-length signals prior to FFT calculation. This approach mitigates the occurrence of unwanted ripples in the frequency response.

Autoregressive modelling: The autoregressive (AR) modelling technique is an alternative to the Fourier transform in calculating spectral attributes of EEG signals. It models EEG as output of a filter that receives white noise as its input. Since white noise encompasses all frequencies, the filter adjusts its parameters to reflect EEG spectral characteristics. A critical factor in AR modelling is optimal order determination. Note that EEG signals are considered to encompass up to five spectral peaks comprising δ (0–4 Hz), θ (4–8 Hz), α (8–13 Hz), β (16–30 Hz), and lower γ (30–50 Hz) (Pfurtscheller and McFarland 2012). Therefore, the order of the AR model must be more than 10 for proper modelling of EEG signals (Krusienski *et al.* 2012). However, the order must be increased when large

sampling rates are used (Pfurtscheller and McFarland 2012). The Burg algorithm (Hayes 2009) is a preferred method for calculating AR model parameters as it guarantees model stability. The power spectrum is obtained using the formula 3.1:

$$P_{AR}(\omega) = \frac{E_p}{|1 + \sum_{k=1}^p a_p(k)e^{-jk\omega}|^2} \quad (3.1)$$

where E_p is the prediction error, $a_p(k)$ is the k_{th} filter weight, p is the order of the AR model, and $P_{AR}(\omega)$ is the spectral power at the angular frequency of ω .

Wavelet transform: To overcome the drawbacks of FFT and AR modelling that lose temporal information when transforming a signal to the frequency domain, wavelet transform has been proposed. Wavelet analysis convolves the EEG signal with both stretched and compressed versions of specifically shaped wavelets. Whenever it finds a large correlation, it creates larger wavelet coefficients and vice versa. Therefore, not only do wavelets reveal spectral attributes of the EEG signal, but they also disclose how the spectral behaviour of the signal changes over time. Another aspect of a wavelet transformation is that it adjusts the signal window length in order to maximize its frequency resolution. Notably, by applying longer wavelets for low frequencies and shorter wavelets for high frequencies, it extracts frequency domain features with optimal resolution. The wavelet transform has two versions: (i) a more computationally efficient version is discrete wavelet transform (DWT) that minimizes redundancy, and (ii) the continuous wavelet transform (CWT), which is more robust in extracting subtle features (Bostanov and Kotchoubey 2006).

3.3.3 Post-processing

Prior to transferring the extracted features to classifiers, further processing of features is required to optimize feature distribution and mitigate redundancy among features. Post-processing of features is typically carried out through the following procedures to enhance the performance, accuracy, and speed of the classifier.

Normalization: The extracted feature sets may have different means and dynamic ranges, non-related to the BCI task conditions. In such cases, a normalization

3.3 EEG signal processing

procedure is applied. It involves subtracting the average value from all features, followed by dividing the resultants by the standard deviation. This technique renders zero mean and unit variance features that enhance classification outcomes.

Log-Normal transformation: The FFT amplitude lower range is bounded by zero whereas the higher range is limited by the sampling frequency. In addition, EEG power is inversely proportional to frequency. Thus, it is very likely to produce a non-Gaussian distribution of spectral power features with EEG signals. Most classifiers provide optimum results when receiving normally distributed features. A logarithmic transformation in most cases normalizes the non-normal EEG spectral features, and makes them optimal for classification.

Dimension reduction: To provide real time feedback in a BCI framework, it is necessary to keep the computational cost as low as possible. To decrease computational cost of the classification, it is required to extract the lowest possible number of features that represent EEG signals. In addition, representing the EEG signals with larger than optimal number of features causes the *curse of dimensionality* (Bellman 1957) and degrades the classification accuracy with novel observations. Principal component analysis (PCA) and independent component analysis (ICA) are among the most commonly applied methods that remove correlated and redundant features from the feature space and define the optimal features (Krusienski *et al.* 2012).

3.3.4 Feature translation

Despite the ideal cases in which the extracted features of BCI signals directly reflect a subject's intent, a feature translator is necessary to transform the features into signals amenable to external devices.

A feature translator, that is also referred to as classifier, is a mathematical model that includes a number of parameters. The parameters of the model become adjusted using observations in which the subject's intent is clear. Then the adjusted (trained) model is used to predict the subject's intention from new observation data (generalization).

To determine a high-performance classifier for a specific BCI system, its model type, input features, and parameters need to be selected optimally (McFarland and Krusienski 2012). The following describes these aspects of BCI classifiers.

Model selection

The primary function of a classification model is to determine whether the user's intention is reflected in the extracted features. The goodness-of-fit of a selected model will be subsequently determined through the accuracy, and speed of classification. Model selection depends mostly on two critical factors: BCI application, and the amount of available training data.

Classifiers that produce continuous outputs have a regression model whereas those with discrete outputs have a discriminant model. While models are typically used in a specific manner to provide either discrete or continuous outputs, they are usually able to produce both types of outputs. A number of most commonly used classifier models for BCIs are listed as follows:

Linear least-squares discriminant classifier: This model is one the simplest and meanwhile most powerful models used for BCI classification (McFarland and Krusienski 2012, Theodoridis and Koutroumbas 2006b). Its general form is:

$$Y = b_1X_1 + b_2X_2 + \dots + b_nX_n + a \quad (3.2)$$

where Y is the predicted value (classifier output), $b_1, b_2, b_3, \dots, b_n$ and a are the model weights that need to be determined, and $X_1, X_2, X_3, \dots, X_n$ are features. The b_i parameters are defined using the following formula:

$$b = (X'X)^{-1}X'Y. \quad (3.3)$$

Bayesian classifier: This classifier uses the maximum likelihood concept to extract information from *a priori* knowledge to classify novel data as posterior probabilities. More specifically, it calculates the possibility of belonging to each class of outputs given a set of features. The class with the highest possibility is most likely the class that the novel observation belongs to. The general form of a Bayesian classifier is as follows:

$$P(Y|X_1, X_2, \dots, X_n) = \frac{P(Y)P(X_1|Y)P(X_2|Y)\dots P(X_n|Y)}{P(X_1)P(X_2)\dots P(X_n)} \quad (3.4)$$

where Y is the predicted value (classifier output), $X_1, X_2, X_3, \dots, X_n$ are features, and $P(X_i|Y)$ is the probability of X_i given Y .

3.3 EEG signal processing

Bayesian classifier is simple and robust even when a small number of observations for classifier training is available. However, for a large set of training data, a linear least-squares discriminant model that takes into account the relationship among features may provide a better performance (Theodoridis and Koutroumbas 2006a).

Support vector machines: The aforementioned classifiers originate from statistical methods. However for another family of classifiers such as support vector machines, machine learning approaches are employed to iteratively improve the classifier performance. Notably, support vector machines find the support vectors across the boundaries between classes that: i) minimize the Euclidean distance between the support vectors (hyper planes) and incorrectly classified data; ii) maximize the Euclidean distance between support vectors (Duda *et al.* 2012). This model is believed to be robust against outliers and generalizes well, even with limited number of observations for adjusting the parameters (Parra *et al.* 2005).

Non-linear methods: Advanced machine learning approaches transform non-linear problems into linear ones through application of kernel methods. Commonly used kernels include Gaussian and radial basis function (RBF) kernels. Gaussian kernels allow producing fairly distinctive hyperplanes from features that in their original form would have created very irregular shapes (McFarland and Krusienski 2012).

Another method to deal with feature non-linearity is to exploit the robustness of artificial neural networks that are able to estimate (theoretically) any function, where a sufficient number of artificial neurons have been used (Müller *et al.* 2003). However, complex functions necessitate employing a large number of artificial neurons that require large numbers of observations to fine tune the model parameters for artificial neural networks (McFarland and Krusienski 2012).

For a through review on BCI classification techniques refer to Lotte *et al.* (2007), and Makeig *et al.* (2012).

Feature selection

Regardless of feature types used for BCI classification, be it event-related potentials or spectral power, the brain usually produces correlated (redundant) features.

In addition, the number of features used in any model is proportional to its classification accuracy of the training data. However, the model generalizability degrades when very large number of features are used for parameter adjustment as it causes overfitting to the training data. Therefore, a trade-off must be made between minimizing the error of the classifier with training data, and its generalizability through selecting optimal number of features. Heuristic methods, iteratively select the optimum features that fulfil the mentioned trade-off. Step-wise heuristic methods such as forward and backward stepwise heuristic techniques, instead of examining all possible combination of features, start with the best features and add or subtract other features and check whether they make the classifier more accurate in each step. The search for optimal features continues until a stopping criterion such as reaching a minimum r^2 value, that defines the percentage of correct outputs that can be predicted given the selected features, is fulfilled.

Parameter estimation

Parameters of a model can be estimated using direct methods such as the LDA Equation 3.2 or using an iterative optimization algorithm (Press 2007). The latter approach has the advantage of being able to estimate even non-linear systems, while the former method is fast and computationally efficient. A common technique in parameter estimation is the least-mean squares (LMS) algorithm (Haykin 1996) in which using Equation 3.5, the parameters are adjusted and iteratively decrease the estimation error. Here, $b(t + 1)$ is the updated parameter at time $t + 1$, l is the learning-rate parameter, $e(t)$ is the prediction error, and $X(t)$ is the current feature vector

$$b(t + 1) = b(t) + l \cdot e(t) \cdot X(t). \quad (3.5)$$

The LMS algorithm belongs to a family of parameter estimators referred to as adaptive parameterization methods. They perform well when the relationship between the error, features, and class labels are simple. If the relationship is complex, LMS may not provide an optimal solution. In such cases evolutionary algorithm such as Genetic Algorithms, and Particle Swarm Optimization may perform better than LMS as they are robust against falling into local minima and sub-optimal final points (Krusienski and Jenkins 2005).

3.3 EEG signal processing

Classifier evaluation methods

Accuracy, sensitivity, selectivity, and specificity: In a typical BCI application, depending on the subject's intention and the BCI output command, four scenarios might occur. To describe these conditions we use a typical BCI system that translates neural activity to commands for an exoskeleton that opens the subject's fingers:

Scenario 1: The user aims to open his fingers and the BCI opens his fingers; this is referred to as *true positive* (TP)

Scenario 2: The user does not aim to open his fingers and the BCI does not open them; this is referred to as *true negative* (TN)

Scenario 3: The user does not aim to open his fingers but the BCI opens them; this is referred to as *false positive* (FP)

Scenario 4: The user aims to open his fingers but the BCI does not open his fingers; this is referred to as *false negative* (FN).

The most commonly used BCI measure is *accuracy* that in terms of the aforementioned indices is:

$$\text{accuracy} = \frac{\text{TP} + \text{TN}}{\text{TP} + \text{TN} + \text{FP} + \text{FN}}.$$

Other BCI measures including *sensitivity*, *selectivity* (positive predictive value), and *specificity* (negative predictive value) are defined as follows:

$$\text{sensitivity} = \frac{\text{TP}}{\text{TP} + \text{FN}}$$

$$\text{selectivity} = \frac{\text{TP}}{\text{TP} + \text{FP}}$$

$$\text{specificity} = \frac{\text{TN}}{\text{TN} + \text{FN}}.$$

There is no specific measure that is suitable for all BCI applications and it is the attributes of the BCI system that makes one or a specific collection of the mentioned metrics more suitable than others.

Measures for continuous BCIs: For BCIs with continuous outputs such as cursor position updates on monitors, the mentioned measures may not be suitable and other specific measures are required. One such possibility is the Chi-squared (χ^2) measure that sums the squared errors. This measure reflects the output variance

that is caused by the BCI error ($1 - r^2$). Then, r^2 indicates the model's goodness-of-fit that can be calculated.

Bit-rate measure: Information transfer rate is a measure that accounts for the speed and accuracy of a BCI system, simultaneously (Wolpaw *et al.* 2000). This measure calculates the amount of information units transferred per unit time and is calculated using the following formula:

$$B = \log_2 N + P \log_2 P + (1 - P) \log_2 \frac{1 - P}{N - 1}$$

where B is the bit-rate, N represent the number of classes, and P is the accuracy of the classifier.

3.4 Different BCI paradigms

In the following sections, different paradigms are highlighted to motivate the area and understand the chosen paradigm of the study in this context.

3.4.1 P300-based BCIs

An oddball paradigm (Donchin and Coles 1988) is a process in which (i) a user receives a collection of stimuli that fall into two categories; (ii) exposure to members of one class is less frequent than those of the other class; (iii) the user is asked to classify the stimuli to one of two classes. It has been shown that being exposed to the less frequent class members (oddball event) produces a positive shift in the EEG amplitude occurring about 250–750 ms post-stimuli referred to as *P300*. Thus, recording EEG signals that are time locked to stimuli presentation enable the detection of P300 phenomenon following the occurrence of the oddball event.

3.4.2 Steady-state evoked potential-based BCIs

Exposure to visual stimuli creates two types of responses in the brain: i) exogenous responses that occur earlier and reflect the brain's unconscious reaction to the stimuli; ii) endogenous responses that occur with longer latencies (such as P300) and indicate

3.4 Different BCI paradigms

conscious responses of the brain to the stimuli. While the latter creates the foundation for P300-based BCIs, the former responses are considered *steady-state visual evoked potentials* (SSVEP) and are the selected signal for another BCI paradigm referred to as SSVEP-based BCI. In the standard SSVEP-based BCI a user is exposed to a number of objects shown on a monitor that blink repetitively with distinct frequencies. When the user fixates on a specific object, the EEG frequency spectrum indicates distinctive peaks at the frequency that the target object is blinking (Allison *et al.* 2012).

3.4.3 Slow cortical potential-based BCIs

Prior to motor execution or motor imagery of a motor skill, a change occurs in the EEG signal that is referred to as the *slow cortical potential* (SCP). The SCP occurs in one of these manifestations in the time domain: i) contingent negative variation (CNV) that is a negative shift starting 200–500 ms after a primary stimulus that prepares the user for a following command that cues the user to perform the motor or cognitive task; ii) *Bereitschaftspotential* (readiness potential) is another form of SCP that begins 500–1000 ms prior to self-decided movement or motor imagery tasks. Slow cortical potentials are also referred to as movement related cortical potentials (MRCP) (Jochumsen 2015, Shibasaki and Hallett 2006).

3.4.4 Motor imagery-based BCIs

Motor planning prior to motor execution and motor imagery of the same task, similarly decrease the spectral power in the α (8–13 Hz) and β (16–30 Hz) frequency bands (Pfurtscheller and Aranibar 1979, Neuper and Pfurtscheller 2001). Thus, having a subject to imagine their limb movement produces specific spectral features that provides the basis for motor imagery based BCIs (MI-BCI) that is the selected BCI paradigm in this thesis.

Even though in this thesis we have chosen ERD as the feature of interest that reflects down-regulation of cortical oscillatory activity, other measures such as readiness potentials (MRCP) or motor evoked potentials (MEP) may also be used to study the effect of feedback optimization on the efficacy of our approach to optimize feedback of restorative BCIs for stroke rehabilitation. Whilst beyond the scope of the present study, these may form the basis of a comparative study on suitability of the mentioned measures in

the context of restorative BCIs. More details on neurophysiological aspects of restorative BCIs have been discussed in Chapters 4–7.

3.5 BCI applications

When a classifier translates features to a command, it affects the outside world via a myriad of methods that are generally referred to as BCI applications.

A BCI output can replace a body function that has been lost due to an injury or a disease. For instance, BCI commands that control exoskeletons for people with amputees replace their *replace* their lost motor functions.

Some tasks, e.g. driving a car, require continuous attention of the user and losing attention may lead to fatal consequences. Here, BCI can be employed to *enhance* neural outputs through continuously monitoring attention and providing alarms when attention has lapsed.

Note that BCIs may be used to *supplement* natural motor outputs such as sending neural commands directly to a robotic arm to complement their natural motor skills.

A BCI may also be designed to improve or *restore* lost or impaired motor functions after a stroke. This BCI application is the key focus of this thesis and for simplicity it will be referred to as *restorative* BCI and will be used interchangeably with the term *BCI application for stroke rehabilitation* throughout this thesis. Fig. 3.1 illustrates the mentioned applications of BCIs.

This section described only key BCI applications. Further details on real world and clinical BCI applications have been thoroughly discussed in Moore (2003), and (Mak and Wolpaw 2009), respectively. A more recent review on BCI applications can be found in Wolpaw and Wolpaw (2012a). One may also visit <http://bnci-horizon-2020.eu/> that is a European project to determine future directions for BCIs.

3.6 Feedback optimization for restorative BCIs

One of the key elements in restorative BCIs and neurofeedback training is feedback provision. In the course of this thesis we examine two main aspects of feedback: feedback update rate (FUI) and feedback modality.

3.6 Feedback optimization for restorative BCIs

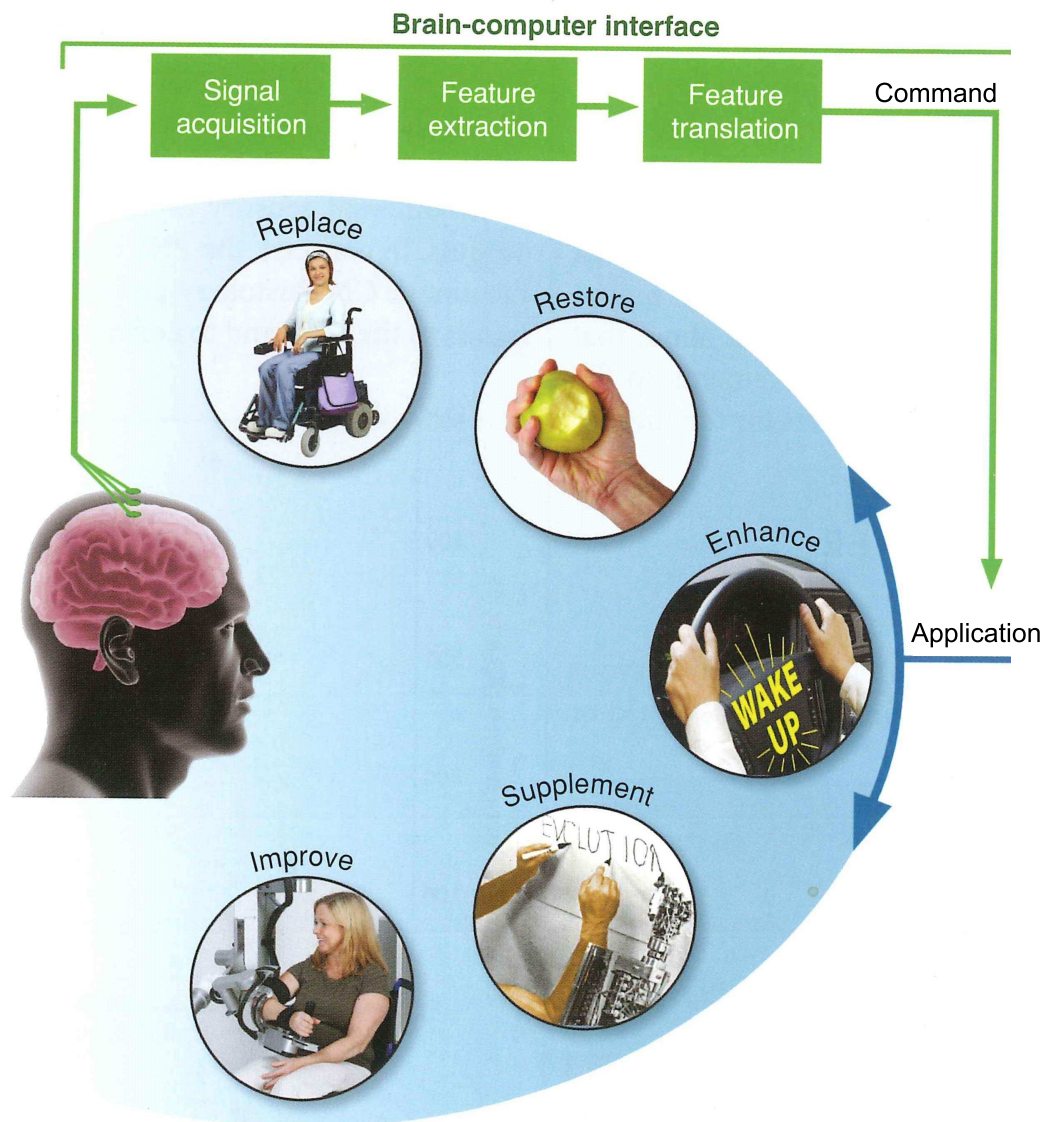


Figure 3.1. BCI main components and its application. A BCI can replace a body function, enhance a driver's attention, supplement a motor function, and improve or restore impaired or lost motor functions following a stroke. After Wolpow and Wolpow (2012a).

Feedback update rate Operant conditioning is thought to play a critical role in MI-BCI training in the behavioural level (Fetz 2007). It has been suggested that Hebbian learning may also play a role in the context of BCI training (Kraus *et al.* 2016, Naros *et al.* 2016). As discussed in Chapter 2, in this thesis we examine whether harnessing the early effects from the arrival of the afferent volley in the sensori-motor cortex plays a role in boosting Hebbian learning within a BCI framework. Specifically, in this thesis we have explored different FUIs for restorative MI-BCIs.

Feedback modality Feedback provision for restorative BCIs is mainly implemented through either visual (Shindo *et al.* 2011) or proprioceptive (Ramos-Murguialday *et al.* 2013) feedback. Functional electrical stimulation (FES) (Rushton 1997) is also used to provide visual and proprioceptive feedback for motor rehabilitation following stroke (Daly *et al.* 2009, Young *et al.* 2015). Among them, FES provides the most similar feedback to feedback provision during motor learning. However, in this study we only study visual and proprioceptive feedback as FES has a long transition time after each stimulation and therefore, is not suitable to study high frequency feedback provision for restorative BCIs, which is another aspect of feedback that is explored in this thesis (see above).

In this thesis we compare the effect of visual and proprioceptive feedback provision for neurofeedback training. Visual feedback was provided through either a cursor position update on a monitor or observing flexion/extension of a free-running (with no hand involvement) orthosis. Instead, proprioceptive feedback was delivered using flexion/extension of an orthosis involved with the BCI users' target hand during motor imagery of four finger flexion/extension. For further details on these, refer to Chapters 5–7. Note that flexion/extension of the fingers of the target hand by the orthosis provided both proprioceptive and visual feedback, since the participants were instructed to observe their target hand movement during motor imagery. Therefore in total, three forms of visual feedback was provided in the studies reported in this thesis: i) visual feedback by a cursor position update on a monitor; ii) visual feedback via observing a free-running orthosis movement during relaxation trials; iii) visual feedback (in addition to proprioceptive feedback) where the participant observed their target hand's movement during motor imagery.

The following section provides a literature review for application of MI-BCIs for motor recovery after stroke.

3.7 The state of the art in restorative BCIs

Restorative BCIs aim to restore or improve lost or impaired motor functions following a stroke. A number of studies have investigated different BCI paradigms to harness BCI potentials for stroke rehabilitation. In the current thesis, the adopted BCI paradigm is motor imagery-based BCI. Therefore the following section, that reviews

3.7 The state of the art in restorative BCIs

major contributions in the realm of restorative BCIs, only considers studies with the motor imagery-based BCI paradigm.

The first application of BCI for stroke rehabilitation was reported by Mohapp *et al.* (2006) as a methodology study on ten stroke patients who performed motor imagery and actual movement of their affected hands. Then Bai *et al.* (2008) conducted a study in which modulation of β -ERD was rewarded by visual feedback with one stroke patient. The first clinical study that applied MI-BCI with clear performance metrics for stroke rehabilitation was carried out by Buch *et al.* (2008). They used MEG as their neural signal with cursor position update on a monitor as feedback. Using the mentioned design they investigated the effect of neurofeedback training on stroke patients' Medical Research Council (MRC) scale and reported no significant change. Ang *et al.* (2009) compared the effect of MI-BCI coupled with robotic training to robotic rehabilitation without BCI and found the studied paradigm outcomes to be equivalent.

Shindo *et al.* (2011) tested MI-BCI for eight stroke patients where motor imagery of the instructed task was rewarded by real time visual and delayed proprioceptive feedback. While their study revealed significant recovery for stroke patients with some residual hand motor functions, it did not provide clinically significant outcomes for the ones who totally lost their hand motor functions following stroke. Prasad *et al.* (2010) also used MI-BCI to investigate the effect of neurofeedback training paired with physiotherapy on five stroke patients. They adopted the Action Research Arm Test (ARAT) and grip strength as their behavioural measures to study the effect of BCI training and reported that all participants improved according to at least one of the applied measures.

Gomez-Rodriguez *et al.* (2011) also examined the effect of coupling ERD modulation with real time proprioceptive and visual feedback. Their specific design enhanced the BCI accuracy and ERD modulation for both healthy and stroke patient populations only with proprioceptive feedback. Ramos-Murguialday *et al.* (2013) studied the effect of pairing proprioceptive feedback with ERD modulation using specifically designed orthoses that extended stroke patients' fingers when they modulated α -ERD. This study involved neurofeedback training followed by physiotherapy with 32 stroke patients divided equally into target and control groups. It was reported that significant improvement of Fugl-Meyer assessment of motor recovery after stroke (FMA) scores were found only in the target group. Thus, it suggests that MI-BCI training

may be used to prime lost motor functions in chronic stroke patients with no residual finger movements. Also a recent study on restorative BCIs has been performed by Pichiorri *et al.* (2015), in which they recruited 28 stroke patients who were divided equally into target and control groups. For target groups, participants performed motor imagery that was rewarded by visual feedback, whereas the control group performed motor imagery without BCI support. They reported significant improvement in both FMA scores and modulation of stronger ERDs only in their target group. This finding further consolidates the feasibility of MI-BCIs for stroke rehabilitation.

Note that BCI-FES has also been used in several studies for stroke rehabilitation. It mainly rewards ERD modulation or MRCP elicited via performance of motor imagery or motor attempt by electrical stimulation of the target muscles and thereby delivers both visual and proprioceptive feedback. Daly *et al.* (2009) examined the feasibility of BCI-FES for stroke motor recovery with one stroke survivor who attended nine training sessions over three weeks. They found the technique feasible as the participant controlled the system accurately and achieved recovery in volitional index finger movement. Also, Young *et al.* (2015), trained one stroke patients with BCI-FES for six weeks and found that his ARAT score improved by 10 points. In another study by McCrimmon *et al.* (2014) they worked with three chronic stroke survivors with foot drop and trained them with three 1-hour sessions over a week using BCI-FES. All participants were able to use BCI-FES with high accuracy and their dorsiflexion active range improved by 3–8 degrees. in another proof-of-principle study with two patients with tetraplegia, Vuckovic *et al.* (2015) tested applicabilty of BCI-FES where they trained the fist and second participants with four and ten training sessions in addition to conventional therapy. They both showed a high level control over the BCI-FES sytem and one of them showed modearte improvement in their muscle strength. The BCI-FES has also been proposed as one the key paradigms for motor stroke rehabilitation in a European project known as 'BNCI Horizon 2020' that determines future directions for BCI research http://lamp.tugraz.at/~karl/verlagspdf/Roadmap_BNCI_Horizon_2020.pdf.

Regardless of the adopted measures, and different paradigms cited above, it can be concluded that: i) BCI training is a feasible intervention for stroke rehabilitation with results that are relatively promising; ii) despite the primary promising results that suggest MI-BCI as a novel intervention for stroke rehabilitation, it needs optimization to provide clinically significant outcomes with both mild and severe post-stroke impairments.

3.8 Chapter summary

This chapter has presented the basic components of brain-computer interfaces, their applications and feedback. Different signal acquisition and processing techniques applied for BCI systems have been discussed. Major BCI paradigms in which a variety of the brain responses are exploited have also been explained. Motivations and aspects of feedback that are explored in this thesis have been highlighted. Since the focus of this dissertation is on optimization of restorative BCIs, only this specific application of BCI was considered for the literature review.

After presenting the required background information on BCI components, feedback and applications in the current chapter, we will investigate an optimal trade-off among the parameters of a restorative BCI in the next chapter that produces real time feedback with the largest possible accuracy.

Chapter 4

Optimizing Parameters for Restorative Brain-Computer Interfaces

RECENTLY, the application of restorative brain-computer interfaces (BCIs) has received significant interest in many BCI labs. However, there are a number of challenges, that need to be tackled to achieve efficient performance of such systems. For instance, a restorative BCI needs an optimum trade-off between its time window length, classification accuracy and classifier update rate. Such a trade-off ensures that real time feedback is provided with the highest possible accuracy. In this study, we have investigated a feasible trade-off for these parameters by using a dataset provided by the University of Graz, Austria. We have used a continuous wavelet transform and the Student t-test for feature extraction and an SVM for classification. We observed that real time feedback for restorative BCIs may be achieved by using a 750 ms time window with an average classification accuracy of 67% that updates every 32 ms.

4.1 Introduction

Based on the findings that imagination of motor functions can facilitate stroke rehabilitation (Boe *et al.* 2014, Halsband and Lange 2006) BCIs have been used by many BCI groups as a tool to assist stroke patients with mental practice to enhance their recovery after stroke (Buch *et al.* 2008, Shindo *et al.* 2011, Ramos-Murguialday *et al.* 2013, Pichiorri *et al.* 2015). Restorative BCIs have been proposed to monitor the motor imagery performance and reward it with sensory feedback and reorganize the impaired neural networks for stroke patients (Soekadar *et al.* 2011). Restorative BCIs may be invasive that involve implanting electrodes on the surface or within the brain, or non-invasive. For non-invasive restorative BCIs, the signal of interest may be EEG, MEG, fMRI, or NIRS. However, EEG-based BCI is the most commonly used paradigm for stroke rehabilitation as a low-cost and portable approach and thus was selected for this study. Mechanisms of recovery (largely neuroplastic, (Murphy and Corbett 2009)) are not fully understood. However, Hebbian-based learning and metaplastic effects are thought to be important (Murphy and Corbett 2009). Hence, presuming the importance of coincidence between motor imagery performance and receiving sensory feedback, providing real-time feedback during neurofeedback training is expected to have a constructive effect on restorative BCIs.

In a recent study by Gomez-Rodriguez *et al.* (2011) a motor imagery based BCI was used to actuate a robotic system for upper limb rehabilitation of stroke patients. In that study, the BCI classifier output controlled the robot movement according to the spectral power within 8–30 Hz frequency band calculated from the most recent 500 ms time window. Then the BCI command was updated every 300 ms. Furthermore, Buch *et al.* (2008) and Shindo *et al.* (2011) in very similar designs, used motor imagery based BCIs rewarded by visual feedback for neurofeedback training aimed at recovery of finger movements. Complementary proprioceptive feedback was also provided after successful performance of the instructed motor imagery at the end of the trial. Besides a number of similarities between the studies of Buch *et al.* and Shindo *et al.*, they also had two main differences. One difference was in the signal acquisition, where Buch *et al.* used MEG while Shindo *et al.* used EEG. The other difference in their study designs was the classifier update rate, which was 300 ms for the former and 30 ms for the latter. Even though in a previous study (Grosse-Wentrup *et al.* 2011) the optimal delay between motor imagery performance and feedback provision, i.e. the classifier update rate, was proposed to be in the 200–300 ms range, which implicitly assumes that only

consciously perceived responses to sensory stimuli are valid. However, according to findings of Hiremath *et al.* (2015) that reported the occurrence of implicit learning during BCI training, potentially early sensory responses to stimuli may also play a role in BCI training.

Within a BCI framework, there is a reciprocal relation between the time window length, the classifier update rate, and the classification accuracy. Notably, a long time window typically results in more representative features and thereby, a high classification accuracy. On the other hand, lengthening the time window necessitates a longer processing time and consequently a longer classifier update rate. Therefore, in the current study, we chose a relatively short classifier update rate, i.e. 30 ms, to explore the interplay between the time window length and the classification accuracy.

Also, application of restorative BCIs typically starts with a calibration session to extract the optimum channels and frequency bands for feature classification followed by training the patients based on the results of the calibration session. However, as reported in Shindo *et al.* (2011), stroke patients experience various difficulties, including spasticity and excessive tones in their muscles and lack of proper sleep. Thus, minimizing the number of sessions may improve stroke patients' adherence to therapy through restorative BCIs. Therefore, in this study, we also examined whether it is viable to improve classification accuracy of a restorative BCI for a typical healthy subject by adding further healthy subjects' training data. This approach that we refer to it as *subject-independent classifier* is compared with another method i.e. *subject-dependent classifier*, that uses only the training data of the same subject for testing the classification accuracy with novel observations.

Most of the contents of this chapter have been published in the *Proceedings of 35th Annual International Conference of the IEEE Engineering in Medicine and Biology Society*, 2013 (Darvishi *et al.* 2013a).

4.2 Analysis setup

4.2.1 Dataset

Since this study was run prior to running the experiments reported in Chapters 5–7, it was run using publicly available data. We utilized a widely used dataset (Dataset 2b of BCI 2008 competition) from the University of Graz, which is accessible via

4.2 Analysis setup

Table 4.1. Dataset specifications. This table shows the specification of the used dataset.

Dataset Name	BCI Competition	Number of Classes	Channels	Number of Subjects	Training Trials	Test Trials
2b	2008	2 (left/right hand)	2(C3,C4)	9	1182	2239

<http://www.bbci.de/competition/iv/>. This dataset comprises EEG data from nine healthy right-handed subjects, who were asked to perform motor imagery instructed by visual cues. For each subject there is 120 calibration trials with no feedback, 80 training trials with feedback and 320 test trials with feedback for motor imagery of each hand. For every subject, some trials (around 20%) were contaminated with EOG artefacts that were rejected and analysis was conducted on artefact-free data. Data were recorded with three electrodes (C3, Cz and C4). The recordings had a dynamic range of 100 V for the screening and 50 V for the feedback sessions. They were bandpass-filtered between 0.5 Hz and 100 Hz, and a notch filter at 50 Hz was enabled. The placement of three bipolar recordings (large or small distances, more anterior or posterior) were slightly different for each subject (for more details see (Leeb *et al.* 2007)). The electrode position Fz served as EEG ground. Note that only C3 and C4 channels were employed to decrease the computational overhead. During training and test sessions, continuous visual feedback started 2 s after the presentation of the visual cue and lasted for 4 s. Table 4.1 summarizes the specifications of the purified dataset used for the current study.

4.2.2 Feature extraction

Pfurtscheller and Lopes da Silva (1999) have demonstrated that event related desynchronization (ERD) is followed by synchronization (ERS) in both the α (8–13 Hz) and β (16–26 Hz) frequency bands during motor imagery. Furthermore, such ERD and ERS phenomena only occur in short and non-stationary periods. Thus, we decided to use a continuous wavelet transform for feature extraction, as it has been shown to be more potent than its discrete version in the extraction of subtle EEG features (Bostanov and Kotchoubey 2006). Moreover, it has been demonstrated by Pfurtscheller and Lopes da Silva (1999) that 500 ms after the cue onset a β -ERD occurs in the contralateral hemisphere, coincidentally with a β -ERS in the ipsilateral hemisphere. Thus, to be able to extract such distinctive features, which in turn leads to higher classification accuracy, we based our feature reduction methodology on finding the most discriminating features

using the Student t-test. Further details on feature extraction procedures are illustrated in Fig. 4.1. Since the exploited dataset contained 3421 trials, to make its classification more computationally efficient, we decided only to extract six features per channel for each α and β frequency bands that in total provided 24 features for each time window.

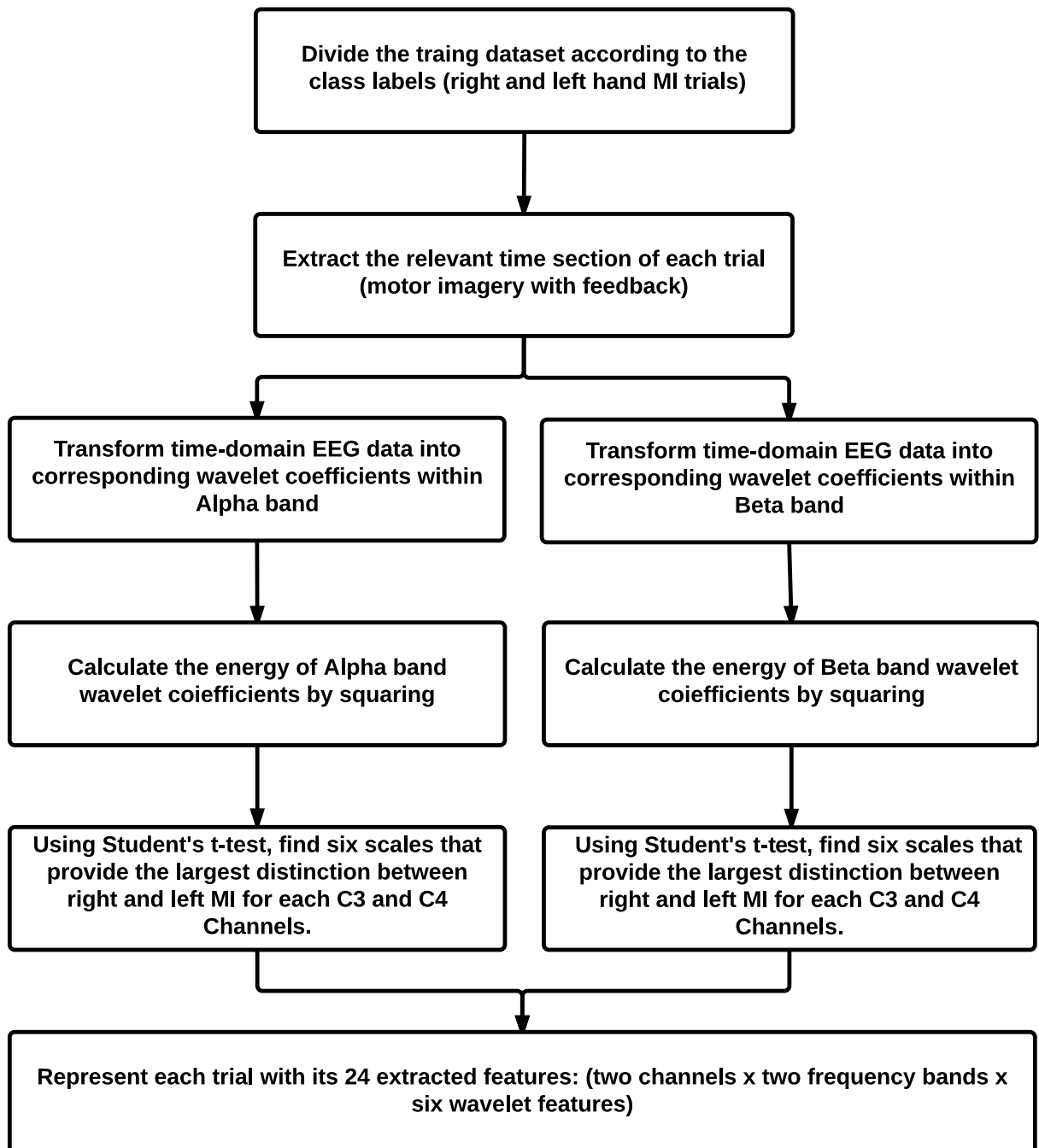


Figure 4.1. Feature extraction steps. This diagram illustrates the steps taken to extract features for each time window of the trials.

4.3 Trade-off results

4.2.3 Classification

For classification, we used an SVM classifier with a linear kernel, which was demonstrated to be one of the most powerful techniques for EEG classification (Darvishi *et al.* 2012). To compare the accuracy of the classification for different window lengths, we defined the window length of the training and test data to be 250, 500, 750, or 1000 ms and then shifted the time windows in steps of 32 ms. We chose the classifier update rate to be 32 ms, which was the closest value to the 30 ms classifier update rate of the Shindo *et al.* (2011) study.

Regarding the comparison between different classifier training methods, for the subject-dependent method, we used only each subject's training data (around 120 trials) for classifier training and tested its accuracy with the same subject's test data. However, for the subject-independent method, we used the entire subjects' training data (1182 trials) and then checked its accuracy for each subject's test data.

4.3 Trade-off results

Based on the described methodology, we achieved the results summarized in Fig. 4.2. The accuracy level for time windows 250 and 500 ms started with classification accuracies very close to chance, however, for wider time windows (750, 1000 ms), the classifiers begin with accuracies higher than 60%. Moreover, with all time windows, after almost one second the classification reaches its maximum and that maximum level has a direct relationship with the length of the time window. Fig. 4.3 and Table 4.2 present a comparison of the average values and standard deviations of the classification accuracies for different time windows. They demonstrate the direct correlation between time window lengths and the average accuracy values and an inverse correlation between time window lengths and accuracy values' standard deviations. Considering the highest observed accuracy of almost 75%, the mean accuracy achievable by 750 ms and 1000 ms time windows seems to provide maximal accuracies.

Regarding the feasibility of subject-independent classifier, we tested both subject-dependent and subject-independent methods. The results of the experiments are shown in Fig. 4.4 where it depicts that training the classifier with the entire subjects

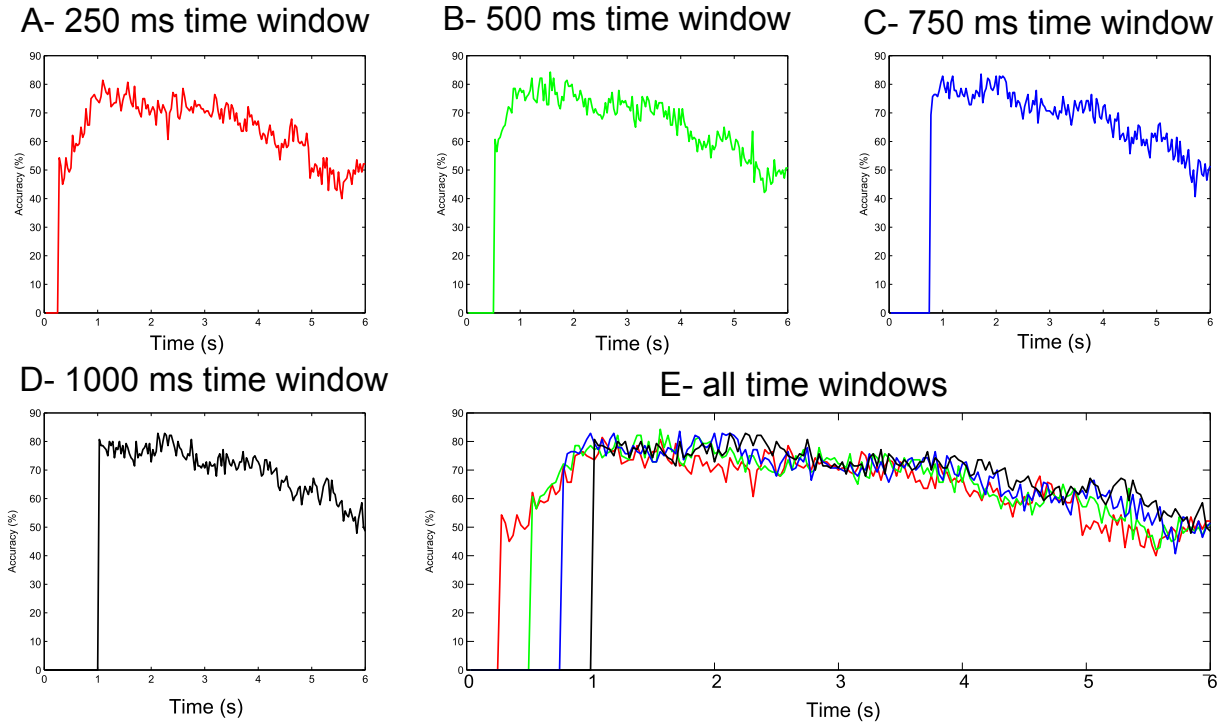


Figure 4.2. Classification accuracy results for different time window lengths. This figure compares the trend of the average classification accuracy with the subject-independent classifier along 4-second-long trials with time window lengths of 250 (panel A), 500 (panel B), 750 (Panel C), and 1000 ms (panel D). Panel E compares the classification trends for all adopted time windows.

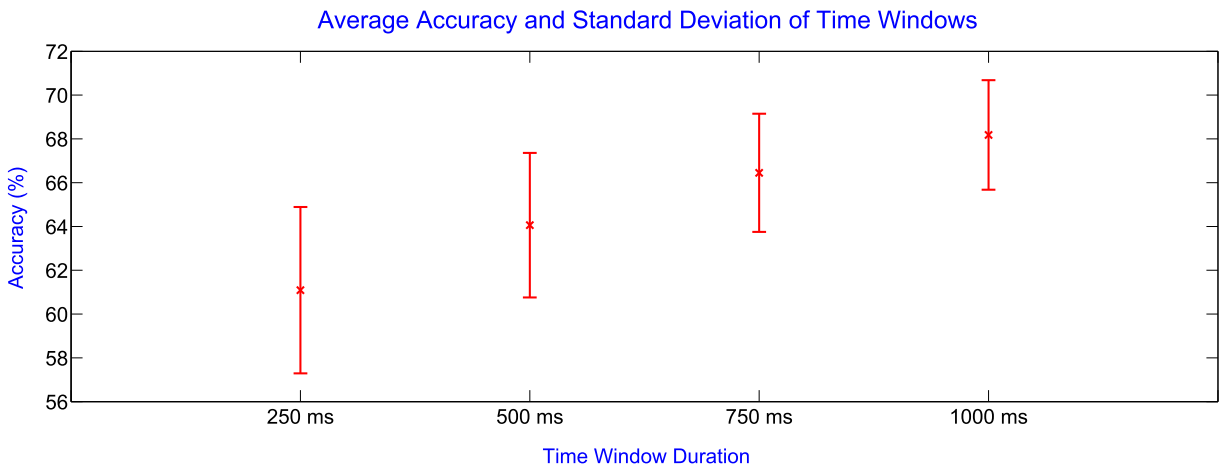


Figure 4.3. Mean and standard deviation of accuracies for different time windows . This figure compares the average and standard deviation for time window lengths of 250, 500, 750, and 1000 ms with the subject-independent classifier.

training data (subject-independent method) improved the average accuracy of the classifier for six subjects by 6.06% while, decreasing it by 2.34% for the other three. On average, training the classifier obtained with the subject-independent method improved the classifier accuracy by 3.26%.

4.3 Trade-off results

Table 4.2. Classification statistics for different window lengths. This table compares the mean, standard deviation, rise time (the time that it takes to reach to the maximum accuracy), maximum, and last accuracies of different time windows with 250, 500, 750, and 1000 ms length for the subject-independent classifier.

Window Length	First Accuracy(%)	Rise Time(ms)	Max. Accuracy(%)	Last Accuracy(%)	Mean Accuracy(%)	Std.
250	49	1000	67	60	61.09	3.8
500	54	900	71	62	64.06	3.3
750	61	1000	72.3	62	66.45	2.7
1000	65	750	72.9	64	68.16	2.5

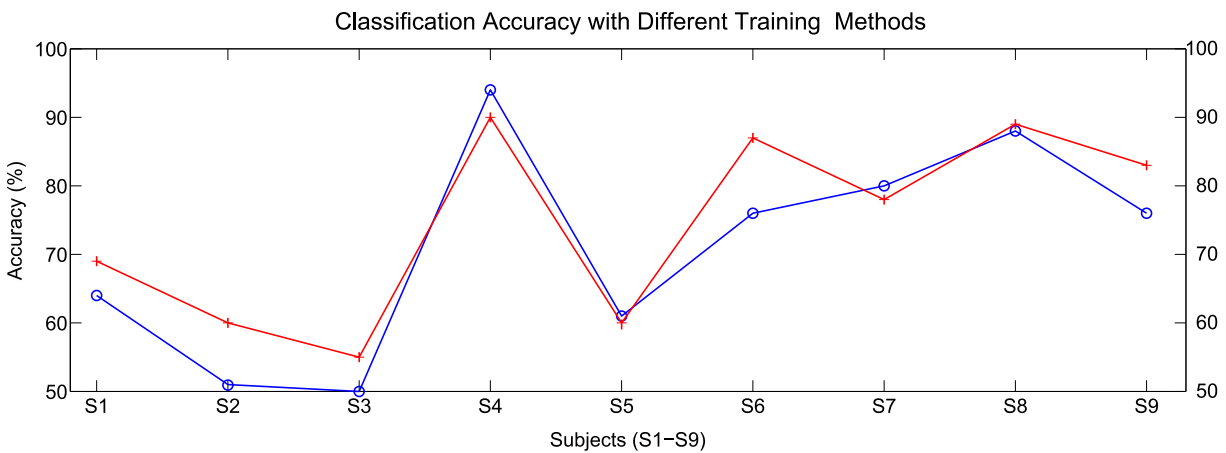


Figure 4.4. Comparison of accuracies for subject-dependent and subject-independent training methods. This figure demonstrates the performance of subject-dependent (blue line) and subject-independent (red line) classifiers in classification of subjects' test data. For most subjects the subject-independent classifier slightly outperforms its rival.

It is also worth mentioning that we examined the classifier performance when the entire subjects' training, as well as calibration (screening) data, were used. We hypothesized that the larger the training dataset, the better the training of the classifier and consequently, the higher its classification accuracy would be. Thus, we only used the first four-second part of each 4.5-second-long trial, because we wanted to make them similar to the calibration data trials, which were only 4 seconds long. However, when we trained the classifier based on the mentioned methodology, it turned out that its average accuracy with 10-fold cross validation was very close to chance (53%). Therefore, it is likely that the absence of feedback provision in the screening session

potentially made the recorded data of the screening session different to training session data. Thus, we decided to use only training data for classifier training based on the sub-optimal performance of the classifier where both training and calibration data were used.

4.4 A feasible trade-off

The main finding of our study is that whenever a part or whole of the time windows lies within the first 500 ms period of trials, accuracy is lower compared to the rest of the times as demonstrated in Fig. 4.2. This finding is in conformity with the literature (Grosse-Wentrup *et al.* 2009, Pfurtscheller *et al.* 2000, Pfurtscheller *et al.* 1999) showing that the EEG data recorded during the first 250–500 ms of motor imagery trials do not include discriminant information. This delay between modulation of the spectral power in the α and β bands and motor imagery onset may reflect the few hundred milliseconds of time that subjects need to recognize the visual stimulus and then perform the motor imagery.

The trends of the classification accuracy with all time windows show that after reaching a maximum value, which varies between 750 to 1000 ms after the trials onset for different time windows, the classification accuracy degrades towards the end of the trial. This behaviour might reflect the decrease in subject attention to the task as the trial continues. Also, it may be concluded that based on the accuracies provided by the 250 ms time window, the most particular time window is the 750–1750 ms period after the cue onset as this segment of the trials provides the highest classification accuracies.

Considering the optimum choice for time window length while taking into account the trade-off between its length and transient as well as stable accuracy levels, it seems that the 750 ms long time window is the optimum choice. It starts with 61% accuracy and ends with 62% while its mean value is 66.45% that is only 1.71% less than the average accuracy level of the 1000 ms window. Besides, the 750 ms time window allows the exploitation of the aforementioned particular period, i.e. 750–1750 ms period, in which the most distinctive features can be extracted.

Comparing the rehabilitation outcomes of stroke patients in the studies by Buch *et al.* and Shindo *et al.*, it appears that patients in the Buch *et al.* study had a more severe impairment in their affected hand's finger movement (no residual finger movement) compared to most patients in the Shindo *et al.* study, who had some residual motor

4.4 A feasible trade-off

function. Note that recovery in mild to moderate stroke patients is more likely than in more severely paralysed stroke patients (Oujamaa *et al.* 2009). Nonetheless, the role of providing ten times faster feedback in the Shindo *et al.* study, compared to the Buch *et al.* study cannot be ruled out and it may have affected the higher recovery level in the Shindo *et al.* study.

The classifier update rate for any BCI must be greater than the sum of data transfer time, signal processing time and the application delay (Wilson *et al.* 2012). Otherwise, the provided feedback is not real time that consequently degrades the performance of the BCI. Also, it has been explicitly indicated elsewhere (Oujamaa *et al.* 2009) that a 30 ms classifier update rate, is sufficient as the total required time for data transfer, signal processing and the application delay when recording data with four channels. This time (30 ms) is very close to the 32 ms that we used in this study as the classifier update interval. Wilson *et al.* (2012) used a typical home PC for data recording and signal processing, a 16 channel *gUSB amp* EEG amplifier, and the open source BCI2000 (Schalk *et al.* 2004) as their software platform. Thus, considering the accessibility of the hardware and software to any BCI laboratory, our suggested classifier update rate seems to be feasible and practical.

In the quest for the reason of the poor classification results when it was trained using both training and calibration data, we noticed that calibration data, due to lack of feedback provision, can be dissimilar to training data in which subjects received real-time visual feedback. In other words, while increasing the training dataset size may lead to improving classification accuracy, it only occurs when we provide consistent data for classifier training.

As for the possibility of increasing the classification accuracy, which plays a significant role in neuroplasticity (Grosse-Wentrup *et al.* 2011), it has been demonstrated in this study, that it is possible to increase the average accuracy level by using other healthy subjects training data. Thus, It might be feasible to use a similar approach to remove the calibration session for stroke patients and minimize the number of required sessions.

Last but not least, recent novel approaches such as transfer learning (Wang *et al.* 2015, Jayaram *et al.* 2016) for training subject-independent classifiers for BCI applications have been proposed. Transfer learning involves improvement of learning for novel users through investment on already learned tasks by previous users appears to have

the potential for further development of the reported results regarding the subject-independent classifier in this study. Moreover, a study to compare the classification trends with different time windows between healthy and stroke patient populations is out of scope of the present study, but may provide a topic for future investigation. Another topic for further investigation of the reported results may be a comparative study on performance of AR modelling and common spatial patterns to extract features for a subject-independent classifier.

4.5 Conclusion

This chapter has presented that a 750 ms long time window with a classification accuracy rate of 32 ms and an average classification accuracy of 67% may be adopted as a feasible model for therapeutic BCI applications. This model potentially provides patients with fast feedback that is likely to be critical for Hebbian learning and leads to greater functional recovery of stroke patients (Murphy and Corbett 2009).

Following the current study on signal processing aspects of restorative BCIs, in the next chapter, we investigate the effect of feedback modality on the performance of therapeutic BCIs.

Chapter 5

Feedback Modality Impact on Restorative Brain-Computer Interfaces

NEUROFEEDBACK training of sensorimotor oscillations related to motor imagery (MI) is used for motor restoration after stroke. However, knowledge concerning the impact of feedback modality on task-related cortical activity during operant learning is still scarce. Right-handed healthy subjects performed two tasks, i.e. MI and relaxation. Their sensorimotor desynchronization during MI or synchronization during relaxation was rewarded with contingent feedback. Feedback onset was delayed to study the cortical activity in the absence of feedback as well. The reward modality was alternated every fifteen trials between proprioceptive and visual feedback. It was found that proprioceptive input was superior to visual input to increase the range of task-related spectral perturbations in the α - and β -band, and was necessary to consistently achieve MI-related sensorimotor desynchronization (ERD) below the baseline. These effects occurred in task periods without feedback as well. The increased accuracy and duration of learned brain self-regulation achieved in the proprioceptive condition was specific to the β -band. Overall, it suggests that rewarding motor imagery with proprioceptive feedback facilitates fast operant learning of modulation of cortical oscillatory activity.

5.1 Introduction

When motor learning via physical practice (Doyon and Benali 2005, Halsband and Lange 2006) is compromised due to motor deficits following stroke, motor imagery (MI) may provide an alternative training modality (Boe *et al.* 2014, Halsband and Lange 2006). Motor imagery activates the sensorimotor system independent of actual movements (Gao *et al.* 2011, Szameitat *et al.* 2012) and might be facilitated by neurofeedback contingent on the event related changes in the oscillatory activities i.e. ERD/ERS (Bauer and Gharabaghi 2015, Vukelić and Gharabaghi 2015a). First studies applying neurofeedback in stroke rehabilitation to prime subsequent physiotherapy are promising with the largest clinical gains in the subacute patient population (Pichiorri *et al.* 2015). Oscillations in the β -band (15–30 Hz) over the sensorimotor cortex have particular relevance for this approach (Gharabaghi *et al.* 2014a, Gharabaghi *et al.* 2014c, Naros and Gharabaghi 2015) since they mediate the cortico-muscular communication during motor tasks (Boulay *et al.* 2011, Davis *et al.* 2012, Kilavik *et al.* 2013, Riddle and Baker 2005, Witham *et al.* 2011) and are linked to the extent of functional impairment after stroke (Rossiter *et al.* 2014).

Feedback may be provided via visual or proprioceptive input using brain-computer interfaces (BCI) or brain-robot interfaces (BRI), respectively (Bai *et al.* 2014, Bauer *et al.* 2015, Boe *et al.* 2014, Vukelić and Gharabaghi 2015a, Vukelic *et al.* 2014, Kraus *et al.* 2016). Functional electrical stimulation (FES) (Rushton 1997) is also implemented to provide feedback for motor rehabilitation following stroke (Daly *et al.* 2009). However, in this study we only study visual and proprioceptive feedback as FES has a long transition time after each stimulation and therefore, it is not possible to employ FES with rapid feedback update rates as required for our study. Feedback provision with a BCI setup for healthy subjects increased both laterality (Boe *et al.* 2014) and movement-associated desynchronization of the targeted β frequency band (Bai *et al.* 2014). Feedback provision with a BRI setup induced a distributed increase of corticospinal connectivity (Kraus *et al.* 2016), involved an extended cortical network including precentral, postcentral and parietal areas (Vukelic *et al.* 2014), and bridged the gap between individuals' abilities and cortical activation patterns for motor imagery and motor execution (Bauer *et al.* 2015). Moreover, a direct comparison between BCI and BRI feedback revealed that proprioceptive feedback was superior to visual feedback in activating a distinct cortical network resembling its activation during overt movement (Vukelić and

Gharabaghi 2015a). Furthermore, pairing MI-related cortical activity and afferent input increased the corticospinal excitability that is further evidence for the critical role of afferent input to improvement in task performance (Gharabaghi *et al.* 2014a, Mrachacz-Kersting *et al.* 2012, Niazi *et al.* 2012, Xu *et al.* 2014).

Physiological knowledge concerning the impact of feedback modality on operant learning of the MI task, i.e. brain self-regulation is, however, still scarce. A detailed exploration would necessitate a refined study design for disentangling the contribution of the task condition and the feedback modality, separately. Previous studies compared the cortical activity during the MI task with concurrent feedback (MI with feedback condition) to cortical activity during the relaxation task where no feedback was provided (relaxation without feedback condition). The observed differences might, therefore, be related to either the task or the feedback. A proper comparison would necessitate studying a relaxation condition with feedback and a MI task condition without feedback as well.

Moreover, particularly proprioceptive input, e.g. by passive movement, is known to modulate the ongoing cortical activity in itself in a similar way to MI, but independently of any volitional brain modulation (Muller-Putz *et al.* 2007, Pfurtscheller *et al.* 2002, Reynolds *et al.* 2015, Salenius *et al.* 1997). However, previous studies explored BCI/BRI related brain oscillations during the feedback period, which potentially clouds the MI-related cortical activity by the additional input of the feedback modality. Thus, knowledge on task-related cortical activity independent of the feedback period, i.e. during MI without feedback, is necessary. Additionally, feedback-independent modulation of MI-related cortical activity potentially indicates fast operant learning of modulation of intrinsic sensorimotor oscillations.

We, therefore, compared visual and proprioceptive feedback during either sensorimotor MI-related desynchronization or relaxation-related synchronization. Furthermore, we applied a delayed feedback onset paradigm to study the cortical activity over the sensorimotor cortex without feedback provision.

5.2 Experimental design

5.2 Experimental design

5.2.1 Ethics

The study conformed to principles outlined in the Declaration of Helsinki and was approved by the local human ethics committee of the University of Adelaide. All participants gave their written informed consent to participate in the study, and all recorded data were de-identified.

5.2.2 Participants

In this study, 10 participants (four females, six males) aged 24–40 years were recruited. Participants were asked to remain alert, immobile, and to concentrate during the trials. The different types of MI, i.e. visual and kinaesthetic MI, were explained to the participants, and it was explicitly stated that they were expected to perform kinaesthetic MI only. Participants were asked to minimize head and facial movements, swallowing, and blinking during the signal recording. They were given break periods to relax or move between consecutive runs when necessary.

5.2.3 Brain-interface system

For data acquisition, a 72-channel Refa TMSi EXG amplifier, containing 64 unipolar and eight bipolar channels, and a 64-channel Waveguard EEG cap were used. The EEG data were recorded from 8 channels (F3, F4, T7, C3, Cz, C4, T8, Pz) positioned according to the international 10-20 system of electrode placement. The AFz channel was used as the ground channel based on the recommendation of the manufacturer. The impedance between electrodes and the scalp was kept below 50 k Ω and this is sufficient due to the amplifier input impedance in the order of tera-Ohms (Volosyak *et al.* 2010). The amplifier does not require a reference channel as it uses built-in common average referencing of the recorded channels. It also disregards any electrodes with very high impedance (more than 256 k Ω) and excludes them from the common average reference. The signals were digitized at 1024 Hz and were then passed through a 50 Hz notch filter (3rd order Chebyshev) followed by a band pass filter (1st order Butterworth) with corner frequencies set to 0.1 and 49 Hz.

The BCI software was a customized version of the BCI2000 Cursor Task (Schalk *et al.* 2004). The source code was modified to provide auditory commands. The application module of the software was also modified to operate the orthoses.

Chapter 5 Feedback Modality Impact on Restorative Brain-Computer Interfaces

Two orthoses (one for each hand) were designed and installed on a laptop board to flex four fingers passively and recurrently following the MI of the target (right/left) hand. Each orthosis comprised a mechanical structure made of PVC and a Blue Bird BMS-630 servomotor. The control commands for servomotors were generated through the customized BCI2000 software and then translated to the servomotors of each orthosis using a Micro Maestro servo controller module. The Micro Maestro servo controller received an updated command simultaneously with every cursor update on the monitor. Fig. 5.1 depicts the elements of the fabricated orthoses.

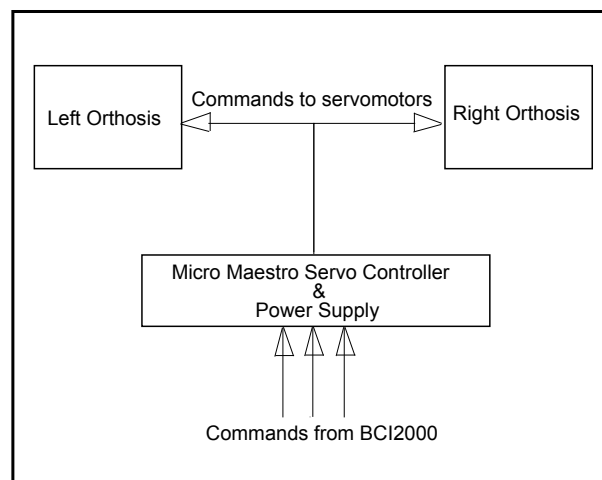


Figure 5.1. Orthoses. The orthoses comprise two mechanical parts that flex/extend left and right hand fingers and operate by two servomotors, independently. Servomotors are controlled by a Micro Maestro servo controller. The servo controller receives commands and returns the angles of the orthoses through an RS-232 connection with the application module of BCI2000 software.

5.2.4 Study design

Every participant attended two sessions: one screening session and one neurofeedback training session. During the screening sessions, the optimum features of the EEG that resulted in the highest discrimination between MI and relaxation trials of each participant were defined. Then the established optimum features of each participant's MI were used in the subsequent neurofeedback session. Eight out of ten participants (four females, four males) who had EEG signals with distinctive features during hand MI passed the screening test and attended the neurofeedback training session. Note that, each participant performed 60 trials, which is more than the required number of trials

5.2 Experimental design

that is usually used to calculate r^2 value for screening session (Guger *et al.* 2003, Pichiorri *et al.* 2011). However, for two participants r^2 values were very small (less than ; 0.05), indicating that they were unable to properly discriminate left/right hand imagery with relaxation trials in their first BCI session. Also, note that during the screening session only motor imagery without feedback was performed and no classification tasks were carried out. However, the data recorded during the feedback sessions were processed in real time to provide control signals that were used to drive either visual or proprioceptive feedback.

Note that MI periods are paralleled by feedback while relaxation periods are usually not. The impact of the concurrent feedback may potentially cause cortical activities uncorrelated with MI. To overcome this limitation, we chose a design that disentangles the MI and relaxation phases into two different tasks. Moreover, each of these tasks is performed with and without feedback. The former condition (with feedback) allows studying the effect of feedback modality on different tasks¹. The latter condition enables investigating the impact of the feedback pattern on operant learning of the brain self-regulation.

5.2.5 Screening session

Every participant attended a screening session in which three runs of right/left hand motor imagery were recorded. Each run included 20 randomized trials of motor imagery, ten of the left and ten of the right hand. Each trial started with an auditory command of “left” or “right” in parallel with a matching visual stimulus provided as an arrow pointing to the left or right. This arrow appeared in the centre of a monitor that was placed 1 metre away from the participant. The sound levels of the auditory commands were kept constant throughout the study. The arrow was shown for three seconds during which the participants were instructed to imagine finger flexion of the indicated hand. Then the arrow disappeared for three seconds; during this time the

¹It is believed that movement observation can also activate the brain similar to movement execution and motor imagery (Kilner and Lemon 2013). However, note that in Gazzola *et al.* (2007) it is explicitly mentioned that: “The mirror system was activated strongly by the sight of both human and robotic actions, with no significant differences between these two agents. Finally we observed that seeing a robot perform a single action repeatedly within a block failed to activate the mirror system. This latter finding suggests that previous studies may have failed to find mirror activations to robotic actions because of the repetitiveness of the presented actions.” Likewise, observing repetitive flexion of the free-running orthosis during the relaxation trials with a BRI condition is unlikely to activate the mirror neurons.

participants had to stop MI and concentrate on their breathing. The instruction to concentrate on breathing was given to ensure that (i) participants switch between MI and relaxation at the right time, and (ii) to provide participants with a tangible example of mental relaxation.

Previous studies (Pfurtscheller *et al.* 1997) demonstrated that performance of hand MI leads to a decrease in the spectral power of sensorimotor rhythms, i.e. event related desynchronization (ERD), followed by an increase in their spectral power, i.e. event related synchronization (ERS)². In most participants these phenomena occur in the contralateral sensorimotor area within the α (8–13 Hz) and β (18–26 Hz) frequency bands. Thus, MI of the right or left hand is expected to lead to ERD followed by ERS in channels C3 or C4, respectively. However, some participants exhibited concurrent ERD over both contralateral and ipsilateral hemispheres during MI (Pfurtscheller *et al.* 1997). With this in mind, we analysed the recorded data from the screening session of each participant. The spectral power of all 2-Hz-wide frequency bins within the α and β frequency bands was considered for analysis. The spectral power of the imagery and relaxation trials were compared to determine the combination of tasks that delivered the highest value of the coefficient of determination (r^2 , which determines how distinct the members of different classes are). Right vs. left hand MI often leads to the highest discrepancy in sensorimotor rhythms. However, we only selected right vs. relaxation and left vs. relaxation in this study to minimize the cognitive load and exhaustion level. Using r^2 as the measure, the optimum channels (considering C3 and C4) and the centre of the optimum frequency bins were selected for the neurofeedback sessions.

5.2.6 Participants' optimum features

After analyzing the screening session data, six participants (P1–P4, P7, P8) exhibited contralateral ERD, while two participants (P5, P6) revealed simultaneous ERD over both C3 and C4 channels (Table 5.1). For these two participants, spectral power was averaged across C3 and C4 channels during the training session.

²The occurrence of post imagery ERS was not explored here as (1) it is a well-established concept in the field, and (2) it was not in line with the goal of this study.

5.2 Experimental design

Table 5.1. Screening session results. Results of the screening session indicating the optimum side of imagined hand movement, channels and frequency bands for each participant, and number of runs performed in the following training session.

Participants	Side of imagined hand movement	Channels	Frequencies	Number of runs
P1	Left vs. Relax	C4	18 Hz	4
P2	Right vs. Relax	C3	13 Hz	4
P3	Right vs. Relax	C3	15 Hz	4
P4	Right vs. Relax	C3	17 Hz	8
P5	Right vs. Relax	C3, C4	15 Hz, 15 Hz	8
P6	Right vs. Relax	C3, C4	12 Hz, 18 Hz	4
P7	Left vs. Relax	C4	15 Hz	8
P8	Right vs. Relax	C3	15 Hz	8

5.2.7 Neurofeedback training session

The eight participants with discriminable EEG features were invited to return for an online feedback session within two weeks of their screening session. During the training session, four runs of MI of right/left hand four-finger flexion were performed. Those participants who were not exhausted participated in additional four runs (Table 5.1). Feedback modality (proprioceptive or visual) was interleaved over consecutive runs, and there was a 2-minute break between runs. Each run included 15 trials with eight or seven MI and seven or eight relaxation trials, respectively, which were sequenced randomly. Each trial started with an auditory command of “right” (“left” for P1 and P7) or “relaxation”. Participants were expected to perform MI or relaxation upon hearing the auditory command. No feedback was provided for the initial 2 s after the onset of the auditory stimulus. After this 2 s delay period, feedback was provided and updated every 24 ms for the following 2.5 s, followed by an audible “beep” signal, indicating the end of the trial. After a break of 4 s the next trial started. The chosen value for feedback update rate (every 24 ms) was adopted as the closest possible value to 20 ms as our proposed optimal value (Darvishi *et al.* 2013b). Fig. 5.2 illustrates the neurofeedback training time course.

Chapter 5 Feedback Modality Impact on Restorative Brain-Computer Interfaces

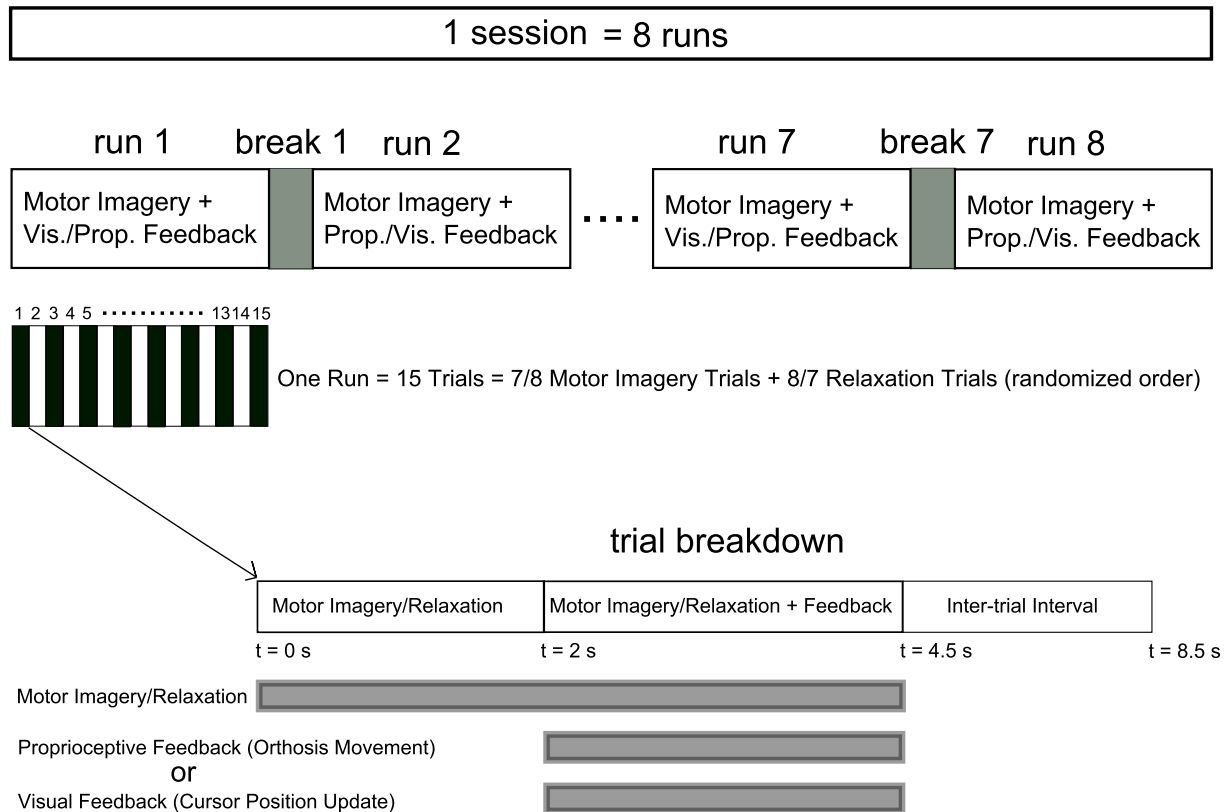


Figure 5.2. Time course of the neurofeedback training sessions. Each session comprised at least four runs (eight runs for P4, P5, P7, P8) with a 2 min break between runs. Each run included 15 trials with relaxation and imagery trial performed in a randomized order. The feedback modality was interleaved between visual and proprioceptive across consecutive runs. Each trial started with a 2 s interval of imagery/relaxation without feedback followed by a 2.5 s section during which real time visual or proprioceptive feedback was provided. Following a 4 s inter-trial interval the next trial started.

5.2.8 Signal processing

A large Laplacian (LLP) spatial filter was used to derive surrogate channels C3-LLP and C4-LLP. The maximum entropy method (MEM) (Marple 1987) was used to define the autoregressive (AR) model of the EEG data. Using a 20th order AR model, the spectral power of the most recent 500 ms was estimated at the subject-specific frequencies and electrode positions determined from the screening session. To minimize the occurrence of false positives in the classifier, the following normalization procedure was adopted: (i) the spectral power of the most recent 18 s period of imagery and relaxation trials (equally represented) were buffered and continuously updated. Equally representation of motor imagery and relaxation trials in the buffer means that 9s of

5.2 Experimental design

motor imagery and 9s of relaxation trials were buffered; (ii) the average and standard deviation of the buffer contents were calculated; (iii) every calculated spectral power component using the AR model was normalized by subtraction of the buffer's average followed by division of the buffer's standard deviation; (iv) if the normalized spectral power was negative, it was classified as ERD, whereas positive values were considered as relaxation. Normalized classifier outputs were used to update either the vertical velocity of the cursor on the monitor (visual feedback) or the flexion angle of the orthosis (proprioceptive feedback) every 24 ms.

5.2.9 MI+BCI

In runs with visual feedback, a red rectangle was displayed at the start of each trial as a target at either the upper or lower half of the right side of the monitor, simultaneously with auditory commands indicating "relaxation" or "right" ("left" for P1 and P7), respectively. After 2 s, a cursor was shown on the middle of the left side of the monitor to indicate the start of the feedback period. The cursor was then moved horizontally from left to right with a constant speed within the next 2.5 s. Every 24 ms (105 times in 2.5 s), the vertical position of the cursor was updated depending on the classification result. The cursor went up and down during ERS and ERD, respectively. After reaching the right side of the screen, either with a hit or miss of the target, the next trial started after a 4 s inter-trial interval.

5.2.10 MI+BRI

Participants sat in an armchair with their target hand placed on the orthosis (e.g., right hand on right orthosis) and their non-target hand placed on the armrest. For imagery trials ("right" or "left"), participants received proprioceptive feedback through congruent passive flexion of their target hand by the orthosis. For "relaxation" trials, participants received feedback by observing the flexion of the non-target orthosis with no hand engagement. This feedback design was intentionally chosen to overcome inherent limitations of providing real proprioceptive feedback for relaxation (see Section 5.4 for further details). In short, the BRI setup studied here was intended for stroke rehabilitation and thus had to avoid feedback that might lead to maladaptive conditioning. For simplicity, this condition will, however, be referred to as the BRI/proprioceptive

Chapter 5 Feedback Modality Impact on Restorative Brain-Computer Interfaces

condition as well in contrast to the BCI/visual condition where feedback for “relaxation” was provided by the position of a cursor. The auditory command, (i.e. “relaxation” or “right”/“left”), initiated the trial. After 2 s, the feedback period commenced by instantly returning the orthosis to the fully extended start position. Every 24 ms, the orthosis flexed, if ERD was detected (see Section 5.2.8), with up to 105 incremental flexions per 2.5 s feedback period. At the end of each feedback period, a “beep” signaled an inter-trial break and the next trial started after 4 s.

It is also worth mentioning that flexion/extension of the fingers of the target hand by the orthosis provided both proprioceptive and visual feedback, since the participants were instructed to observe their target hand movement during motor imagery. However, it was assumed that the proprioceptive feedback was the major modality in this paradigm and therefore was considered as ‘proprioceptive feedback’ throughout this chapter.

5.2.11 Offline spectral analysis

Offline spectral analysis of the EEG signals was performed with EEGLAB (Delorme and Makeig 2004) and custom-made Matlab scripts. Here, EEG signals were spatially filtered to derive C3-LLP and C4-LLP surrogate channels as in the online processing. For the two participants with the left hand as the target hand, C3-LLP and C4-LLP were swapped resulting in group-wide ‘contralateral’ and ‘ipsilateral’ channels. Channel data were bandpass filtered between 3 and 47 Hz using the `pop_eegfiltnew()` function of EEGLAB that employs a Hamming windowed sinc finite impulse response (FIR) filter. Next, they were resampled at 128 Hz. Channel data were then segmented into epochs from -2 to 4 s after the auditory command and each trial had its average baseline value subtracted. Outlier trials were automatically rejected using EEGLAB based on signal amplitude, variance, probability, and spectral power. In total, 4.1% of trials were rejected. For each retained trial, the spectral band power was integrated over two frequency bands: α (8–13 Hz) and β (16–26 Hz).

The spectral power for MI without feedback was calculated for 1 s during the delay period, i.e. in the interval from +1 to +2 s after the auditory command. Accordingly, the spectral power of MI with feedback was estimated for 1 s as well, i.e. from +3 to +4 s after the auditory command.

5.2 Experimental design

5.2.12 Performance measures

We employed the following indices to compare the effect of visual and proprioceptive feedback on MI performance with and without feedback: (i) accuracy, i.e. the percentage of trials in which the feedback conformed to the MI task, i.e. equivalent to the classical target hit rate in the cursor position update paradigm, (ii) ERD duration in imagery trials, i.e. the average percentage of times in each trial that the classifier output conformed to the MI task and moved either the orthosis (with BRI) or the cursor in the expected direction (with BCI). These measures were computed for the subject specific frequencies (Table 5.2) and were then re-calculated for α and β bands (Figs. 5.3–5.5).

To re-calculate accuracy, a 10-fold cross-validated linear discriminant analysis was used to classify trials as “relaxation” or “imagery”. Predictors included spectral power in contralateral, central and ipsilateral channels. The classification was performed separately for α and β power, and for visual and proprioceptive feedback. Time windows for the “without” and “with” feedback conditions were defined as 1–2 and 3–4 s, respectively.

To re-calculate ERD duration in α and β bands with and without feedback, the same time windows as for the accuracy (see above) were used. To simulate the real time situation, the spectral power of a 500 ms target window (shifting 24 ms at each step across the one-second time window) was calculated until the whole time window was swept. This methodology provided a collection of 42 (1000/24) spectral power data for each condition (relaxation/imagery). Then, using the z-scored values of all spectral data (both relaxation and imagery trials), the spectral data were normalized, and only negative values (indicating ERD) were counted. The resultants were divided by 42 and multiplied by 100 to determine offline ERD duration percentage for motor imagery trials.

5.2.13 Statistical analysis

GraphPad Prism version 6.05 was used for statistical analysis. For the accuracy and ERD duration with and without feedback, an unpaired Wilcoxon rank-sum test was applied for statistical analysis. Due to the application of multiple comparisons, Bonferroni correction was adopted.

Before statistical analysis, the spectral power in the α and β bands were normalized via calculation of their z-scores, resulting in intra-individual zero mean and unit variance spectral data. The normalized spectral data were subjected to repeated-measures 2-way ANOVA with factors Task (levels “relaxation” and “imagery”) and Feedback Modality (levels “proprioceptive” and “visual”) and two-sided t-tests (Holm-Sidak’s multiple comparison tests) for *post-hoc* comparisons. The statistical analysis of spectral data was performed separately for with and without feedback conditions.

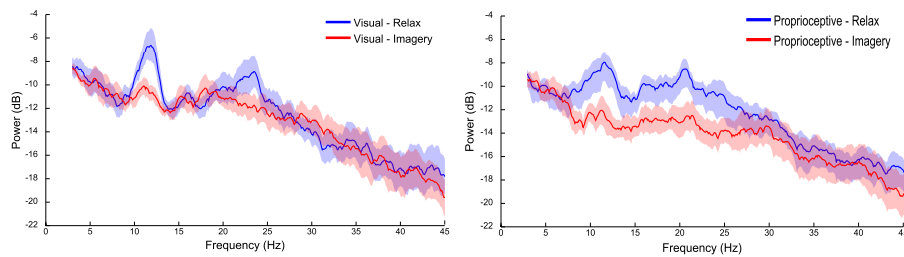
5.3 Comparing visual and proprioceptive feedback effects

5.3.1 Spectral analysis of MI with feedback

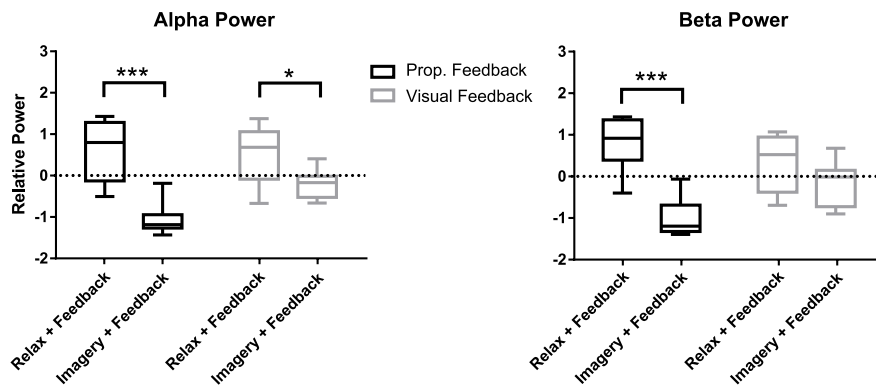
Fig. 5.3 illustrates the spectral power of the 3–4 s post-stimulus period in which either relaxation or motor imagery was performed with proprioceptive (BRI) or visual feedback (BCI). There were task-related changes in spectral power in the α and β bands (Fig. 5.3-A). Analysis of the α band revealed a significant main effect for task ($F(1,7) = 97.37, p < 0.0001$) and a significant interaction between task and feedback modality ($F(1,7) = 6.128, p = 0.0426$). The *post-hoc* test showed that during both proprioceptive and visual feedback there were significant differences between relaxation and imagery trials ($t(7) = 6.09, p = 0.0010$, and $t(7) = 2.59, p = 0.0358$, respectively). Moreover, feedback modality was indifferent for relaxation trials ($t(7) = 0.44, p = 0.6710$), whereas imagery trials produced significantly stronger ERDs with proprioceptive feedback than with visual feedback ($t(7) = 3.06, p = 0.0365$). Similarly, the β band showed a significant main effect for task ($F(1,7) = 62.76, p < 0.0001$) and a significant interaction between task and feedback modality ($F(1,7) = 10.23, p = 0.0151$). The *post-hoc* test between imagery and relaxation trials revealed a significant difference with proprioceptive feedback ($t(7) = 6.326, p = 0.0003$) but not for visual feedback ($t(7) = 1.803, p = 0.1145$). Investigation of the impact of feedback modality on the β power indicated that imagery with proprioceptive (BRI) and visual (BCI) feedback were significantly different ($t(7) = 2.94, p = 0.0429$), whereas relaxation trials showed no significant difference between feedback conditions ($t(7) = 1.582, p = 0.1576$). In summary, α ERD was facilitated by both feedback modalities with stronger impact of proprioceptive feedback; whereas β ERD was facilitated by proprioceptive feedback

5.3 Comparing visual and proprioceptive feedback effects

A. Power-Frequency Plots



B. Task Effect



C. Feedback Effect

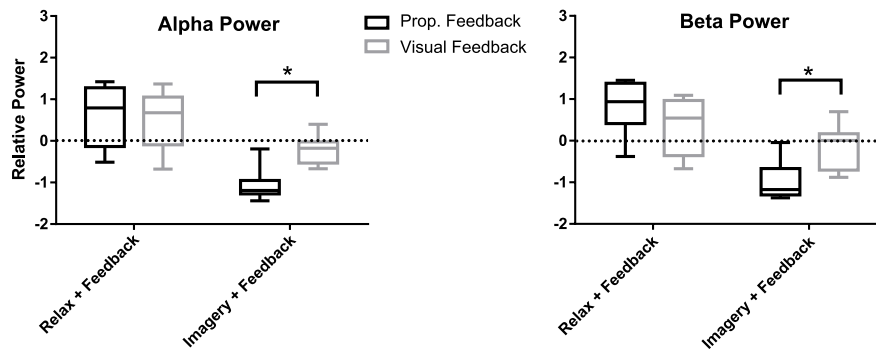


Figure 5.3. Spectral analysis of imagery and relaxation with feedback. Panel A illustrates the spectral power of imagery and relaxation trials during visual or proprioceptive feedback. The solid lines represent mean spectral power for each task and their circumscribing shaded area indicate the standard deviation. Panel B depicts task effect on the relative spectral power (z-scored) of imagery and relaxation trials with visual or proprioceptive feedback in α and β bands. Panel C shows feedback effect on the relative spectral power (z-scored) of imagery and relaxation trials in α and β bands with visual or proprioceptive feedback (*: $p < 0.05$; ***: $p < 0.001$).

only. In addition, proprioceptive feedback was essential to achieve ERD consistently below baseline across both α and β frequency bands ($t(7) = 9.017, p < 0.0001$ for proprioceptive feedback and $t(7) = 2.225, p = 0.1192$ for visual feedback).

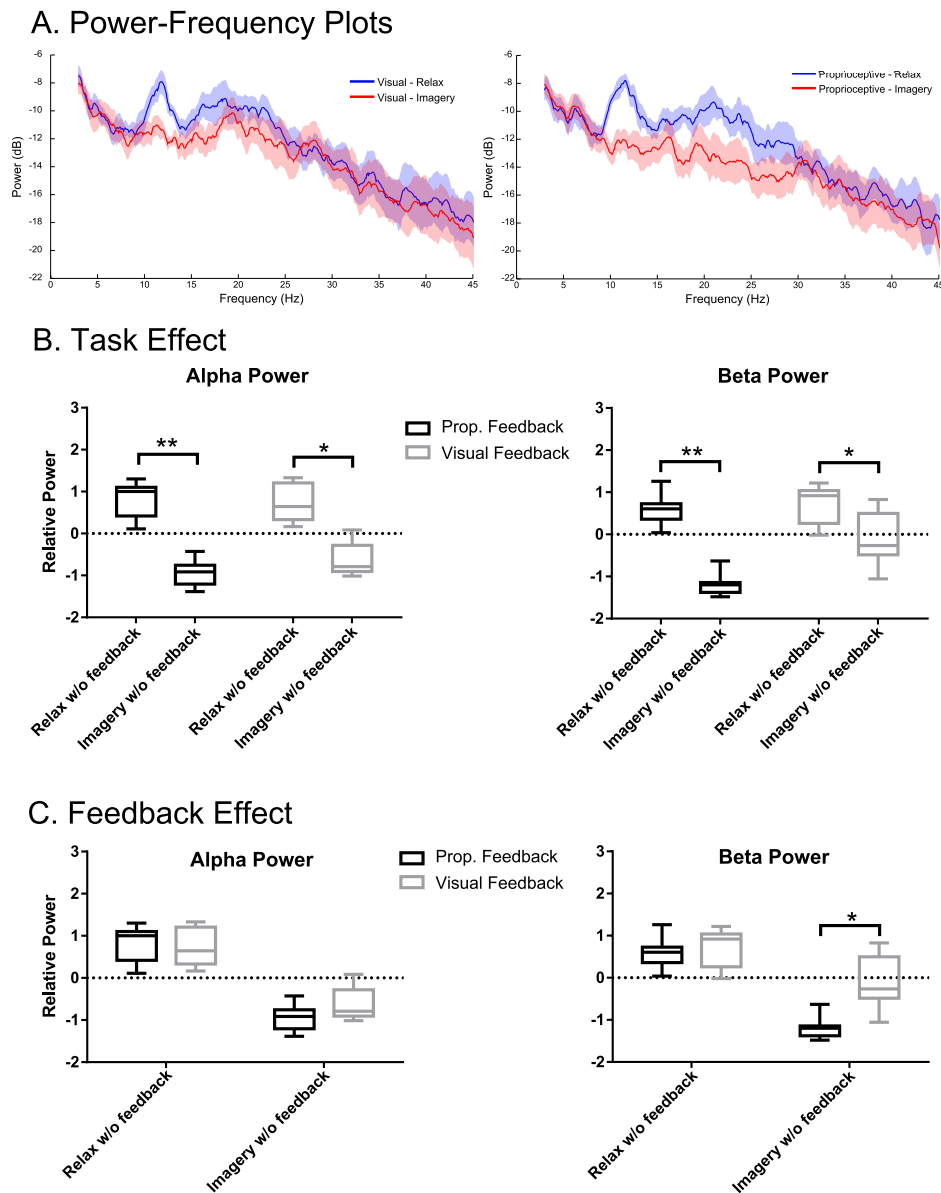


Figure 5.4. Spectral analysis of imagery and relaxation without feedback. Panel A illustrates the spectral power of imagery/relaxation trials without visual or proprioceptive feedback. The solid lines represent mean spectral power for each task and their circumscribing shaded area indicate the standard deviation. Panel B depicts task effect on the relative spectral power (z-scored) on imagery and relaxation trials without visual or proprioceptive feedback in the α and β bands. Panel C shows the persisting visual and proprioceptive feedback effects on the relative spectral power (z-scored) of imagery and relaxation trials in the α and β bands in the absence of visual or proprioceptive feedback (*: $p < 0.05$; **: $p < 0.01$).

5.3 Comparing visual and proprioceptive feedback effects

Table 5.2. Accuracy and ERD duration comparison. Comparison of subject-specific accuracy and ERD duration with and without visual/proprioceptive feedback.

Studied Conditions	Accuracy			ERD Duration		
	Visual	Proprioceptive	<i>p</i> -value	Visual	Proprioceptive	<i>p</i> -value
with feedback	75%	83%	0.0011	65%	75%	< 0.0001
without feedback	60%	75%	0.0027	63%	76%	0.0028

5.3.2 Spectral analysis of MI without feedback

Fig. 5.4 shows the spectral power from the 1–2 s period of the BRI and BCI conditions during which participants performed the task without feedback. Fig. 5.4-A depicts the spectral power in the α and β bands for each feedback modality. Analysis of the α band showed significant main effects only for task ($F(1,7) = 840.8, p < 0.0001$), but neither for feedback ($F(1,7) = 1.116, p = 0.3258$) nor interaction ($F(1,7) = 0.7129, p = 0.4264$). The *post-hoc* test showed that relaxation and imagery trials were significantly different for both BRI ($t(7) = 4.961, p = 0.0033$) and BCI ($t(7) = 3.767, p = 0.0140$) conditions. However, analysis of the β band power showed a significant main effect for both task ($F(1,7) = 79.68, p < 0.0001$) and feedback modality ($F(1,7) = 11.30, p = 0.0121$) but revealed no interaction between two factors ($F(1,7) = 4.869, p = 0.0631$). The *post-hoc* test between imagery and relaxation showed a significant difference for both the BRI ($t(7) = 5.994, p = 0.0011$) and the BCI condition ($t(7) = 2.87, p = 0.0478$). Comparing the effect of feedback modality on the β power revealed significant differences between conditions for motor imagery ($t(7) = 3.54, p = 0.0189$), but not for relaxation ($t(7) = 0.42, p = 0.69$). The findings indicate that in both BRI and BCI conditions sufficient α and β ERD was achieved, even prior to feedback onset. However, the BRI condition was superior to the BCI condition with regard to β band modulation. Similar to the situation “with feedback”, the BRI condition was essential to keep ERD consistently below baseline across both α and β bands ($t(7) = 12.00, p < 0.0001$ for the BRI condition and $t(7) = 2.831, p = 0.0501$ the BCI condition).

5.3.3 Accuracy and ERD duration for individual frequencies

Motor imagery performance with and without feedback was quantified using average accuracy, and the average percentage of ERD length in each trial. These measures were obtained through calculation of spectral power in each subjects’ optimum frequency

Chapter 5 Feedback Modality Impact on Restorative Brain-Computer Interfaces

according to their screening session. Results are summarized in Table 5.2 where medians of all studied measures and their corresponding p-values are reported. For motor imagery with feedback, accuracy was 8% higher for the proprioceptive compared to the visual feedback condition ($p = 0.0011$). The ERD duration was also longer with proprioceptive than with visual feedback by 10% ($p < 0.0001$). Considering motor imagery without feedback, the BRI condition was superior to the BCI condition for both the accuracy and ERD duration by 15% ($p = 0.0027$), and 13% ($p = 0.0028$), respectively.

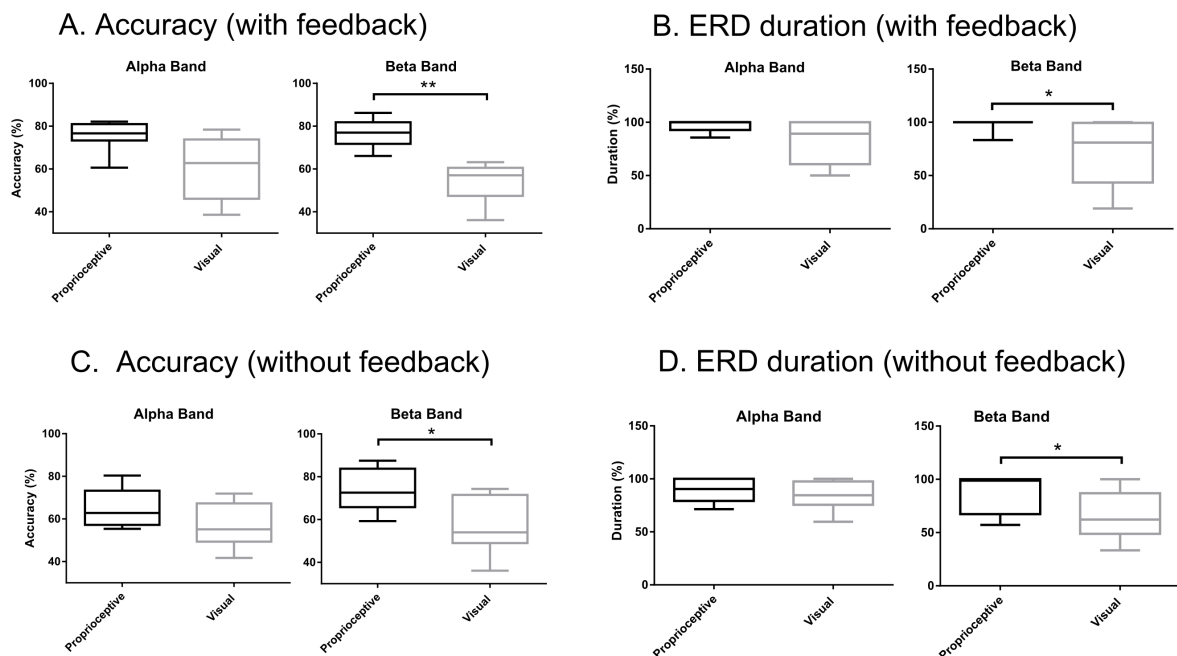


Figure 5.5. Accuracy and ERD duration with and without feedback. (A): Classification accuracy with visual or proprioceptive feedback in the α and β band. (B): Event-related desynchronization (ERD) duration with visual or proprioceptive feedback in the α and β band. (C): Classification accuracy without visual or proprioceptive feedback in the α and β band. (D): ERD duration without visual or proprioceptive feedback in the α and β band (*: $p < 0.05$; **: $p < 0.01$).

5.3.4 Accuracy and ERD duration for the α and β bands

Fig. 5.5 depicts the accuracy and duration of ERD with (4A–4B) and without feedback (4C–4D) in α and β bands. Trial task (“Imagery” vs. “Relaxation”) was classified by linear discriminant analysis using band-power in three channels (ipsilateral, Cz,

5.4 Feedback modality impact on modulation level and operant learning

and contralateral), separately for the α and β bands, and separately for proprioceptive and visual feedback. According to the paired Wilcoxon rank-sum tests, BRI accuracy was superior to BCI accuracy for the β band with ($p = 0.0078$) and without feedback ($p = 0.0234$). Similarly, ERD duration was longer for the BRI as compared to the BCI condition for the β band with ($p = 0.0313$) and without feedback ($p = 0.0156$). In summary, there was a significantly different behavioural impact for BRI and BCI with regard to accuracy and duration of ERD specific to the β band.

5.4 Feedback modality impact on modulation level and operant learning

This study demonstrated that MI and BRI training, i.e. providing proprioceptive feedback, were superior to MI and BCI training, i.e. providing visual feedback, to increase the spectral modulation range in the α - and β -band. Moreover, proprioceptive feedback was necessary to achieve consistently MI-related ERD significantly below the baseline. These effects on both the modulation level and MI-related ERD persisted, even in the absence of feedback, thereby indicating fast operant learning of oscillatory self-regulation. The increased accuracy and duration of learned brain self-regulation achieved in the proprioceptive feedback condition was mediated in the β band.

5.4.1 Feedback modality and oscillatory modulation level

The modulation level of the power in the α and β bands was influenced by the feedback modality. The power in the α band, which typically reflects sensorimotor activation and visual information processing (Pfurtscheller 2001), was modulated by both visual and proprioceptive feedback, with stronger effects of the latter (Fig. 5.3-B left). By contrast, the power in the β band, which is thought to be associated with cortico-muscular communication (Miller *et al.* 2010, Schulz *et al.* 2014, Takemi *et al.* 2013a, Takemi *et al.* 2013b) during MI (Kilavik *et al.* 2013) and actual movement (McFarland *et al.* 2000), required proprioceptive input for modulation (Fig. 5.3-B right). This significant feedback effect on the modulation range of both the α and β bands was caused by the proprioceptive input on the MI task and not on the relaxation task (Fig. 5.4-C). Task-dependency of the feedback effect on cortical activity may be interpreted as follows: (i) The feedback during the relaxation task was visual in both conditions, i.e. observing

cursor movement vs. orthosis movement (with no hand involvement). Providing real proprioceptive feedback during the relaxation trials, instead of a modified version of visual feedback (observing orthosis movement), might have resulted in power changes in comparison to the visual feedback condition (observing cursor movement). (ii) The relaxation task might, in general, be insensitive to the feedback modalities applied in this study. (iii) The proprioceptive input might reveal its effects on cortical physiology during specific brain states only, which is especially receptive to afferent input, e.g. sensorimotor desynchronization. Note that providing proprioceptive feedback during relaxation, i.e. sensorimotor synchronization, might lead to maladaptive changes and may thus be contraindicated from a motor restoration perspective. Notably, proprioceptive feedback was essential to achieve consistently MI-related sensorimotor ERD significantly below baseline in both α and β bands. Thus, it suggests that coupling proprioceptive feedback with MI provides a better substrate for closing the sensorimotor loop than visual feedback only. This finding is particularly relevant for future rehabilitation applications as ERD has been suggested as a biomarker for corticospinal excitability which is mediated via down-regulation of intracortical inhibition in the human primary motor cortex (Takemi *et al.* 2013a, Takemi *et al.* 2013b). Furthermore, the amount of β ERD during a BRI task has been shown to correlate with robust increases in corticospinal excitability following the intervention (Kraus *et al.* 2016). In this context, the present study revealed that rewarding motor imagery with contingent proprioceptive feedback will result in stronger (Fig. 5.3-C) and longer lasting β ERD (Fig. 5.5-B), compared to visual feedback only, and might, therefore, be especially relevant for restorative approaches.

5.4.2 Feedback modality and operant learning

The participants of this study regulated their brain oscillations in both the α and β bands even in those task periods in which they did not receive any feedback. This finding might be interpreted in different ways: At first glance, this result might suggest that (i) no feedback at all was necessary to achieve brain self-regulation. However, such a notion would be challenged by several other observations of this study. (ii) The oscillatory modulation range was relatively larger in the BRI than in the BCI condition (Fig. 5.4-B). Since the BRI and BCI conditions of this study were alternating from run to run, i.e. every fifteen trials, such a finding would most likely be related to the feedback modality within one run. (iii) Moreover, the ERD remained consistently below

5.4 Feedback modality impact on modulation level and operant learning

baseline only in the BRI condition. (iv) There was a significant difference between the β ERD levels of the BRI and the BCI condition with stronger desynchronization in the former (Fig. 5.4-C). We interpret these converging findings, therefore, as evidence for fast operant learning of oscillatory self-regulation with a stronger impact of the BRI condition.

Operant conditioning of neural activity was initially demonstrated in animal models (Engelhard *et al.* 2013, Fetz 2007, Fetz 1969, Ganguly and Carmena 2009, Hiremath *et al.* 2015). In humans, the reinforcement learning of self-regulated changes in cortical activity is usually acquired after several training sessions (Boe *et al.* 2014, Florin *et al.* 2013, Kaiser *et al.* 2014). The fast learning in the present study might be due to different reasons: The delayed feedback onset design may have facilitated brain self-regulation by (i) providing the participants with a preparation period for ramping volitional oscillatory modulation (Donoghue *et al.* 1998, Fetz 2013), and/or (ii) increasing their reward expectation (Leon and Shadlen 1999, Savage and Ramos 2009) during the 2 s lag. Moreover, the interleaved feedback design, switching every 15 trials between proprioceptive and visual feedback, might have caused (iii) sustained attention levels (Lorenz *et al.* 2014) and/or provided (iv) sufficient novelty to keep up motivation; a moderate level of novelty during learning has been shown to correlate with the highest level of motivation (Heckhausen and Heckhausen 2008). Finally, applying a particular relaxation task that is (v) rewarded by feedback as well appears to be more able to enhance the modulation of the oscillatory range than a relaxation condition without feedback.

However, even within such an optimized environment for operant learning, the feedback modality seems to play a relevant role, suggesting that the BRI condition may provide a better mean for self-regulation of sensorimotor rhythms than the BCI condition.

5.4.3 β band and the sensorimotor loop

Optimum frequencies for which participants received feedback, lay within 12–18 Hz frequency band (Table 5.1). However, subjects modulated their brain oscillations in both the α and β bands. This might be unexpected at first glance, because successful neurofeedback is known to be frequency-specific (Florin *et al.* 2013, Naros and

Gharabaghi 2015, Zoefel *et al.* 2011, Reynolds *et al.* 2015). However, it has to be considered that this previous frequency-specificity was achieved in the course of several sessions while the current intervention lasted for one session only. Moreover, the feedback modality was alternated in the present examination, while it remained unchanged in previous studies. Furthermore, recent findings suggest that neurofeedback may not only reinforce the feedback frequency band itself but may be related to different cortical oscillations as well, thus, suggesting cross-frequency interactions. More specifically, a distributed α network has been shown to regulate the local sensorimotor β activity in a performance dependent way, i.e. with good and poor performers of β band brain-self-regulation revealing different extents of α network lateralization (Vukelic *et al.* 2014). Along the same lines, a single neurofeedback session that rewarded spatially selective and spectrally distinct cortical activities with proprioceptive feedback modulated the connectivity of distributed resting state networks of the sensorimotor cortex in different frequency bands (Vukelic and Gharabaghi 2015b). The reported finding of Vukelic and Gharabaghi (2015b) is particularly relevant for new rehabilitation strategies, since resting state functional connectivity of the motor cortex seems to be of interest for motor learning (Mottaz *et al.* 2015) and for prediction of functional improvement after stroke (Nicolo *et al.* 2015).

In the present study, the feedback modality had a behaviourally relevant impact, as well, by improving the online classification accuracy and duration of brain self-regulation in the proprioceptive as compared to the visual condition (Table 5.2). Importantly, the BRI condition allowed the subjects to achieve accuracies more than 70% even when no feedback was provided, a level which is regarded as the threshold for gaining a sense of self-efficacy during operant learning in brain-interface procedures (Kubler *et al.* 2001). Analysing the α and β bands separately (Fig. 5.5) revealed the relevance of the latter for mediating these performance gains. These findings are in line with the current literature indicating that β band oscillations mediate the cortico-muscular communication (Boulay *et al.* 2011, Davis *et al.* 2012, Kilavik *et al.* 2013, Riddle and Baker 2005, Witham *et al.* 2011), sensorimotor control (Boulay *et al.* 2011, Brittain *et al.* 2014) and motor learning (Herrojo Ruiz *et al.* 2014, Pollok *et al.* 2014). Accordingly, recent proof of concept data indicated that operant conditioning of β band ERD will lead to task-specific motor improvement after stroke (Naros and Gharabaghi 2015) and also suggests the suitability of this biomarker for state-dependent stimulation (Gharabaghi *et al.* 2014a) and restorative neuroprosthetics (Gharabaghi *et al.* 2014b, Gharabaghi *et al.* 2014c) in the context of motor rehabilitation after stroke.

5.5 Limitations of the study

Also, note that all reported results have been made based on the specific visual and proprioceptive feedback that were adopted in this study. Therefore, care must be taken in generalizing the findings of this study results when other forms of visual feedback such as virtual reality, real-time fMRI, and, real-time EEG topographic map are involved.

5.5 Limitations of the study

- In this study participants were discarded from the study based on an *add-hock measure*, i.e. if they could not produce r^2 values greater than 0.05 after 60 MI trials, which reflected that they were not able to discriminate between imagery and relaxation trials, they were excluded.
- Instead of exclusively working with the right hand, in this study the hand that its motor imagery elicited the stronger ERD was chosen. However, stroke patients mostly have a unilateral brain injury and therefore this strategy would not be applicable to them.
- In this study being right-handed was self-declared and no specific test such as Edinburgh handedness inventory was adopted to double check whether or not participants were right handed.

5.6 Conclusion

This chapter has presented empirical evidence that proprioceptive feedback facilitates fast operant learning of brain self-regulation. Reinforcing β -band ERD in a BRI environment may provide a suitable approach for enhancing the sensorimotor loop for rehabilitation.

Following the investigation of feedback modality effect on the performance of restorative BCIs in the current chapter, we will proceed with exploring the impact of feedback update interval on the performance of therapeutic BCIs in the next chapter.

Chapter 6

Feedback Update Interval Impact on Brain-Computer Interfaces

FEEDBACK optimization is believed to enhance the performance of motor imagery based brain-computer interfaces (MI-BCI). Many studies have investigated the effect of feedback modality on MI-BCIs. However, the impact of feedback update interval (FUI) modification on MI-BCI performance remains unexplored. We hypothesized that: (i) information processing speed and BCI aptitude are correlated; and, (ii) the FUI modification affects BCI performance depending on subjects' information processing speed. Thus, in this chapter we investigate the effect of FUI change on ten healthy participants who were dichotomized as good and poor imagers according to their online BCI accuracy. They attended two BCI training sessions with 16 ms and 96 ms FUIs. Simple reaction time (SRT) measure that was recorded as an index of information processing speed was found to be a surrogate for BCI aptitude with 70% accuracy. Also, it was illustrated that for good imagers 16 ms FUI provided higher BCI accuracies whereas poor imagers showed better performance with 96 ms FUI. Overall, this preliminary study suggests that FUI customization may improve the performance of MI-BCIs and may also have implications towards addressing BCI-illiteracy challenge.

6.1 Introduction

Motor imagery based brain-computer interfaces (MI-BCIs) translate movement imagination to commands readable by a machine or robot. Thus, MI-BCIs can provide artificial communication channels for locked-in-syndrome patients who are not able to communicate naturally (Birbaumer *et al.* 2008). Note that MI-BCIs are also used for therapeutic applications such as rehabilitation of motor functions after a stroke (Prasad *et al.* 2010). While preliminary results of MI-BCI applications in these areas are promising, their dissemination necessitates enhancement of their reliability and accuracy (Wolpaw and Wolpaw 2012b).

To improve the accuracy of MI-BCI two main areas for optimization are currently explored: In the machine learning area, the research focus is on the enhancement of feature extraction and classification algorithms (Bashashati *et al.* 2015, Muller-Putz *et al.* 2007, Pradeep *et al.* 2006). User-centred learning strategies, which enable human agents to provide their best possible signals, shape the other area of interest (Lotte *et al.* 2013, Perdikis *et al.* 2014). One main direction in user-centred BCI enhancement is feedback optimization (Huggins *et al.* 2014, Jeunet *et al.* 2014, Lotte and Jeunet 2015). Motor imagery and motor execution of a specific task activate the brain similarly (De Vries and Mulder 2007). Following movement onset in motor execution, sensory and visual feedbacks are provided recurrently to close the sensorimotor loop and complete the proposed function successfully (Magill 2014). Similarly, in MI-BCI setups artificial feedback is delivered recurrently to supply updated knowledge of performance and enhance motor imagery quality. Visual feedback is the most common feedback modality in MI-BCI designs that is provided through cursor position updates on a monitor (Bai *et al.* 2008, Prasad *et al.* 2010). Alternative modalities include proprioceptive feedback via a robot/orthosis (Ramos-Murguialday *et al.* 2012). To investigate the effect of feedback modality on MI-BCI performance a number of previous studies have been conducted (Darvishi *et al.* 2015a, Jeunet *et al.* 2015, Ramos-Murguialday *et al.* 2012, Vukelić and Gharabaghi 2015a). Several studies have suggested that proprioceptive feedback enhances MI-BCI performance compared to visual feedback realization (Darvishi *et al.* 2015a, Jeunet *et al.* 2015, Vukelić and Gharabaghi 2015a).

A further parameter within the user-centred learning strategies that may potentially improve the performance of BCIs, which has been largely unexplored, is the feedback update interval (FUI). As discussed in Chapter 2, there is a growing body of evidence (Kraus *et al.* 2016, Naros *et al.* 2016) suggesting that Hebbian plasticity may play a

role in BCI training. Therefore in this study we aim to explore whether FUI customization affects Hebbian learning and thereby create a synergy with operant conditioning during BCI training. While during motor execution FUI is adjusted continuously through transmission of the efferent motor and afferent sensory information along the sensorimotor loop, there is no established guideline for this parameter in MI-BCIs. Operating MI-BCIs is largely a cognitive task that involves sequential motor planning and feedback realization in a closed loop fashion. Reaction time tests, however, measure how a person interacts with the performance environment while preparing to produce a required action (Magill 2014). Thus, we hypothesized that: (i) reaction time, as a surrogate for information processing speed, is correlated with each individual's BCI performance, and (ii) the FUI customization according to each person's reaction time improves their BCI performance. Notably, for people with short reaction times MI-BCI performance is improved with a short FUI while a longer FUI is more suitable for their slower counterparts.

To investigate these hypotheses, we recruited 10 participants and measured their simple reaction time (SRT) as an index of their speed of information processing. Then, we studied their online BCI performance and brain activation patterns where they attended two BCI training sessions with proprioceptive feedback that had different FUIs in a crossover design.

6.2 Experimental setup

6.2.1 Participants

Ten healthy participants (six males) aged 18–26 years were recruited in this study. The study was approved by the local human ethics committee of the University of Adelaide, and all participants gave their written informed consent to participate in the study.

6.2.2 BCI system

A 72 Channel Refa TMSi EXG amplifier, with 64 unipolar and eight bipolar channels and a 64 channel Waveguard EEG cap were used. The EEG data were recorded only from small Laplacian combination of the channels centred on either C3 or C4 channel.

6.2 Experimental setup

The ground channel was connected to the participants target hand using a wristband. The impedance between electrodes and the scalp was kept below 20 k Ω . The EMG data of the finger flexor muscles of the target hand was recorded using a bipolar channel of the EXG amplifier. The amplifier uses a built-in common average reference (CAR) of the recorded channels and thus does not require a reference channel. The amplifier excludes any unipolar channels with impedances more than 256 k Ω from the common average reference calculation. It also does not consider the bipolar channel used for EMG recording in common average referencing of EEG signals. All EEG and EMG signals were digitized at 1000 Hz and then were passed through a 50 Hz notch filter (3rd order Chebyshev) followed by a high pass filter (1st order Butterworth) with corner frequency set to 0.1 Hz.

To provide the proprioceptive feedback two orthoses were mounted on a platform to serve either the right or the left hand. They passively flexed fingers of the involved hand according to the motor imagery of the target hand. Each orthosis was driven by a Blue Bird BMS-630 servomotor. The commands to operate the orthoses originated from a customized software and then using a Micro Maestro servo controller module were translated to the servomotors.

A customized version of the BCI2000 (Schalk et al., 2004) Cursor Task was used to record the data and run the online experiments. The source code was customized to provide auditory commands and to update the position of the servo motors.

6.2.3 Study design

The data used in the current study are part of a larger study we conducted to investigate the effect of user-centred strategies on BCI performance. In the mentioned crossover study, each of 10 participants attended one screening session followed by six online BCI sessions under different conditions. The six adopted conditions were 1) proprioceptive feedback with FUI of 16 ms, 2) proprioceptive feedback with FUI of 24 ms, 3) proprioceptive feedback with FUI of 48 ms, 4) proprioceptive feedback with FUI of 96 ms, 5) visual feedback, and, 6) No imagery (control condition). The order of different conditions were randomized to compensate for training and fatigue effect over the consecutive sessions of BCI training. The data for the current study have been derived from two of those six conditions in which participants performed MI-BCI and

received proprioceptive feedback that updated every 16 ms and every 96 ms, respectively. We assumed that any potential effect of FUI alteration becomes clear when in one condition feedback is updated six times faster than the other. In the rest of the manuscript, for simplicity, FUIs of 96 and 16 ms will be regarded as “long FUI” and “short FUI”, respectively.

6.2.4 Screening session

In the screening session, the subjects were asked to perform three runs of left and right hand motor imagery according to the visual and auditory instructions. Each run included 20 trials of right/left hand imagery in a randomized order where each trial lasted for 3 s and was followed by 3 s of relaxation. Thus for each subject 60 trials was performed during the screening session³. For each subject, the frequency within 8–30 Hz frequency band that maximized the spectral power discrepancy between the motor imagery of right or left hand and relaxation trials were defined. To minimize cognitive load due to the planned therapeutic application of the BCI design, only right vs. relaxation and left vs. relaxation combinations were considered. Thus, the screening session provided the optimum frequency and the optimum combination of tasks (either right vs. relax or left vs. relax) for each subject. Also according to the selected imagery task (right or left hand movement), the contralateral channel over the hand representation of the sensorimotor area was chosen (C3 or C4 channels). For all participants except participant P3, right vs. relax found to provide larger differences compared to left vs. relaxation. For all participants except P3, channel C3 and its closest neighbours (FC3, CP3, C5, and C1) were recorded to provide small Laplacian combinations. For P3 with left vs. relax as their selected tasks, EEG signals were recorded from C4 and its small Laplacian combination (FC4, CP4, C6, and C2). Table 6.1 summarizes participants selected features.

³As it was discussed in Chapter 5, our adopted number of trials for the screening session is larger than similar studies (Guger *et al.* 2003, Pichiorri *et al.* 2011). Therefore, while we cannot reject the possibility of changing EEG patterns with larger number of trials, it appears that sufficient number of trials have been performed during the screening session.

6.2 Experimental setup

Table 6.1. Screening session results. Results of screening session to define the optimum tasks, channels and frequency bands for each individual.

Participants	Imagery type	Channels	Frequencies
P1	Right vs. Relax	C3	20 Hz
P2	Right vs. Relax	C3	25 Hz
P3	Left vs. Relax	C4	23 Hz
P4	Right vs. Relax	C3	15 Hz
P5	Right vs. Relax	C3	21 Hz
P6	Right vs. Relax	C3	11 Hz
P7	Right vs. Relax	C3	17Hz
P8	Right vs. Relax	C3	11Hz
P9	Right vs. Relax	C3	15Hz
P10	Right vs. Relax	C3	15Hz

6.2.5 Online training session

Each online session comprised eight runs of MI of right/left hand finger flexion. Each run included 20 trials with ten motor imagery and ten relaxation trials presented with a randomized order. Each run took almost four minutes, and consecutive runs had a 2-minute break in between where each recording took less than an hour. Sessions were scheduled using BCI2000 Operator scripts that determined runs operation and the breaks between consecutive runs.

Every trial started with a “start” auditory command that prepared the participant for the following instruction. After 3 s, another auditory command instructed the participant to either relax or perform motor imagery of right hand finger flexion. After another 3 s, the participant was able to receive contingent feedback according to their motor imagery or relaxation as follows. For “right” auditory command the right orthosis briskly initialized the right hand’s fingers to fully extended position. Then within the next 2.5 s, the orthosis was able to flex the right hand’s fingers incrementally if motor imagery classification result was smaller than a threshold value. However, if the command was “relax”, the free running left orthosis was immediately initialized to fully extended position. Then it could be flexed incrementally within the next 2.5 seconds if the classification result was larger than a threshold value. Note that the threshold value is defined according to the pooled average spectral power of motor imagery and relaxation trials within the most recent 18 seconds. Next, an auditory

‘stop’ command cued the end of each trial and after a subsequent 4 s inter-trial interval, the next trial started. Note that each participant’s left hand was on the arm rest and not placed on the left orthosis. As a result, participants received proprioceptive feedback for right hand imagery and visual feedback through observation of the left orthosis flexion on relaxation. For participant P3, however, his left hand was involved with the left orthosis while his right hand was resting on the armrest. Thus, participant P3 was supplied with proprioceptive feedback for left hand imagery and visual feedback of relaxation through the right orthosis. Fig. 6.1 illustrates the training sessions time course.

6.2.6 Online signal processing

To enhance the spatial resolution of EEG signals a small Laplacian (SLP) transform⁴ was used to filter C3 channel (C4 for participant P3). Then a 20th order autoregressive model of the EEG signal was created using Burg method (Marple 1987). Next, according to each participant’s selected frequency and electrode (C3-SLP or C4-SLP), the spectral power of the autoregressive model in the most recent 500 ms was calculated. A linear transform, which was created based on the screening sessions results for each participant, was applied to the estimated spectral power to provide classification outputs. The outputs were normalized using an adaptive normalization procedure to compensate for the effect of EEG non-stationariness. For normalization, data were transformed to become zero mean and unit variance using contents of a buffer that was continuously filled with the most recent 18 seconds of imagery and relax trials (equally represented). Equation 6.1 illustrates the normalization procedure. Here, ‘Out’ refers to the raw classifier output, ‘NorOut’ is the normalized output, while ‘Aver’, and ‘STD’ are the average and standard deviation of the classifier outputs within the most recent 18 seconds, respectively

$$\text{NorOut} = \frac{\text{Out} - \text{Aver}}{\text{STD}}. \quad (6.1)$$

Normalized outputs were used to flex the target orthosis for 0.4 and 2.4 degrees with the short and long FUIs, respectively. Note that the flexion angle for 96 ms condition

⁴Even though a large Laplacian slightly outperforms a small Laplacian, they are both commonly used strategies for deblurring EEG signals. Since channel C5 of our EEG cap became disconnected, the small Laplacian was chosen over the large Laplacian in this study.

6.2 Experimental setup

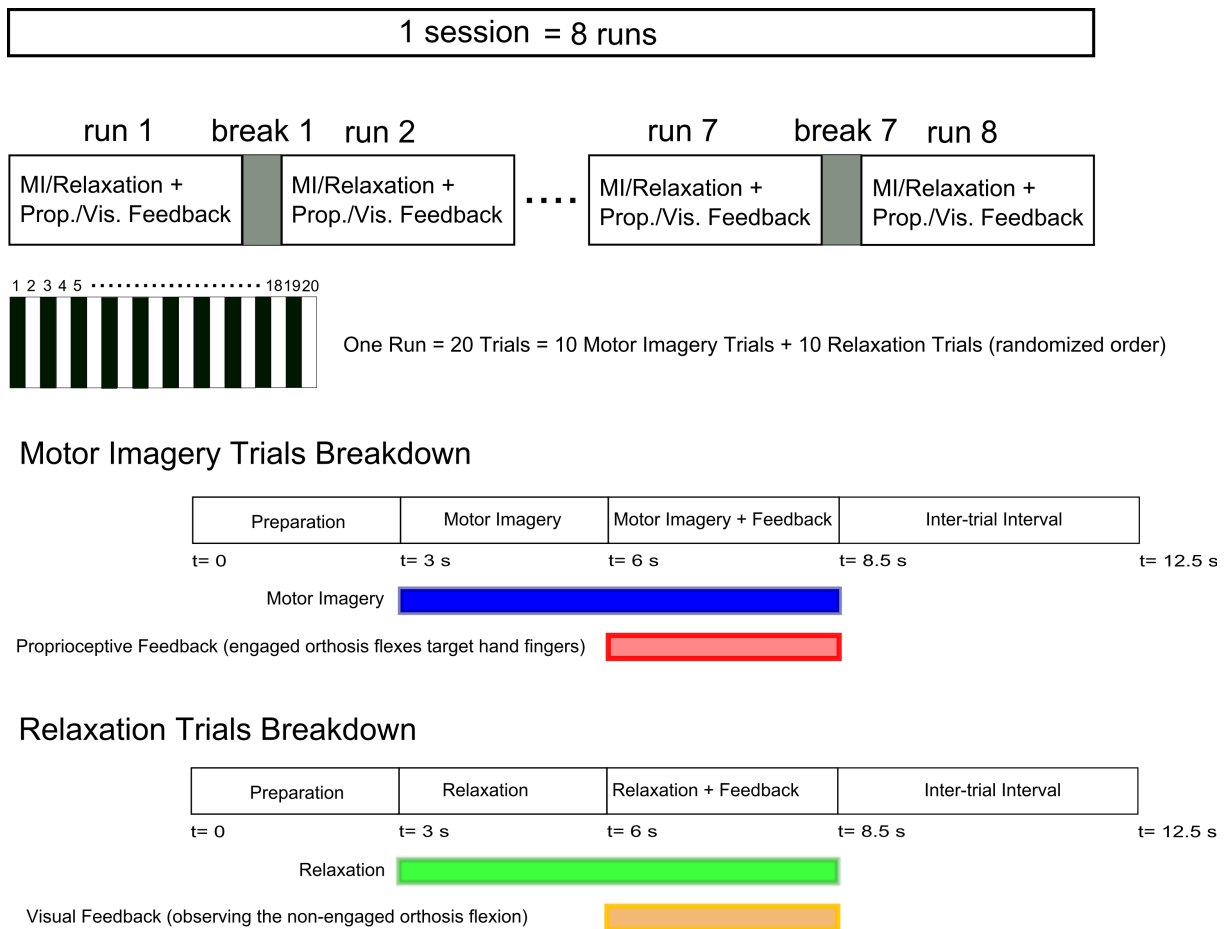


Figure 6.1. Time course of neurofeedback training sessions. This figure illustrates the time course of each neurofeedback training session. Each session encompasses eight runs, where each run includes 20 trials. Each trial starts with a preparation cue at $t = 0$ s, followed by another command at $t = 3$ s that guides the participant to perform relaxation or finger flexion motor imagery. After 3 s of motor imagery/relaxation performance, feedback provision starts and becomes updated recurrently every 16 or 96 ms according to the session's condition. At $t = 8.5$ s the trial finishes and after a 4 s inter-trial interval the next trial starts.

was six times larger than 16 ms condition. This adjustment was made to provide equal total flexion angle of 62.4 degrees received in 156 ($= \frac{2500}{16}$) and 26 ($= \frac{2500}{96}$) steps in each trial for the former and the latter conditions, respectively. Provision of equal total flexion for both FUIs renders the FUI effect unbiased by the amount of movement.

6.2.7 BCI performance measures

We employed one trial-based index and one run-based index to compare the participants' online BCI performance with different FUIs. The indices are as follows: (i) A trial based information transfer rate (ITR) was employed to take into account both the accuracy and the speed of data transfer (Wolpaw *et al.* 2000). The ITR calculation was performed according to Wolpaw's definition (Wolpaw *et al.* 2000) using Equation 6.2 in which it is expressed in bits per minute (bits/min)

$$ITR = \log_2 N + P \log_2 P + (1 - P) \log_2 \left(\frac{1 - P}{N - 1} \right) \left(\frac{60}{8.5} \right) \quad (6.2)$$

where P stands for the accuracy of each trial, N represents the number of classes (two classes: relaxation and motor imagery), and 8.5 is the total length of each trial in seconds. The ITR has been multiplied by 60, to express it in bits/min. Note that the trial-based accuracy (P) was calculated as the percentage of times in the feedback section of each trial that classification outputs conformed to the task and flexed the orthosis. (ii) A run based classification accuracy that indicates the percentage of trials in each run in which the average classifier output is larger or smaller than the threshold value for the motor imagery and relaxation trials, respectively. While the former measure (ITR) considers both the average accuracy and speed of information transfer across all trials, the latter is equivalent to the traditional measure of BCI performance; the target hit rate in each run with visual feedback. The analysis was performed using custom built Matlab scripts.

It has been shown that the threshold for BCI accuracy to consider one is controlling a BCI is 70% (Halder *et al.* 2013). Therefore, in this study participants were dichotomized to *good imagers* if their average accuracy with the short FUI were more than 70%, and *poor imagers* if their average accuracy with the short FUI were between 50% and 70%.

6.2.8 SRT measurement

A simple reaction time (SRT) test (Klemmer 1956) was carried out, using the CANTAB battery test of Cambridge Cognition, to measure the reaction time of participants. Participants sat in a chair and were asked to concentrate on a tablet computer placed on a desk in front of them and to press the button on a press pad as soon as they saw a square on the screen. Each participant performed the task 30 times to obtain the average latency (reaction time), which was used as their SRT index.

6.2 Experimental setup

Note that our reported values for SRT are measured using CANTAB battery test of Cambridge Cognition with subjects aged 18–26 years and using different hardware, software, or participants with different age range may provide different results.

6.2.9 Offline analysis

For offline analysis of the EEG and EMG signals, EEGLAB (Delorme and Makeig 2004) and custom-built Matlab scripts were used. The EEG signals were spatially transformed using a small Laplacian filter to produce single channel EEG data with enhanced spatial resolution (C4-SLP for P3 and C3-SLP for other participants). Next, the data were band-pass filtered (3–47 Hz) and divided into epochs from -2 to 8.5 s centred around the “start” auditory command. Then all relaxation trials were rejected and after removing the average baseline, data purification was performed as follows: (i) to tag the outlier trials, EEG amplitude, spectral power, skewness, kurtosis and variance were checked; (ii) the trial was labelled as irregular if any of the mentioned indices were beyond the regular values of artefact free EEG signals using the guideline provided elsewhere (Daly *et al.* 2012). The EMG signals of the Flexor Carpi Radialis (FCR) of the target hand, which monitored the reflection of actual movement of fingers in the forearm muscle activity, were also band-pass filtered (3–400 Hz). Next, the average baselines of motor imagery trials were removed and then they were epoched using the same time windows as EEG signals. EMG signals recorded during the motor imagery performance were screened, and trials with peak-to-peak values larger than 50 mV were tagged. All tagged trials due to irregular EEG or significant EMG signals were discarded (9.2%).

The spectral power of the feedback section of motor imagery trials (6–8 s) and their preceding inter-trial interval (-2 to 0 s) were extracted in three frequency bands: α (8–13 Hz) and lower β (16–22 Hz) and higher β (22–30 Hz). Only the last 2 s of the 4-second-long inter-trial interval were considered as baseline period. This adjustment ensured that the post imagery ERS had elapsed and had not affected the baseline spectral power estimation. Only the first 2 s of motor imagery with feedback section (6–8 s) was considered, to equalize the length of imagery and baseline time windows. Welch method (Welch 1967) with frequency resolution of 0.25 Hz was used to estimate the

power spectral density (PSD) in decibel (dB). The PSD in the inter-trial interval preceding the imagery trials was also calculated to determine baseline spectral power. The absolute difference between the spectral power during motor imagery and inter-trial interval were calculated as a measure of absolute ERD for each frequency band. The ERD percentage indices were then calculated according to Equation 6.3 (Pfurtscheller 2001)

$$\text{ERD}(\%) = \frac{A - R}{R} \times 100 \quad (6.3)$$

where A and R stand for the spectral power during motor imagery and the baseline period, respectively. Note that ERD percentage measures in each frequency bands were calculated and compared between different FUIs in each group of imagers (good and poor imagers).

6.2.10 Statistical analysis

To investigate the relationship among the online accuracy measures and SRT, a Pearson correlation analysis between SRT and the accuracy was carried out for each FUI. To ensure that the small number of samples did not bias the correlation coefficients, 100,000 bootstrapped data samples were used. Using the bootstrapped samples the mean values (r' , estimated correlation coefficient), standard deviations and 95% confidence intervals (2.5th and 97.5th centiles of the 100,000 correlation coefficients) were calculated. If the 95% confidence interval did not include zero, the correlation coefficient would be considered as significant.

The accuracy and ITR indices of the eight runs of each session with either short or long FUI for each participant were used, to calculate the online BCI performance measures. Since each group (good and poor imagers) had five members, each condition (FUI) comprised 40 (five participants \times eight runs) measures for comparison. We decided to consider all eight runs of each session for each participant's accuracy and ITR measures (instead of their average values) to increase the statistical power. A two-way ANOVA with factors BCI aptitude (levels "good" and "poor") and FUI (levels "16 ms" and "96 ms") was used to explore the interplay between the aforementioned factors and the accuracy and ITR, separately.

In the offline analysis, α , lower β and higher β ERDs were compared. The calculations were performed for each of eight runs of each session with either short or long FUI for all participants. Selecting all runs for the analysis, resulted in 40 (five participants \times

6.3 Feedback customization effect

eight runs) ERD measures with each FUI in each frequency band for each group. In total, it provided 240 ERD measures (40 runs \times two FUIs \times three frequency bands) that were analyzed using a two-way ANOVA with factors frequency band (levels α , lower β , and higher β) and FUI (levels “16 ms” and “96 ms”) for good and poor imagers, separately.

For *post-hoc* tests in the applied ANOVA for online measures, since two correlated measures (accuracy and ITR) were used, only planned comparisons between FUI values (16 and 96 ms) were carried out. Therefore, Holm-Sidak’s two-sided t-test was adopted for *post-hoc* analysis to adjust for multiple comparisons. However, in the two-way ANOVA on ERD measures, since spectral analysis in α and β bands are independent, no adjustment for multiple comparisons were made and thus, uncorrected Fisher’s LSD two-sided t-test was adopted for *post-hoc* analysis.

6.3 Feedback customization effect

Table 6.2 summarizes the online accuracies and ITR values of all participants at short and long FUIs and their SRT results. Our reported results for SRT test corroborate with findings of another study by Philip *et al.* (1999) who found the SRT values for subjects less than 30 years old as 236 ± 32 ms⁵. Subjects with accuracies $> 70\%$ at an FUI of 16 ms (P2, P3, P6, P9, P10) were grouped as good imagers. The remaining participants (P1, P4, P5, P7, and P8) who achieved accuracies between 50% and 70% at the same FUI were grouped as poor imagers. We observed a linear relation between the accuracy and SRT (Fig. 6.2). The Pearson correlation coefficient between SRT and accuracy at an FUI of 16 ms was $r = -0.671$ ($p = 0.033$) while its value between SRT and accuracy at an FUI of 96 ms was $r = -0.725$ ($p = 0.018$). Bootstrapping the samples for FUI of 16 ms resulted in $r' = -0.671 \pm 0.140$ with 95% confidence interval of $(-0.371 - -0.889)$ between SRT and the accuracy. For FUI of 96 ms bootstrapping resulted in $r' = -0.7165 \pm 0.1654$ with 95% confidence interval of $(-0.346 - -0.957)$ between SRT and accuracy. Since none of the calculated 95% confidence intervals contained zero, bootstrapping further demonstrated the significance of the observed correlations. It suggests that SRT is a surrogate for BCI aptitude with both long and short FUIs. The green horizontal lines in Fig. 6.2 represent the accuracy threshold of 70% that has been used to classify participants as

⁵Note that the adopted measure in this study is simple reaction time (SRT) and not choice reaction time (CRT) that is always longer than SRT

Table 6.2. Summarizing SRT, ITR and accuracy results. Accuracy, information transfer rates with feedback update intervals of 16 and 96 ms and the results of reaction time test

Participants	Accuracy (16) (%)	Accuracy (96) (%)	ITR (16) (bits/min)	ITR (96) (bits/min)	SRT (ms)
P1	53	59	3.15	3.45	244
P2	86	80	4.68	4.80	206
P3	84	76	4.60	4.28	214
P4	59	69	3.33	4.05	230
P5	67	61	3.44	4.40	245
P6	97	86	6.95	4.65	214
P7	56	57	3.20	3.15	221
P8	64	81	4.17	4.98	219
P9	89	90	6.13	5.26	221
P10	83	91	4.12	4.45	208

good and poor imagers. As illustrated, the boundary margin for classification is wider at 16 ms FUI compared to that of 96 ms FUI. Therefore, the accuracy with the short FUI was employed to dichotomize subjects as good and poor imagers.

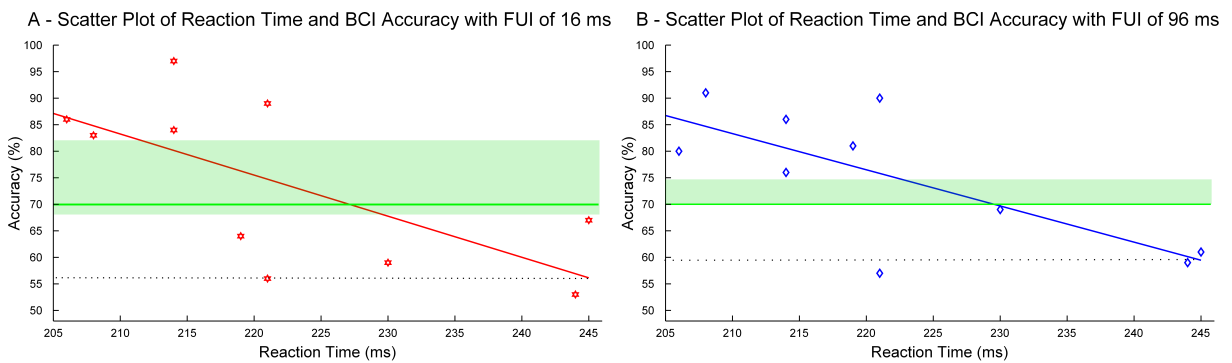


Figure 6.2. Illustration of the relationship between SRT and BCI accuracy. Scatter plot of the simple reaction time measure and BCI accuracy with feedback update intervals of 16 ms (panel A) and 96 ms (panel B) of 10 participants. The red and blue lines show linear regression lines for 16 and 96 ms conditions, respectively. The green horizontal lines at 70% accuracy were used to segment subjects as good and poor imagers. Since the boundary margin (the green shadowed area around the green line) in panel A was wider than that of panel B, the online accuracy with 16 ms FUI was adopted to label participants as good and poor imagers.

6.3 Feedback customization effect

To analyze the online BCI performance, the run-based accuracy and trial based ITR were used to compare the effect of long and short FUIs on good and poor imagers, separately. According to Fig. 6.3, the direction of accuracy and ITR change following FUI modification was dependent on the BCI aptitude. Two-way ANOVA of the accuracy showed significant main effects for BCI aptitude ($F(1, 78) = 172.2, p < 0.0001$) but not for FUI ($F(1, 78) = 0.6704, p = 0.4154$), with a significant interaction ($F(1, 78) = 8.212, p = 0.0053$). The *post-hoc* analysis showed that for poor imagers the short FUI improved the accuracy significantly compared to the long FUI ($t(78) = 2.605, p = 0.0219$). However, changing FUI provided no significant difference between accuracies for good imagers ($t(78) = 1.447, p = 0.1518$). The two-way ANOVA for the ITR showed a significant interaction between two factors ($F(1, 78) = 17.80, p < 0.0001$) and a significant main effect for BCI aptitude ($F(1, 78) = 38.16, p < 0.0001$). However, FUI factor did not have a significant main effect ($F(1, 78) = 0.4037, p = 0.5270$). The *post-hoc* analysis showed a significant outperformance of the short over long FUI for good imagers ($t(78) = 3.432, p = 0.0019$). In contrast, for poor Imagers ITR was larger with long FUI than those of short FUI ($t(78) = 2.534, p = 0.0264$). Overall, poor imagers appear to produce larger accuracies and ITRs with long FUI, whereas good imagers revealed larger ITRs with short FUI. Furthermore, there was a highly significant main effect of BCI aptitude with both the accuracy and ITR across good and poor imagers.

Power spectral density of feedback section of motor imagery trials and the baseline period preceding imagery trials were calculated for all participants and averaged in both groups in the 3–45 Hz frequency band (Fig. 6.4-A, Fig. 6.4-B). For each FUI in each group the difference between the spectral power of motor imagery and baseline periods were calculated and plotted in Fig. 6.4-C and Fig. 6.4-D. Also, ERD percentage measures for both groups and both condition in α , lower β and higher β frequency bands were calculated according to Equation 6.3 and are demonstrated in Fig. 6.4-E, and Fig. 6.4-F. The statistical analysis was performed on the ERD percentages as the neural signature of increased cortical activity during motor imagery performance (Pfurtscheller 2001). The ERD indices were analyzed using two-way ANOVA with factors frequency bands (levels α , lower β , and higher β) and FUI (levels “16 ms” and “96 ms”) across good and poor imagers, separately. Two-way ANOVA of good imagers revealed significant main effects for both frequency band ($F(2, 234) = 6.178, p = 0.0024$) and FUI ($F(2, 234) = 32.06, p < 0.0001$). The *post-hoc* analysis with Holm-Sidak’s two-sided *t-test* showed a significant outperformance for 16 ms FUI over 96 ms in the α ($t(234) = 4.155, p < 0.0001$), lower β ($t(234) = 2.896, p = 0.0041$), and higher

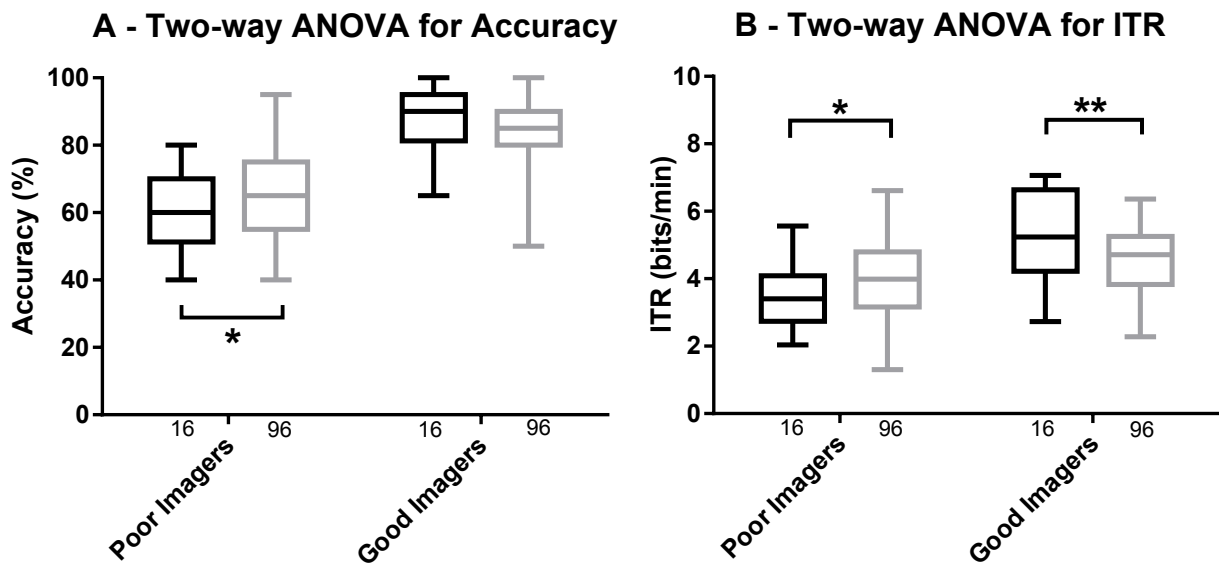


Figure 6.3. Accuracy and ITR comparison. This figure compares the accuracy and information transfer rate (ITR) for good and poor imagers with different feedback update intervals. Panel A illustrates accuracies with 16 and 96 ms feedback update intervals for poor and good imagers. Panel B depicts ITRs with 16 and 96 ms feedback update intervals for poor and good imagers, respectively (*: $p < 0.05$, **: $p < 0.01$).

β ($t(234) = 2.757, p = 0.0063$) bands. However, for poor imagers, there was not any significant main effects neither for frequency band ($F(2, 234) = 2.563, p = 0.0792$) nor for FUI ($F(2, 234) = 1.647, p = 0.2007$). However, there was a significant interaction between factors ($F(2, 234) = 3.343, p = 0.0370$). The *post-hoc* analysis for poor imagers showed that lower β band supplied significantly larger ERDs with the long compared to those of the short FUI ($t(234) = 2.036, p = 0.0428$). Overall, good imagers showed significantly stronger ERDs across all frequency bands with the short FUI while poor imagers showed significantly larger ERDs at lower β band with the long FUI.

6.4 Reaction time and feedback update rate

The main findings of this study are as follows: (i) the SRT and BCI aptitude measures are inversely correlated, i.e. a short SRT is a surrogate for possessing a high-level BCI aptitude and vice versa⁶; (ii) the FUI customization affects the BCI accuracy, ITR, and down-regulation of sensorimotor rhythms when operating MI-BCIs with proprioceptive feedback depending on the participants' level of BCI aptitude. Notably,

⁶Note that SRT may not be as helpful in acute phases of stroke where patients take large amount of medications that negatively affect their cognitive functions.

6.4 Reaction time and feedback update rate

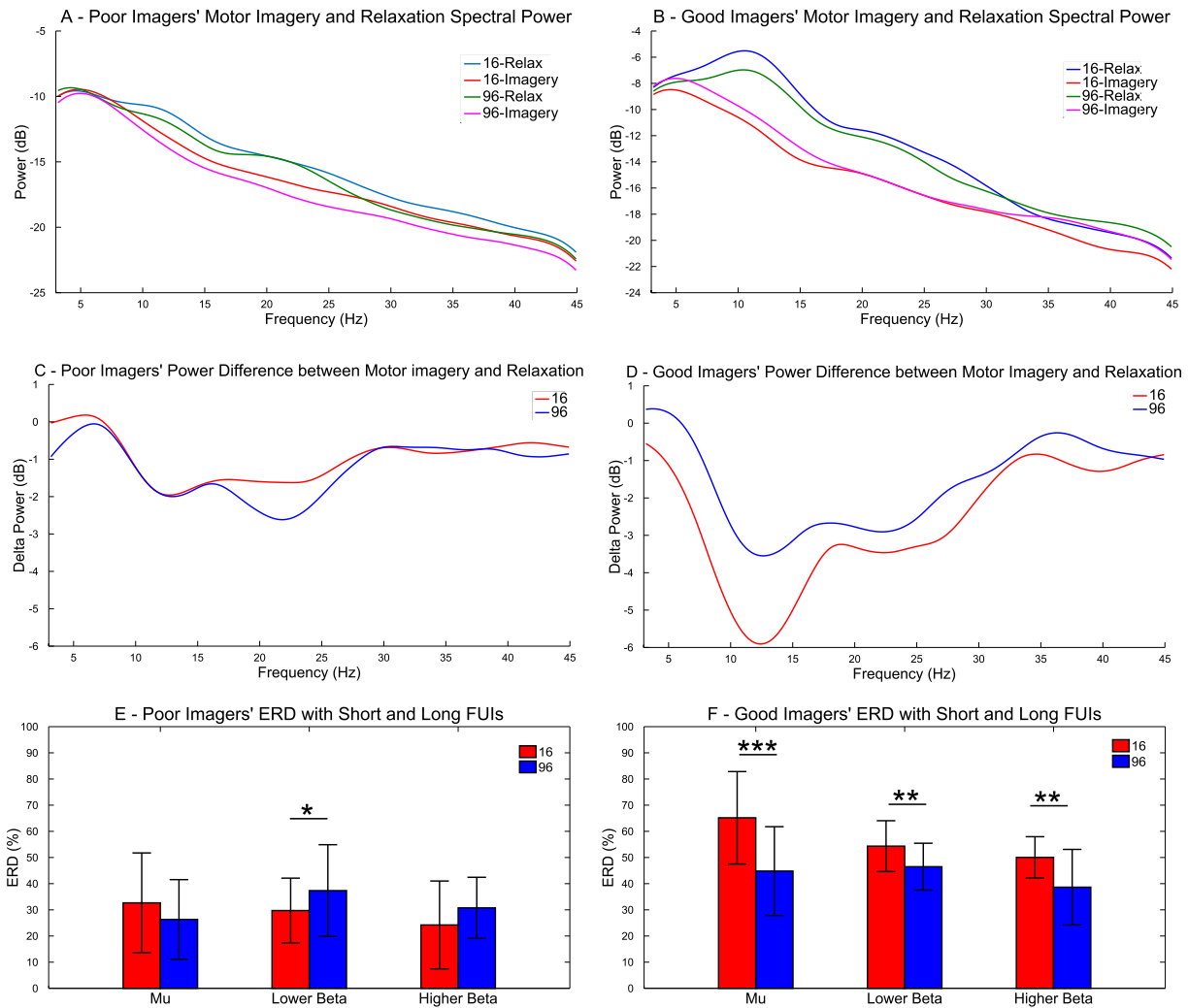


Figure 6.4. Power spectral density in 3–45 Hz with different feedback update intervals.

Fig.4-A and Fig.4-B show the averaged PSDs for poor and good imagers, respectively. The difference between spectral power of motor imagery and baseline periods are plotted in Fig.4-C for poor imagers and Fig.4-D for good imagers. ERD percentage measures for both groups and both condition in α , lower β and higher β frequency bands are plotted in Fig.4-E, and Fig.4-F (FUI: feedback update interval, ERD: event related desynchronization, *: $p < 0.05$, **: $p < 0.01$, ***: $p < 0.001$).

participants with poor BCI aptitude produce higher accuracies and larger ERDs with feedback updated every 96 ms, while good imagers provide a higher ITRs and elicit stronger ERDs with feedback updated every 16 ms.

We hypothesized that FUI affects BCI performance differently depending on subjects' reaction time. SRT was found to be inversely correlated with BCI accuracy at both short and long FUIs. Moreover, the slope of the regression line fitted between SRT and the accuracy for 96 ms FUI showed to shift slightly lower for good imagers and more

clearly higher for poor imagers. If increasing FUI had a symmetric effect on good and poor imagers, we should have observed a symmetric shift in the slope of the regression line of the 96 ms FUI. Thus, it appears that increasing FUI from 16 to 96 ms improved BCI performance for poor imagers, but degraded the performance of good imagers to a lesser extent. Accordingly, it may suggest that people who possess a high level of BCI aptitude benefit more from shorter FUIs. However, longer FUIs do not degrade their BCI performance significantly. In contrast, poor imagers with a lower BCI aptitude appear to respond positively to FUI prolongation.

In this study, participants were dichotomized according to their online performance with the 16 ms FUI. Besides the provision of a wider boundary margin for classification, another reason for choosing 16 ms over 96 ms FUI was hypothesizing that using shorter FUIs would make the distinction between good and poor imagers more pronounced due to their different speed of information processing. Our results indeed illustrate that changing FUI from 16 to 96 ms improves the BCI performance for poor imagers while decreases those of good imagers. Thus, it appears that people with shorter reaction time can perform motor planning and feedback realization quickly and thus gain more with a short FUI. In contrast, a short FUI may be even distracting for people with longer SRTs as the updates occur faster than their processing speed and therefore, may degrade their BCI performance. Overall, both online and offline measures suggest that dichotomizing participants according to their BCI performance accuracy with a 16 ms FUI was effective according to the distinct responses of good and poor imagers.

To investigate neural substrates underlying FUI effect on BCI online metrics, the spectral power of the EEG signals over the contralateral hand representation of the primary motor cortex (M1) in α and β bands were analysed. Good imagers showed more pronounced ERDs in both frequency bands than their poor counterparts. Besides, good imagers showed larger α and β ERDs with the shorter FUI. Poor imagers, however, showed significantly larger ERDs with longer FUIs only in the lower β band. Since poor imagers showed weaker ERDs compared to good imagers, it might explain why they failed to show distinctive ERDs with different FUIs in α and Higher β bands. Overall, offline analysis results corroborate the findings from the online analysis. While increasing FUI elicited significantly larger ERDs in the α band for good imagers, poor imagers appeared to be indifferent. However, in the β band, changing FUI affected ERDs in the lower or both lower and higher β bands for poor and good

6.4 Reaction time and feedback update rate

imagers, respectively. This responsiveness of β ERDs to FUI change is congruent with prior studies that highlight the role of β oscillation in motor control (Feurra *et al.* 2011), and cortical and muscular coherence (Halliday *et al.* 1998, Mima *et al.* 2001a, Mima *et al.* 2001b, Witham *et al.* 2011). Distinctive β oscillations are also supported by the findings of Vukelić and Gharabaghi (2015a) that highlight the relationship between proprioceptive feedback and modulation of β ERD during motor imagery.

The opposite effect of FUI change on poor and good imagers may be explained by the findings of Witham *et al.* (2011), who studied how descending and ascending pathways affect corticomuscular coherence. They demonstrated that both cortical to muscular activity time lag and its reafferent feedback (muscular to cortical) time delay vary across subjects, implying individual variations in sensorimotor loop duration. Therefore, it is plausible that customized FUI optimizes sensorimotor information processing through consideration of intra-subject bidirectional corticomuscular delays.

For good imagers changing FUI did not alter online accuracies substantially, as they provided average accuracies more than 80% with both conditions. For poor imagers the slower FUI elicited stronger ERDs in lower β band and thus improved their average accuracy by almost 6%. However, their average accuracy was still sub-threshold compared with the baseline 70% accuracy of good BCI performance (Halder *et al.* 2013). Nonetheless, testing only two values for FUI customization has elevated poor imagers accuracy from 59% to 65% which halves their distance from the 70% threshold. Thus, further studies on the effect of a range of FUIs on BCI performance of poor and good imagers may explain the phenomenon of BCI illiteracy.

BCIs for communication and rehabilitation require different key performance indices. Notably in BCIs for communication, accuracy is a critical measure (Wolpaw and Wolpaw 2012b) whereas, in therapeutic BCIs, both online accuracy and brain facilitation are equally important (Grosse-Wentrup *et al.* 2011). Thus, in BCI for communication, poor imagers are more likely to provide higher accuracies with FUI customization while good imagers' accuracy may change to a lower extent with FUI change. However, in BCI for rehabilitation, it is expected that all imagers receive benefit from FUI customization through enhanced brain facilitation.

6.5 Limitations of the study

- Instead of exclusively working with the right hand, in this study the hand that its motor imagery elicited the stronger ERD was chosen. However, stroke patients mostly have a unilateral brain injury and therefore this strategy would not be applicable to them.
- This study was done in healthy participants and whether the findings translate directly to a stroke population is not clear.
- In this study no motor imagery questionnaire such as KVIQ questionnaire was used. If such a measure was administered, it could be used as a validator of SRT for BCI aptitude.
- Even though the statistical analysis of the data showed significant differences between SRT and ERD patterns of two groups, considering the small number of group members, it is recommended to verify the reported results with larger groups.

6.6 Conclusion

As presented in this chapter, participants can be categorized as poor and good imagers according to their online BCI accuracy with FUI of 16 ms. However, underlying neural substrates of motor imagery performance are not fully understood yet, and subjects take a variety of different approaches to perform motor imagery. Therefore, we propose adding one more factor to the screening sessions to find the optimum FUI for each subject through testing their performance with short, medium, and long FUIs. Alternatively, SRT index can predict whether a long or short FUI suits each individual with almost 70% accuracy. Also, it would be interesting to see in the future a similar study repeated on larger number of participants.

In the next chapter, we will investigate whether and to what extent, customizing a restorative BCI through our findings reported in the current and the last chapters may affect the motor performance of a stroke patient.

Chapter 7

Feedback Optimization May Promote Restorative BCIs

THIS chapter is aimed at exploring how shorter than usual feedback update intervals affect behavioural and neurophysiologic measures following BCI training for stroke patients using a single-case and proof-of-principle study design.

The ARAT score that was used as the primary and behavioural measure showed an unprecedented (more than 30%) increase over the course of training, while neurophysiologic measures including MEP and MVC showed distinctive changes in early and late phases of BCI training.

Thus, this preliminary study may pave the way for running larger studies to further investigate the role of confounding factors such as early and late phases of motor training along the course of BCI training.

7.1 Introduction

In Chapter 5, we investigated the effect of feedback modality on restorative BCIs. We found that proprioceptive feedback outperforms visual feedback in both eliciting stronger β -ERDs and the occurrence of conditional learning. Then, in Chapter 6, we studied the effect of feedback update interval (FUI) on restorative BCIs and established that FUI customization enhances the BCI performance. As discussed in 2, in addition to operant conditioning, Hebbian learning is also suggested to be important in neurofeedback training. Shortening the FUI within a restorative BCI framework reduces the latency between activation of the motor (via motor imagery) and sensory cortices (by sensory feedback). Thus, it seems that neurofeedback training with shorter FUIs may promote the occurrence of Hebbian neuroplasticity and thereby reorganization of the impaired neural connections following stroke. Therefore, to investigate the potential synergy between findings of the studies reported in Chapter 5, and Chapter 6, in this study we employed proprioceptive feedback and investigated whether shortening FUI in neurofeedback training sessions affects motor performance in a participant who had suffered a stroke 3.5 years ago.

To study the effect of neurofeedback training with shorter than usual FUIs on motor function change after stroke, we adopted a proof-of-principle study design and recruited one stroke patient. The FUI values were chosen randomly among 16, 24, 48, or 96 ms that were at least two time shorter than earlier studies (Gomez-Rodriguez *et al.* 2011, Ramos-Murguialday *et al.* 2013). The action research arm test (ARAT) was used as our primary clinical test. We also used rest and active motor evoked potentials (MEP) as well as maximum voluntary contraction (MVC) as our secondary neurophysiological tests.

7.2 Methods

7.2.1 Ethics, subjects, and inclusion criteria

Since in this phase of our studies, we planned to shift from healthy participants to stroke patients, we applied for an amendment to our current ethics approval that was approved by the Ethics Committee of the University of Adelaide. As a proof-of-principle study, it was planned to recruit one stroke patient. The prospective participant had to fulfil the following inclusion criteria: (1) being in the chronic stable phase of

Table 7.1. Screening session results. Results of the screening session presenting the scores achieved by the participant that were all above the defined thresholds (ARAT: action research arm test, MMSE: mini-mental state examination).

Time after stroke	ARAT score	MMSE score	Mobility	TMS contra-indicator	Modified Ashworth score	BCI accuracy	Proprioception
3.5 years	34	30	Fully mobile	Nil	2	75%	95%

stroke—at least six months post-stroke; (2) having impaired motor capabilities in their arms—by screening them using action research arm test (ARAT) scores (Lyle 1981) to be less than 54 out of 57; 3) having intact cognitive functions—by screening them using mini-mental state examination (MMSE) score (Folstein *et al.* 1975) to be more than 26 out of 30; (4) being independently mobile—with or without a walking aid; (5) not having any transcranial magnetic stimulation (TMS) contraindications—by screening them using TMS adult safety screen (TASS) questionnaire (Rossi *et al.* 2009); (6) not having excessive tone in their arm and hand muscles—by screening them using modified Ashworth test score (Bohannon and Smith 1987) to be less than three out of four; (7) having the ability to perform vivid motor imagery—by screening their accuracy in running a motor imagery based BCI system to be more than 70%; (8) having an intact sense of proprioception—by screening their blind judgement of comparing size of seven polystyrene balls (Kattenstroth *et al.* 2013) with more than 90% accuracy.

We screened three stroke patients and only the last one met all the requirements. For the first candidate while he passed all the requirements, after attending the BCI screening session he reported having muscle cramps in his leg and arm on the affected side of his body and withdrew from the study. The second patient had had two strokes: one in the left and another in the right hemisphere of her brain. However, her motor functions had recovered almost perfectly and except for her speech that was slightly unclear, her motor functions were too good to be considered for the study. Finally, the last candidate who was a 65-year old man and had a stroke in his right hemisphere 3.5 years prior to the screening, passed all the tests with the results summarized in Table 7.1.

7.2 Methods

7.2.2 Study design

In this study we planned to investigate: (i) whether and how neurofeedback training with FUIs selected from 16-96 ms range (16, 24, 48, or 96 ms) affects the motor performance, and (ii) in case of observing any potential effect of these shorter than usual FUI values on behavioural and/or neurophysiological measures, how long the impacts last. Therefore, we made a specific setup that not only recoded the performance measurements during neurofeedback training sessions; it also measured the indices up to 5 weeks after BCI training interventions.

To fulfil the aforementioned goals, the study was designed as a proof-of-principle study with a ABABCC setup (Nock 2007). The selected participant took part in a number of index measurements (IM) in no intervention weeks (A), intervention weeks (B), and follow-up weeks (C). In the no intervention weeks (A), only the IM were done on Monday, Wednesday and Friday. However, in intervention weeks (B), besides the measurement of indices similar to week (A), on every weekday a BCI training session was also performed. Then, in the follow-up weeks (C) performance indices were measured once per week, to investigate how long potential changes last, one and five weeks after the last neurofeedback training session (weeks 5, and 9). The design schedule is shown in Table 7.2.

7.2.3 Neurofeedback training setup

According to the results of the participant's screening session that is described in detail in Section 5.2.4., an optimum frequency of 15 Hz with a large Laplacian configuration of EEG channels centred on CP4 channel produced the highest coefficient of determination (r^2) for the left hand motor imagery versus relaxation trials. These features were used to provide feedback during the training sessions. Every session comprised of eight runs of 20 trials (ten left hand finger extension motor imagery, and ten relaxation trials). The setup for neurofeedback training sessions was quite similar to the design that was adopted for studying the effect of FUI on BCI performance and was described in Section 6.2.5. Following a stroke, the fingers often assume a flexed position and to obtain useful function in the hand, strengthening control of the finger extensors is desirable. Therefore, unlike the last phases of our studies with healthy populations, here we rewarded the motor imagery of the stroke patient by extending his fingers. Fig. 7.1

Table 7.2. Time course of the study design. The study was of nine weeks duration and was set as ABABCC. In A weeks (weeks 1 and 3), only performance measures were recorded three times per week. In B weeks (weeks 2 and 4), in addition to recording performance measures three times per week, five neurofeedback sessions were carried out where the FUI value for each session are shown in braces. In C weeks (weeks 5 and 9), only one recording of performance measures was performed. During weeks 6–8, no recording sessions were performed. In weeks 2 and 4, all measures were recorded after BCI training (IM: index measurement, BCI: neurofeedback training session).

	Monday	Tuesday	Wednesday	Thursday	Friday
Week 1 (A)	IM	—	IM	—	IM
Week 2 (B)	BCI(96) + IM	BCI(48)	BCI(48) + IM	BCI(16)	BCI(24) + IM
Week 3 (A)	IM	—	IM	—	IM
Week 4 (B)	BCI(16) + IM	BCI(24)	BCI(48) + IM	BCI(96)	BCI(48) + IM
Week 5 (C)	—	—	—	—	IM
Week 9 (C)	—	—	—	—	IM

illustrates the setup for BCI training session, and Fig. 7.2 demonstrates the time course of neurofeedback training sessions

7.2.4 Performance measures

All adopted measures in B weeks (weeks 2 and 4) that included BCI training, were recorded after BCI training.

Action research arm test (ARAT)

The ARAT (Lyle 1981) was employed as the primary and clinical measure to investigate the effect of neurofeedback training on the recovery of the affected arm following stroke.

Maximum voluntary contraction (MVC)

To investigate how BCI training sessions affect the participant's volitional contraction of finger extensor muscles, we adopted the MVC measure (Meldrum *et al.* 2007). The participant sat in an armchair while his left arm was placed on the armrest. An auditory command of "GET READY" signalled the participant to be prepared for recording.

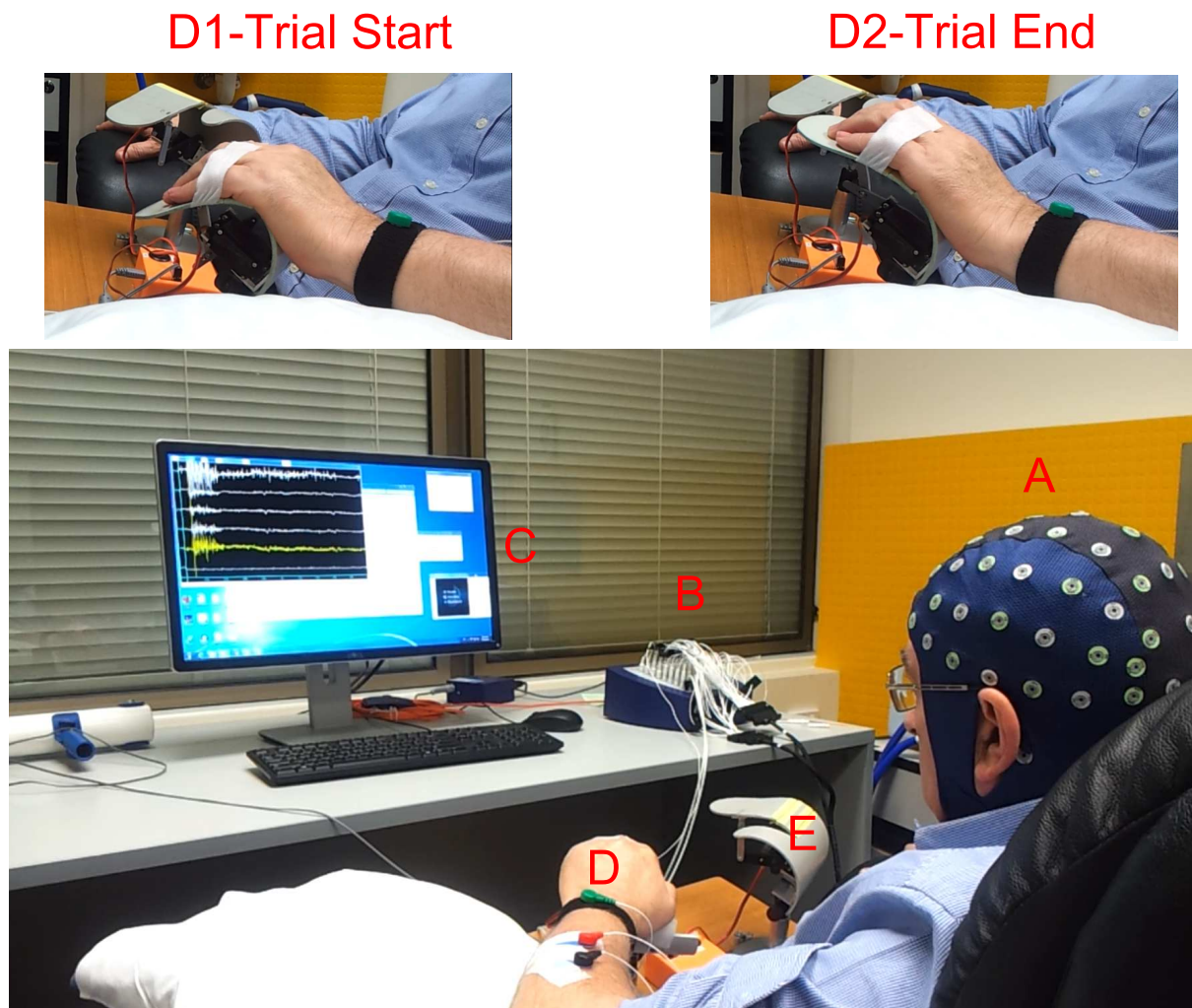
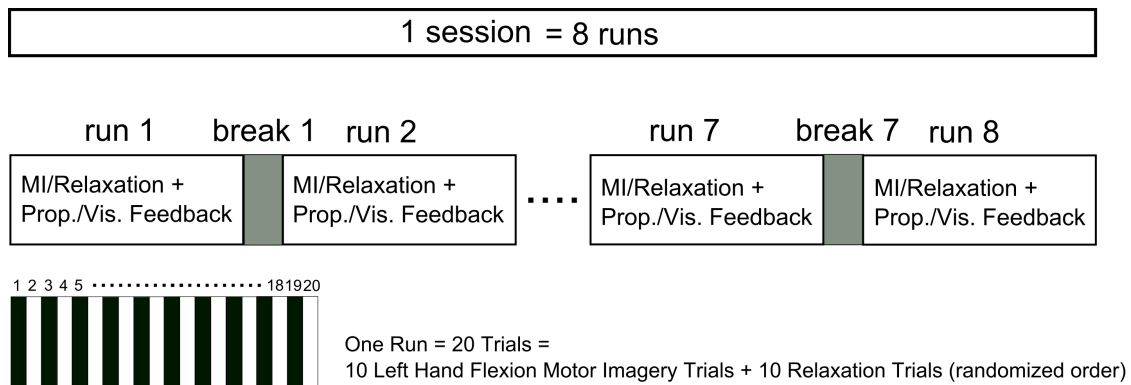
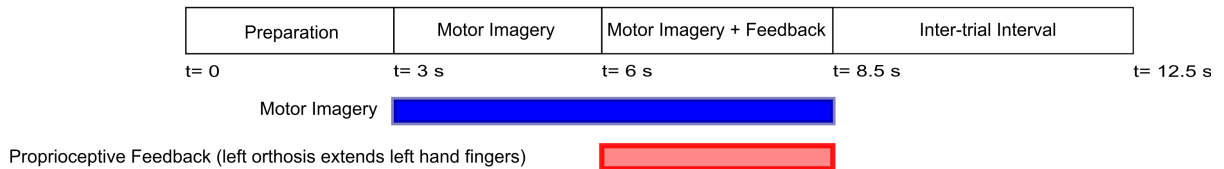


Figure 7.1. Illustration of the setup of the neurofeedback training session. This figure illustrates the setup of the neurofeedback training sessions. (A) the EEG cap records EEG signals. (B) the Refa EXG amplifier that receives and amplifies the EEG and EMG signals and then sends them to a PC for processing and screening. (C) the PC monitor that screens the EEG and EMG signals for the study instructor. (D) the left orthosis which is hidden under the participant's left hand and provides proprioceptive feedback during motor imagery. (D1) and (D2) present side views of the left orthosis at the start and the end of each motor imagery trial. (E) the free running orthosis that provides visual feedback during relaxation.

Then, a “START” auditory command, instructed him to extend his left hand fingers with maximum power while an experienced physiotherapist was holding his hand. After 2.5 second of recording, a “STOP” auditory command cued the end of the trial. Each MVC recording session encompassed three trials with 10-second inter-trial intervals. The root mean square of the EMG activity recorded from the finger extensor



Motor Imagery Trials Breakdown



Relaxation Trials Breakdown

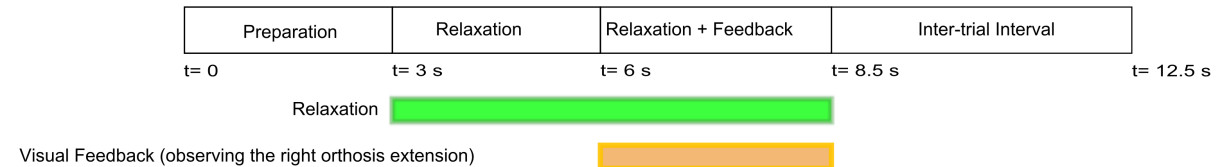


Figure 7.2. Time course of the neurofeedback training sessions. This figure illustrates the time course of each neurofeedback training sessions. Each session encompasses eight runs, where each run includes 20 trials. Each trial starts with a preparation cue at $t = 0$ s, followed by another command at $t = 3$ s that guides the participant to perform relaxation or motor imagery of left hand finger extension. After 3 s of motor imagery/relaxation performance, feedback provision starts and becomes updated recurrently every 16/24/48/96 ms according to the randomized and predetermined FUI value for each session. At $t = 8.5$ s the trial finishes and after a 4 s inter-trial interval the next trial starts. Note that the adopted measures for FUI were the values that belonged to a shorter than usual range (less than 100 ms). Here the aim was to show whether application of such shorter feedback delays within 16–96 ms range can potentially affect BCI training and therefore the order was randomized to exclude any potential effect of a specific FUI value.

muscles (surface recording electrodes) for each of the three trials was calculated and then averaged, to determine the MVC measure for each session.

7.2 Methods

Motor Evoked Potentials (MEP)

Additionally, motor evoked potentials (MEP) were recorded from the finger extensor muscles in both rest and active conditions through application of transcranial magnetic stimulation (TMS)⁷. We used a Magstim 200 (The Magstim Co., Dyfed, UK) machine with a figure-of-eight D70² coil. This made it possible to record rest MEPs for stroke patients that perhaps would not show MEPs with peak-to-peaks more than 50 mV with regular coils. The coil was positioned at almost 45 degrees to the medial line where its handle pointing towards the back of the head. The induced current in the brain with this orientation of the coil flew in a posterior to anterior direction which is optimal to activate the hand representation area in the motor cortex (Ridding and Taylor 2001).

Recording Rest MEPs

To record rest MEPs we used a Refa TMSi 72 channel EXG amplifier and used one of its bipolar channels to record EMG of the finger flexor muscles of the participants affected, i.e. left, forearm. We used disposable electromyogram (EMG) snap electrodes with a belly-tendon setup to record MEPs. To make a communication between Magstim 200 machine and the EMG amplifier, we used a custom built Matlab program that almost every 8 seconds (7.2–8.8 s), sent a trigger pulse through an RS-232 communication channel to both the Magstim 200 machine and the digital input of the EMG amplifier. The recording of both digital input pulse as well as the EMG signal were performed using a customized version of Polybench software provided by TMSi. To find the hotspot, first the best point over the right motor cortex that evoked the largest MEP in the finger extensor muscles was found and marked using maker pens. Next, the intensity was increased in a number of steps and the rest motor threshold was defined as the minimal intensity with which at least five out of ten consecutive MEPs had peak to peak amplitudes of larger than 50 μ V. The rest MEPs were then recorded at 120% of the rest motor threshold and the average peak to peak amplitude of 15 consecutive MEPs was defined as the rest MEP at each recording session.

Recording Active MEPs

To record active MEPs, we designed and fabricated an application specific hardware that measured finger extension force and sent it to the PC for further processing. As

⁷In Weeks 2 and 4 that included neurofeedback training, TMS applications were applied after BCI training sessions to remove a potential effect of TMS application on BCI training

soon as the applied force fell in the range of 150–160 grams, a trigger command was sent to the Magstim 200 machine that stimulated the brain. To define the active motor threshold, the intensity of the stimulation was increased step-wise and MEPs were recorded. The minimal intensity that elicited at least 5 out of 10 MEPs larger than 200 μV was defined as the active motor threshold. Then the active MEP was defined by averaging 15 consecutive MEPs, while participant left hand fingers were applying 150–160 grams of force, at the intensity of 120% of the active motor threshold.

7.3 Results

7.3.1 ARAT scores

In the first week of BCI training (week 2) the average ARAT score was 40.75 that compared to its baseline value in week 1 (36), showed a 13% increase. The ARAT scores reached 42.5 in week 3 (no BCI training) and showed an 18% increase compared to the reference ARAT score of 36. The average ARAT score in week 4, in which another round of BCI training took place, was 48 and revealed a 34% increase compared to the baseline value. In week 5, the ARAT score revealed a subtle increase of less than 2% and reached to 49. The increasing trend of the ARAT scores changed after week 5, and in week 9 its value plateaued at 49. Overall, the ARAT scores revealed a 36% increase over weeks 1–5 and then plateaued at week 9 where the highest increments occurred in weeks with BCI training (week 2 and week 4). Fig. 7.3-A demonstrates the weekly averages and standard deviations of the ARAT scores.

7.3.2 Maximum voluntary contraction

Maximum voluntary contraction (MVC), that was measured by calculating the root mean squares of the EMG signals, was found to be 80 mV in the week 1 (considered as reference value). In week 2, however, The MVC decreased by 16% and was measured at 68 mV. In week 3 the decreasing trend of the MVC changed and with a 34% increase compared to its reference value reached to 108 mV. In week 4, even though it dropped to 91 mV and its value became smaller than that of week 3, it still remained 14% higher than the baseline. In week 5 and week 9, it went again below baseline and reached to 72 mV and 67 mV, respectively. Altogether, the MVC scores were only above the baseline value in weeks 3–4. Fig. 7.3-B summarizes the MVC values across weeks 1-9.

7.3 Results

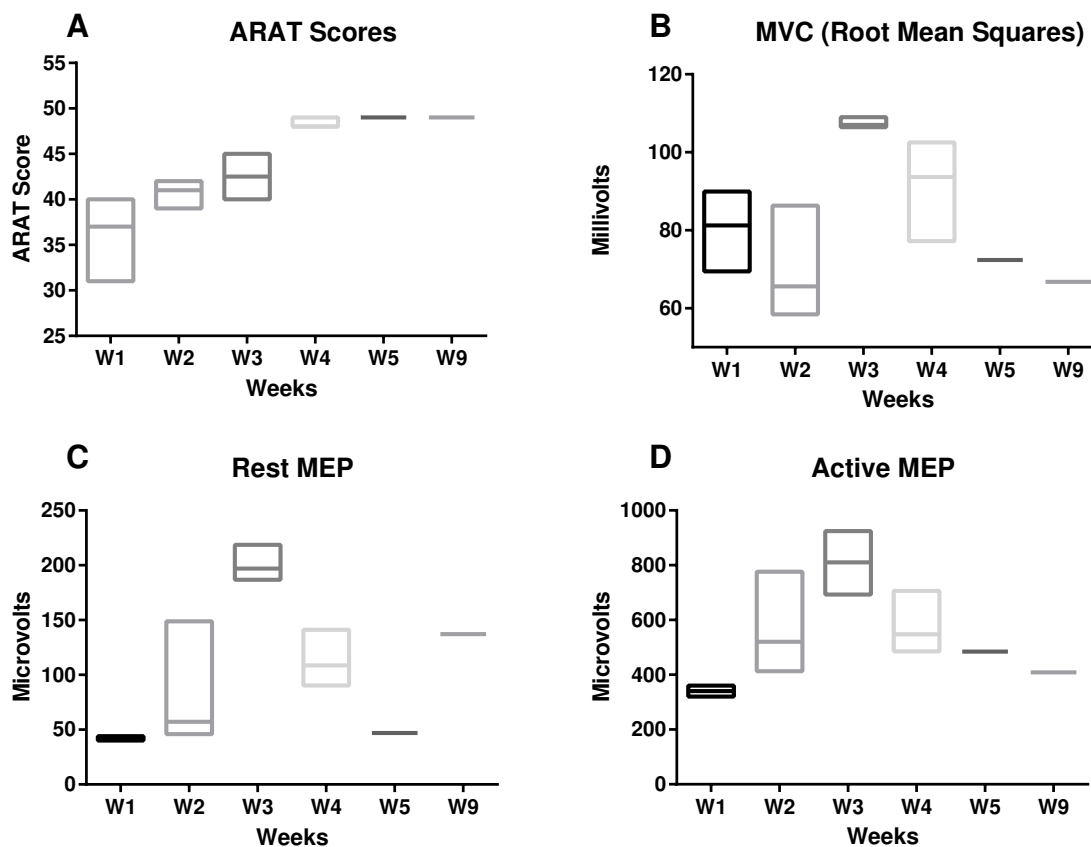


Figure 7.3. The trend of performance measures across the study. figure demonstrates whether application of shorter feedback delays within 16–96 ms range could affect BCI training with randomized FUI values to exclude any potential effect of a specific FUI value. Note that the selected FUI was kept constant along each training session and TMS application occurred after BCI training in weeks 2 and 4. Panel A illustrates the average and standard deviation of ARAT scores along weeks 1–9 where it increase through weeks 2–5 and then plateaus. Panel B shows the trend of MVC scores where it decreases in week 2 and then increases in week 3 and fianlly shows a deceremantal trend along weeks 4–9. Panel C depicts the trend of rest MEP peak to peak amplitudes where it shows increment along weeks 2–3, followed by decrement along weeks 4–5 and finally increase in week 9. Panel D presents the trend of active MEP peak to peak amplitudes that shows an increasing trend over weeks 2–3 and then is decreased along weeks 4–9 (ARAT: arm research action test, MVC: maximum voluntary contraction, MEP: motor evoked potential).

7.3.3 Rest MEP

Measuring the rest MEP in week 1, it showed to be 43 μV . In week 2 it almost doubled (increased by 96%) and reached to 84 μV . Then, in week 3 it revealed the highest rise with 271% increase and became 203 μV . In week 4, even though it was still 164% larger than its reference value in week 1, it dropped to 113 μV . The decremental trend continued in week 5 where the rest MEP was measured at 47 μV and was just 9% larger than its baseline value. However, in week 9 its value raised to 137 μV and showed to be 219% larger than its reference value. Overall, the rest MEP had a rising trend over weeks 2–3 followed by a decrement along weeks 4–5, and finally ended up with an increase in week 9. Fig. 7.3-C depicts the rest MEP values measured along the study.

7.3.4 Active MEP

In week 1 the baseline peak to peak value of the active MEP, where the participant was applying 150 grams of force, was 340 μV . In week 2, the active MEP showed a 67% increase and reached to 570 μV . In week 3 the active MEP value raised for the second time and reached to 809 μV and showed a 138% increase compared with its baseline value. In week 4, the active MEP dropped to 580 μV , but it was still 70% larger than the reference. The decrement continued in week 5 and week 9 where the active MEPs were measured at 484 and 408 μV , though they were still above the baseline level by 42 and 20%, respectively. To sum up, active MEPs, had an increasing trend along weeks 2–3, followed by a decreasing trend across weeks 4–9. Fig. 7.3-D shows the active MEPs trend over the study course.

7.4 Discussion

The main finding of this single case study is that neurofeedback training with FUIs chosen within 16–96 ms range may potentially have a constructive impact on the motor behaviour following stroke. The mentioned possibility is supported by the reported 36% increase in the ARAT scores that was achieved after 10 sessions of neurofeedback training. Other studies on application of restorative BCIs for stroke rehab with real time proprioceptive feedback adopted larger values for the FUI. Gomez-Rodriguez *et al.* (2011) provided real time proprioceptive feedback every 300 ms, whereas in Ramos-Murguialday *et al.* (2013) design, it was provided every 200 ms. However, FUI values in

7.4 Discussion

the current study (16, 24, 48 , or 96 ms were at least two times faster than previous studies. Presuming a critical role for Hebbian learning (Hebb 2005) and STDP (Florian 2007) in stroke rehabilitation (Murphy and Corbett 2009), the adopted shorter FUIs may have enhanced neuroplasticity that was manifested in the observed increment in the ARAT scores.

The second implication of the current study is that short- and long-term impacts of BCI training are reflected distinctively through behavioural measures such as ARAT, and physiological measures such as rest/active MEPs, and MVC. All measures showed an increasing trend (despite some small deviations), both during (week 2) and after earlier sessions of BCI training (week 3). However, the ARAT scores increased, whereas rest/active MEP amplitudes and MVC values decreased both during (week 4), and after (week 5) later sessions of neurofeedback training. Karabanov *et al.* (2012) have explored connectivity between posterior parietal cortex (PPC), which is thought to play a critical role in sensory information processing, and primary motor cortex (M1) in early and late phases of motor learning. They reported that while connectivity between M1 and PPC increases in early phases of motor learning, it degrades during late phases of motor learning. If we presume that acquiring motor imagery skills takes longer than learning motor skills, we can find congruency between the findings of Karabanov *et al* study and the observations of the current study. During week 2 of the current study, that can be considered as early phases of motor imagery training, the connectivity between M1–PPC may have increased and thereby increased rest and active MEPs. However in week 4 that can be regarded as a late phase of motor imagery training, it had potentially become automatized (Wolpaw and McFarland 2004). Therefore, the connectivity between M1-PPC in week 4 had potentially become weaker and thereby resulted in decreased rest/active MEPs.

In a study ran by Pascual-Leone *et al.* (1994), they found that during implicit motor learning, participant reaction time decreased and the cortical map related to the task extended. However, when explicit knowledge of the motor learning task was achieved, the reaction time stopped decreasing and the cortical representation of the related area shrank. The observation we had in the current study was at least to some extent similar to Pascual-Leone results. In their study the reaction time was a behavioural measure that resembles our adopted ARAT score. They also used the paired-pulse TMS as their neurophysiological index that is similar to active MEP measure of the current study.

BCI training in week 2 (first week of BCI training) can also be considered as the implicit phase of the training of the motor imagery task. The implicit phase of training in week 2 was manifested in increasing ARAT scores, and active MEP values, similar to reduction of reaction time and increase of MEP values in Pascal-Leone study. Furthermore, during week 3, where no training took place, we observed that all measures rose that may reflect the consolidation of implicit motor learning during week 3. However after week 4, where the second round of BCI training occurred, the motor learning may have switched to its automatized (explicit) phase similar to a well-learned motor skill (Wolpaw and McFarland 2004). Thus, congruent with Pascal-Leone et al findings, our clinical measure (ARAT score) plateaued in week 5, whereas all other physiological indices such as MVC and MEPs reduced. Thus, these observations may reflect the shrinkage of the cortical representation of the related area to the trained motor imagery task. Altogether, our observations suggest that (i) similar to learning a new skill, in early phases of motor imagery training the cortical representation of the related area extends, and (ii) after consolidation of motor imagery task, the extended cortical representation of the task shrinks while the motor imagery skill remains intact.

7.5 Limitation of the study

In this study we examined the effect of neurofeedback training with shorter than usual FUIs within 16–96 ms range on behavioural and neurophysiological attributes of stroke patients. To exclude a potential effect of any specific values within this range we randomized the four adopted FUIs (16, 24, 48, and 96 ms) in the training sessions. As a result of randomization, in six training sessions followed by measurement, the FUI was 48 ms whereas other FUIs (16, 24, and 96 ms) were used in only one session. If we had designed the study to control the fUI values in a way that equal number of FUIs were used in training sessions followed by TMS application, we could have reported the individual values for each FUI that potentially could add valuable information to the reported results. Thus, it is recommended to consider this point in design of larger studies on the effect of FUI value on neurofeedback training with stroke patients.

7.6 Conclusion

In this single case proof-of-principle study we used a restorative BCI to investigate (i) whether adopting FUIs within the 16–96 ms range with proprioceptive feedback affects

7.6 Conclusion

behavioural and clinical measures of stroke rehabilitation; (ii) the duration of any potential training-induced changes in behavioural or neurophysiological measures. We observed that the adopted shorter than usual FUI values for restorative BCIs may potentially enhance the motor performance following stroke; ii) following earlier phases of BCI training all behavioural and physiologic measures increased (week 3). However, after the later phases of neurofeedback training the behavioural index (ARAT) plateaued while the physiologic measures decreased (week 5). The observed trend may reflect the impact of early (or implicit) and late (or explicit) phases of motor imagery training. Further studies that investigate the mentioned factors (early and late phases of motor imagery training, and each individual FUI) separately with larger sample sizes are required to determine whether and to what extent each factor affects the motor performance following neurofeedback training.

In the next chapter we highlight the key contributions of the thesis and suggest future directions for further development of the reported findings.

Chapter 8

Conclusion and Future Work

THIS chapter outlines a summary of the conclusions of this dissertation and suggests further directions for future research on the investigated topics within the thesis.

8.1 Introduction

Primary applications of restorative BCIs has resulted in promising outcomes for enhancement of motor performance following stroke. However, its widespread clinical application and dissemination necessitates its optimization (Wolpow and Wolpow 2012b). To optimize restorative BCIs, two lines of research are being followed: (i) the signal processing approach investigates how to improve feature extraction and feature translation methods for BCIs using machine learning techniques; (ii) the user-centred approach, however, aims at eliciting more representative features through techniques such as feedback optimization. This thesis reports the studies conducted on both approaches for optimization of restorative BCIs. This chapter summarizes the key findings described in the thesis and discusses potential future works to further investigate suitability of the proposed techniques for optimization of restorative BCIs.

8.2 Thesis summary

Chapter 1 describes the origins of BCIs and their applications for stroke rehabilitation. Then, it outlines the thesis structure and contents. Chapter 3 provides the reader with required backgrounds on BCI components and applications to understand the following chapters of the thesis. BCI components have been divided into the following disciplines: signal acquisition, feature extraction, feature translation (classification), and BCI applications. Then, it provides a literature review on BCI application for stroke rehabilitation (restorative BCIs). Chapter 3 is concluded by listing the current challenges of restorative BCIs.

Chapter 4, that is the contribution of thesis on signal processing techniques, investigates a practical trade-off between parameters of a restorative BCI. It focuses on finding a feasible trade-off among the key parameters that while delivers real time feedback, does not degrade the accuracy substantially.

Chapter 5 describes the first study on feedback optimization and compares visual and proprioceptive feedback modalities. It concludes that the latter modality outperforms the former in eliciting stronger β -ERDs and the occurrence of conditional learning.

Chapter 6 explores the second study on feedback optimization and investigates the effect of FUI alteration on the performance of restorative BCIs. It concludes that FUI customization affects the BCI performance where its manifestation depends on the subjects' BCI aptitude.

Chapter 7 reports the last phase of studies on feedback optimization and explores the synergy between the findings reported in Chapters 5&6. It employs a proof-of-principle study design to explore the impact of neurofeedback training on motor performance of a stroke patient with FUIs within 16–96 ms range where the feedback modality is proprioceptive. It is concluded that neurofeedback training with proprioceptive feedback and FUIs within 16–96 ms range may enhance motor performance for stroke patients.

A number of study outcomes that have been published as conference papers have been added to this thesis in the Appendix section. Appendix A describes another study on signal processing that explores the suitability of particle swarm optimization (PSO) in training adaptive neuro-fuzzy inference system (ANFIS) classifiers. Appendix B proposes a novel feedback provision paradigm for restorative BCIs. Appendix C compares visual and proprioceptive feedback effect on BCI performance but using different measures than Chapter 5. It uses the classification accuracy and information transfer rate (ITR) and demonstrates that according to both metrics visual feedback is inferior to proprioceptive feedback. Appendix D explains a study that was conducted to investigate a novel and accurate predictor for BCI aptitude. It concludes that simple reaction time (SRT) test may be used as a predictor for subjects' BCI aptitude with almost 70% accuracy. Appendix E describes the characteristics of the designed and fabricated orthosis that was employed in the studies for provision of proprioceptive feedback.

8.3 Summary of author's original contributions

- **Investigation of a feasible trade-off between the classifier update rate, time window length, and the accuracy of the classifier:** Through offline analysis of a publicly available dataset, we concluded that adopting a time window length of 750 ms with FUI of 32 ms, provides accuracies of almost 70% while providing real time feedback (Darvishi *et al.* 2013a).
- **Studying the effect of feedback modality on the performance of restorative BCIs:** Through a study on healthy subjects we observed the superiority of proprioceptive over visual feedback in eliciting stronger β -ERDs and the occurrence of conditional learning (submitted to *Frontiers in Neuroscience*).

8.4 Potential future directions

- **Exploring the effect of FUI on restorative BCIs:** We observed that FUI alteration affects the BCI performance and the direction of impact depends on the subjects' BCI aptitude (under final preparation for submission to a journal).
- **Studying how shortening the FUI affects the motor performance following neurofeedback training:** We observed that shortening the FUI may enhance motor performance following BCI training with proprioceptive feedback (under preparation for submission to a journal).
- **Investigation of the suitability of PSO for training an ANFIS classifier:** We found that application of PSO instead of backpropagation for training the ANFIS classifier produces comparable results with traditional ANFIS, SVM, and LDA (Darvishi *et al.* 2012).
- **Exploring the effect of feedback modality on the classification accuracy and ITR:** We observed that proprioceptive feedback outperforms visual feedback with both metrics (Darvishi *et al.* 2015b).
- **Proposing a novel and objective predictor for BCI aptitude:** We demonstrated that the SRT test predicts the BCI aptitude with almost 70% (Darvishi *et al.* 2015a).

8.4 Potential future directions

Here, we discuss in brief some of the directions that future studies may pursue.

- Running studies with larger sample sizes to further investigate the effect of feedback modality on BCI performance.
- Conducting larger studies on the effect of FUI value on BCI performance. The FUIs may be taken with at least four different values within 16–96 ms range to further study the effect of this factor.
- Conducting larger studies on stroke patients to further explore the manifestations of early and late phases of neurofeedback training.
- Investigating the effect of FUIs on stroke patient populations. The FUI alteration effect may be explored through choosing at least four different values within 16–1000 ms range. Here each FUI should be investigated individually so as to extract conclusive information as a result of FUI customization.

- Studying a potential synergy between TMS application and neurofeedback training for stroke rehabilitation.

8.5 In closing

In this chapter we summarized the observations and conclusions made of this thesis followed by listing the potential directions for future work. The thesis has made a number of contributions towards feedback optimization for restorative BCIs. The work herein, is unique and original, providing the basis for further research on enhancement of restorative BCIs.

Appendices

Appendix A

Classification of Motor Imagery EEG Signals using Adaptive Neuro-Fuzzy Inference System Trained by Particle Swarm Optimization

AS discussed in Chapter 3, whenever the relationship between the features and classes is not simple, traditional methods for estimation of the model parameters may fall into sub-optimal points (local minima). Evolutionary algorithms such as particle swarm optimization (PSO) has been shown to be robust against this drawback. Therefore, in this study, we compare the performance of an adaptive neuro-fuzzy inference system (ANFIS) classifier that its parameters have been estimated using PSO, with a traditional ANFIS that uses backpropagation for its parameter estimation. The results depict that tuning ANFIS with PSO provides classification accuracies comparable with traditional ANFIS and other robust classifiers such as support vector machines and linear discriminant analysis.

A.1 Introduction

Brain-computer interfaces (BCI) applications have experienced increasing attention during the last decade (Vaughan and Wolpaw 2006). Among the primary procedures of EEG-based BCI systems, including preprocessing, feature extraction and classification, the last step (classification) is one of the most challenging, due to the highly stochastic nature of the EEG signal. Several linear classifiers such as linear discriminant analysis (LDA), linear support vector machine (SVM) and non-linear classifiers such as neural networks and adaptive neuro-fuzzy inference system (ANFIS) have been proposed to classify EEG signals and each of them has shown to be efficient for different types of EEG features such as P300, steady-state visual evoked potentials (SSVEP) and sensorimotor rhythms (motor imagery signals). Note that ANFIS due to its robustness, originating from both neural network and fuzzy inference systems, appears to have the potential to be used as a suitable classifier for motor imagery EEG signals (Darvishi and Al-Ani 2007). Neural network based methods such as backpropagation and least-mean-squares (LMS) estimation are employed to adjust the parameters of ANFIS fuzzy rules. Particle swarm optimization (PSO), which is an evolutionary optimization technique, has shown to be an efficient method for optimization (Ghomsheh *et al.* 2007). Therefore, in this study, we investigated training an ANFIS classifier using PSO instead of the application of backpropagation for ANFIS training.

The study in this appendix has been published in the *Proceedings of the IEEE EMB/CAS/SMC Workshop on Brain-Machine-Body Interfaces* (Darvishi *et al.* 2012).

A.2 Feature extraction and classification

We used dataset III of the BCI competition 2003 that comprises 140 test and 140 training trials. The EEG signals are recorded using three channels (C3, Cz, C4), and each trial lasts nine seconds. We applied a continuous wavelet transform (CWT) and Student's *t*-test to extract eight features from each trial i.e. four features from α (8–13 Hz) and four features from β (18–26 Hz) frequency bands. Fig. A.1 illustrates the feature extraction procedure and for a full description of the method refer to Darvishi and Al-Ani (2007).

To train the ANFIS classifier by PSO, we created a fuzzy inference system (FIS) by subtractive clustering. Then, we created a swarm of 10 particles; each held a collection of 125 parameters to be used for fine tuning of fuzzy membership functions of the created

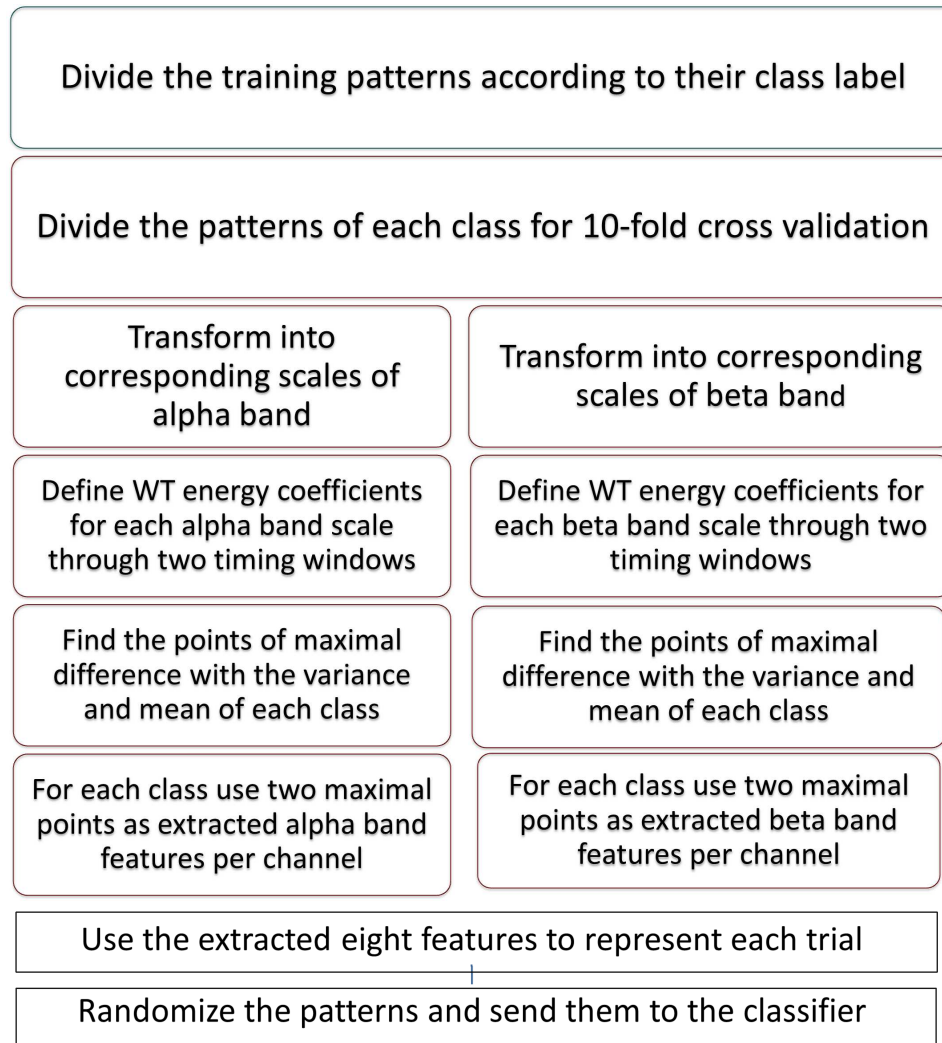


Figure A.1. Feature extraction procedure. This figure illustrates the steps taken for feature extraction.

FIS. Afterwards, all swarm members were evolved for 100 epochs and finally the particle with the best fit function was selected as the winner and the ANFIS parameters were replaced by the members of the winner particle. Fig. A.2 summarizes the adopted steps to train ANFIS using PSO. Using the selected dataset, we compared the results of ANFIS-PSO classifier with the traditional ANFIS that was trained by backpropagation, as well as LDA and SVM as benchmark classifiers which were fed by the same features of the training and test data.

A.3 Results and discussion

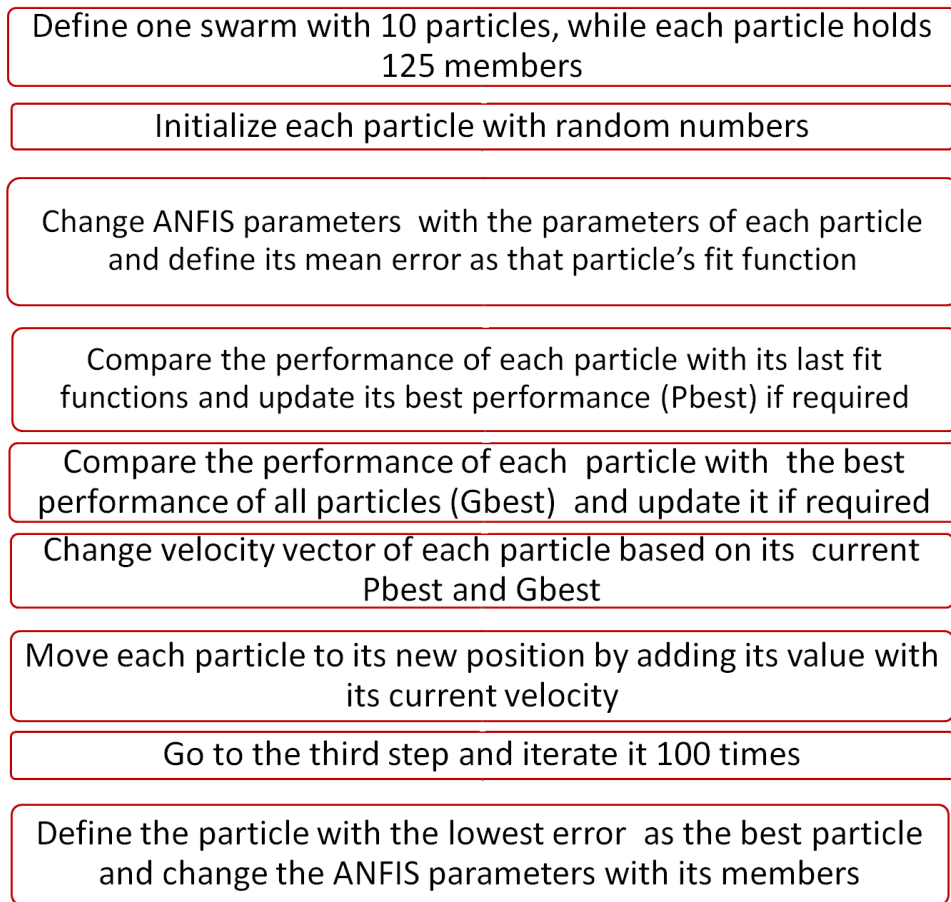


Figure A.2. Procedure for training ANFIS with PSO. This figure illustrates the training procedure of an adaptive neurofuzzy inference system (ANFIS) classifier using particle swarm optimization (PSO).

A.3 Results and discussion

As depicted in Fig. A.3, ANFIS-PSO and SVM classifiers achieved the highest accuracy in classifying training data (85.7%), which outperformed the traditional ANFIS trained by backpropagation. However, when classifying the test data, the traditional ANFIS performed slightly better than ANFIS-PSO, with LDA achieving the highest accuracy. In summary, it has been demonstrated that PSO is suitable for ANFIS training as to classify motor imagery EEG signals, with an accuracy comparable to those of other more common classifiers such as LDA, SVM, and conventional ANFIS.

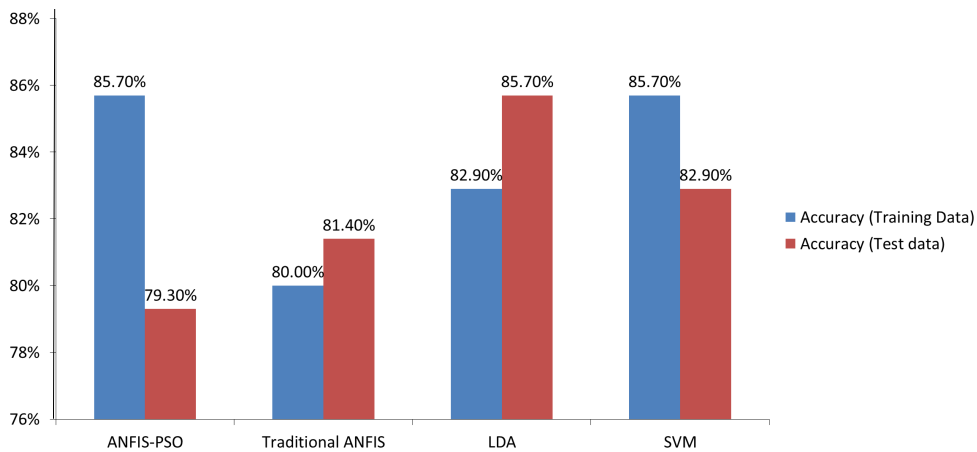


Figure A.3. Comparing the accuracy of classifiers for training and testing data. This figure compares the accuracy of four classifiers, i.e. linear discriminant analysis (LDA), support vector machines (SVM), traditional ANFIS, and ANFIS-PSO, with training and test datasets. Note that ANFIS-PSO provides results that are comparable with those of traditional ANFIS and other robust classifiers such as LDA and SVM.

Appendix B

Novel Feedback Provision for Restorative Brain-Computer Interfaces

RESTORATIVE brain-computer interfaces (BCIs) have been exploited by a number of BCI labs for stroke rehabilitation. The results that are achieved with commonly used methods are rather promising, but inconsistent. Here, we propose a novel paradigm for restorative BCI designs that is based on motor learning theory and the Hebbian learning rules that may promote neuroplasticity following stroke.

B.1 Introduction

Stroke is a major cause of paralysis. In the traditional rehabilitation of stroke, repetitive rehearsal of motor functions is exploited in hope that based on activity-dependent plasticity concept; impaired neural paths become reorganized the same way that they were established during early development of motor functions (Koganemaru *et al.* 2010).

Considering the similarity between activity in sensorimotor area of the human brain during motor imagery and the actual movement, motor imagery has been suggested as an alternative modality to enhance motor performance after stroke (De Vries and Mulder 2007). There is evidence that application of motor imagery in healthy subjects increases the cortical activity and thereby elevates the amplitude of motor evoked potentials (MEP) in response to transcranial magnetic stimulation (Kasai *et al.* 1997). The finding of Kasai *et al.* (1997) suggests that motor imagery can modulate corticospinal excitability in a way similar to motor learning.

In contrast to the actual movement, motor imagery does not produce any muscular activities and thereby, no sensory feedback is received during motor imagery performance. However, sensory feedback is critical for motor learning. Thus, in this study we propose a novel method to provide sensory feedback during motor imagery BCI. In particular, we describe an approach to provide sensory feedback at a timing that will be optimal for practice dependent learning based upon Hebbian learning rules. We anticipate that this approach would offer significantly improved therapeutic options for stroke patients.

The study in this appendix has been published in the *Proceedings of the 5th International BCI meeting* (Darvishi *et al.* 2013b).

B.2 Methods

A combination of proprioceptive and visual feedback is thought to be the optimum sensory feedback for motor functions (Ramos-Murguialday *et al.* 2012). Even though there have been some trials to provide such feedback for motor imagery based restorative BCI designs, there is no clear rationale provided for the latency used between motor imagery performance and feedback reception (Ramos-Murguialday *et al.* 2012, Shindo *et al.* 2011). There is evidence that the latency for efferent route from the primary motor cortex (M1) to the median nerve is approximately 20 ms (Samii *et al.* 1998).

In addition, studies show that the required time for sensory feedback to travel from the median nerve to the M1 is approximately 25 ms (Stefan *et al.* 2000). Thus the total time for a motor learning loop (from cortex to the median nerve) is approximately 45 ms. Presuming a critical role for the Hebbian learning rules in practice dependent motor learning (Murphy and Corbett 2009) it seems crucial to provide sensory feedback during motor imagery based BCI training at an interval, i.e. 45 ms, similar to that of actual motor training. Fig. B.1 illustrates the timing of the proposed paradigm.

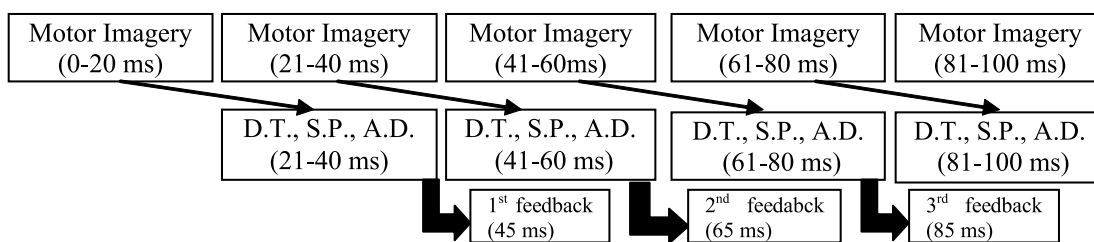


Figure B.1. Illustration of the novel feedback provision paradigm. Demonstration of timing between motor imagery, data transfer (D.T.), signal processing (S.P.), application delay (A.D.), and their consequent feedback arrival time to M1. As depicted, 45 ms after each 20 ms portion of motor imagery, its correspondent feedback reaches M1. Presuming continuous performance of motor imagery by the subject, this paradigm is expected to promote the occurrence of desired neuroplasticity in neurofeedback training following stroke.

B.2.1 The proposed design specification

- Classifier update rate: As the first 250–500 ms of motor imagery does not contain features related to motor imagery (Pfurtscheller *et al.* 1999), the classification of EEG features is proposed to be done using windows of 750 ms length, which slide 20 ms at each classification update. Thus, the classifier update rate is defined to be 20 ms (in conformity with efferent latency from the M1 area to the median nerve). In case of detection of the correct imagery by the classifier, a stimulatory feedback must be provided. Therefore, a fast and real-time BCI system that its total transfer time, i.e. the total time required for signal processing and the application delay, is as low as 20 ms, is required.
- Brain signal: We propose 3 channels of electroencephalogram (EEG) recordings to be used in this design to make classification update result available in the proposed short time frame.

B.3 Discussion

- Feedback modality: we propose visual and proprioceptive feedback through an orthosis such as the M-28 servomotor to flex 4 fingers of the subject for 1 degree every time that classifier detects the requested motor imagery based on the classification result, while having the subjects to look at their hand. A similar paradigm is described in (Ramos-Murguialday *et al.* 2012).
- Trial duration: We propose to use 2 seconds of rest, followed by 1 second of preparation using showing a “+” sign on the monitor to the subject. Then by showing them an arrow pointing towards their target hand, we instruct them to perform the motor imagery task for 2 seconds.
- Software platform: We propose BCI2000 (Schalk *et al.* 2004) to be used as our software platform for its fast and real time processing algorithms.
- Imagery pattern: For the occurrence of Hebbian based plasticity it is crucial that patients keep imagining 4-finger flexion for a period of 2 seconds, continuously.
- Sampling frequency: Regarding the fast proposed update rate (20 ms) sampling frequency is defined to be 500 Hz so as to provide enough sampling data for signal processing.

B.3 Discussion

We propose a novel design for a restorative BCI system for stroke rehabilitation with a timing similar to that of motor learning. Subjects are instructed to perform motor imagery and then every 20 ms receive concurrent proprioceptive and visual feedback. The provided feedback is expected to reach the M1 area after 25 ms and if sensory feedback diffusion to the M1 area coincides with M1 activation through motor imagery, it is expected to strengthen the connection between the primary sensory cortex and the M1. This may provide the basis for reorganization of the damaged neural networks involved with the motor tasks and leading to improvements in the impaired motor functions following stroke.

Appendix C

Feedback modality affects brain-computer interfaces

BRAIN computer interfaces (BCIs) are used for communication and rehabilitation. One of the main categories of BCIs is motor imagery based BCI (MI-BCI). A large number of studies have focused on machine learning approaches to optimize MI-BCI performance. However, enhancement of MI-BCI through the provision of optimized feedback modalities has not received equal attention. Motor imagery and motor execution activate almost the same area of the brain. During motor skills performance, a combination of proprioceptive and direct visual feedback (PDVF) is provided. Thus, we hypothesized that MI-BCI that receives PDVF outperforms the traditional MI-BCI, which only uses indirect visual feedback (IVF). We studied eight healthy subjects performing MI through (i) IVF and (ii) PDVF. We used eight channel electroencephalogram (EEG) signals and extracted features using an autoregressive model and classified MIs using linear regression. On average, PDVF increased the accuracy of MI performance by 11%, and improved information transfer rate (ITR) by more than two times. In conclusion, using PDVF appears to improve MI-BCI performance according to the studied metrics, making this approach potentially more reliable.

C.1 Introduction

Brain-computer interface (BCI) technology has established the foundation for the human brain to communicate with machines directly. Motor imagery (MI) based BCI (MI-BCI) that relies on the rhythm changes occur within the sensorimotor area of the brain during MI (Pfurtscheller and Aranibar 1979), is one of the main BCI paradigms. In non-invasive MI-BCI, the brain activity during MI is recorded using EEG (Birbaumer *et al.* 1999), functional magnetic resonance imaging (fMRI) (Weiskopf *et al.* 2004), or near infrared spectroscopy (NIRS) (Coyle *et al.* 2007). Among the aforementioned techniques, EEG is the most practical and affordable technique and thereby, the most commonly used modality in non-invasive MI-BCI applications.

One of the challenges of MI-BCI is its rather low accuracy and information transfer rate (ITR) (Wolpaw and Wolpaw 2012b). This drawback limits the dissemination of MI-BCIs for widespread application. Provision of optimum feedback is believed to improve MI-BCI performance metrics (Huggins *et al.* 2014). Proprioceptive feedback, visual feedback, or different combinations thereof are among the most common feedback modalities in MI-BCIs (Ang and Guan 2013). While visual feedback is mostly supplied via cursor position update on a monitor (Prasad *et al.* 2010), proprioceptive feedback has been provided using either orthoses (Caria *et al.* 2011) or robots (Ang *et al.* 2009). Nijboer *et al.* (2008), investigated the suitability of auditory feedback for MI-BCI, and found its performance comparable with indirect visual feedback (IVF). Ramos-Murguialday *et al.* (2012), applied concurrent proprioceptive and direct visual feedback (PDVF) as a feedback modality in MI-BCI restorative applications. The PDVF increased the accuracy of MI performance compared to either no feedback or sham feedback. However, they did not compare PDVF with other feedback modalities.

Motor execution and motor imagery of a particular task, activate almost the same area of the brain (De Vries and Mulder 2007). Thus, in search for optimization of feedback modality for MI-BCI, we surveyed different feedback types in motor learning. Enough repetition of a movement, followed by feedback, results in motor learning in healthy subjects. Intrinsic feedback is realized through proprioceptive and/or visual sensory inputs as a result of the performed motor task. Extrinsic (augmented) feedback, however, is provided artificially by an external agent to enhance the motor learning outcomes; an example of this are athletes who learn new moves via auditory feedback from the coach (van Vliet and Wulf 2006). When augmented feedback

is added to intrinsic feedback, it improves the retention and motor learning outcomes by the provision of knowledge of performance and/or knowledge of result (Thorpe and Valvano 2002). In contrast to motor learning, there is no muscle activation during motor imagery and, therefore, no source of feedback. As a consequence, an external actuator is required to supply extrinsic feedback in MI-BCI setups. Provision of IVF through updating the cursor position on a monitor is currently the most ubiquitous feedback modality in BCI applications (Ramos-Murguialday *et al.* 2012). This type of feedback arrangement might be quite sufficient for some BCI applications, such as in the P300-based Speller (Donchin *et al.* 2000). However, considering the outcomes of motor learning studies on feedback modalities (Magill 2014), IVF may not be as effective in MI-BCI because it lacks intrinsic (direct) feedback to close the sensorimotor loop. By contrast, PDVF, in addition to the augmented feedback of IVF, provides intrinsic visual and proprioceptive feedback.

While PDVF provides feedback that is closest to motor learning, supplying IVF via updating cursor position on a monitor remains the most prevalent feedback modality in MI-BCI setups. Recently, Jeunet *et al.* (2014), suggested that current BCI training approaches that use IVF were suboptimal and need to be improved. Thus, we compared two similar BCI designs that used either IVF or PDVF with eight BCI-naive subjects, to investigate alternative feedback modalities for MI-BCIs. According to our results, PDVF seems to be superior to the traditional IVF that promotes the application of PDVF to make MI-BCIs more efficient and accurate.

The study in this appendix has been published in the *Proceedings of the 7th International IEEE/EMBS Conference on Neural Engineering* (Darvishi *et al.* 2015b).

C.2 Methods

C.2.1 Subjects

The study was approved by the human ethics committee of the University of Adelaide and conformed to principles outlined in the Declaration of Helsinki. All subjects provided their written informed consent to take part in the study, and all recorded data were de-identified. Ten subjects (six males) aged 24–40 years were recruited for this study. All subjects were asked to attend an induction session prior to the BCI sessions.

C.2 Methods

During the induction session, they were trained to remain alert, immobile, and concentrate during the experiments. Also, visual and kinaesthetic MI were explained to them, and then they practised these techniques.

Only eight out of ten subjects (four females, four males) whose right vs. left hand MI performance were distinctive, passed the screening test and were allowed to participate in the study (training sessions).

C.2.2 BCI Setup

A 72 Channel Refa TMSi EXG amplifier, containing 64 unipolar and eight bipolar channels and a 64 channel Waveguard EEG cap, were used for data acquisition. Only eight out of 64 channels (F3, F4, T7, C3, Cz, C4, T8, Pz) were used to record EEG data. The AFz channel was used as the ground channel, to follow the recommendation of the manufacturer. Due to the very high input impedance (in the order of tera-ohms) of the instrumentation amplifier (Volosyak *et al.* 2010), the impedance between the scalp and recording electrodes were kept below 50 k Ω . As the amplifier uses a built-in common average referencing procedure, there is no need to use an external reference channel to be attached to nose or ears. Any electrode with impedance more than 256 k Ω is considered as disconnected by the amplifier firmware and is excluded from common average reference calculation. The sampling frequency was 1024 Hz and every sample block contained 24 samples. The EEG signals were passed through a 50 Hz notch filter to remove the power line noise. To remove DC offset and nonrelated high frequency elements, a band pass filter with corner frequencies set to 0.1 and 40 Hz was also applied. After amplification and filtering by the amplifier, EEG signals were transferred through a 10-metre-long fiber optic cable to a FUSBi fibre to USB converter. Then they were conveyed to a PC using a USB cable. The PC contained an Intel Core-2 Duo 3.166 GHz processor, 3 GB of RAM, and used the Windows XP service pack 3 operating system. It was also mobilized with a 23" LCD monitor with a display update rate of 60 Hz to provide the IVF feedback.

Note that BCI2000 (Schalk *et al.* 2004) was adopted as the software platform for the study because of its real time characteristic. We customized the source code of the software to supply auditory commands. We also altered the application module of the software to progressively update servomotors position throughout the feedback section of each trial.

To provide PDVF, we fabricated a platform with two orthoses (one for each hand) to passively flex four fingers incrementally, according to the attributes of the MI of the target hand. Each orthosis included a servomotor (Blue Bird BMS-630) and mechanical structure made of PVC. The BCI2000 supplied the control commands for servomotors operation that were transformed via a Micro Maestro servo controller module to a format readable by the servomotors.

C.2.3 Study design

Each participant took part in one screening session followed by an online training session. The goal of the screening session was to identify the extent to which subjects could produce distinctive EEG signals with right/left hand MI. The most discriminating features of each subject's EEG signals were extracted and used to calibrate their following training sessions. The extracted features of EEG signals, produced during online sessions, were classified in real time to generate control signals that were used to provide either PDVF or IVF.

C.2.4 Screening session setup

During the screening session, each participant went through three runs of MI of right/left hand. In each run subjects were instructed to perform ten right and ten left hand MI in a randomized order. At the onset of each trial, an auditory command of "left" or "right" was supplied concurrently with an equivalent visual stimulus. To present the visual cue, a monitor was placed one metre away from the subject at which an arrow pointing to either the left or right was shown. The sound levels of the auditory commands were kept constant throughout the study. The subjects were instructed to perform MI of their target hands involving four finger flexion within the 3-second-long period in which the arrow was shown. The subjects were cued to stop the MI and concentrate on their breathing (relaxation) when the arrow disappeared. After three seconds of relaxation, they were given new stimuli to perform MI for the next trial. To appreciate the specificity of MI attributes of each subject, the combination (left vs. relax or right vs. relax) that resulted in the highest value of the coefficient of determination (r^2) was selected for each individual, where r^2 represents the proportion of the single-trial variance that is due to the task. While for the majority of subjects right vs. left hand MI generated the highest discrimination in sensorimotor rhythms; only right vs. rest

C.2 Methods

and left vs. rest were considered in the current study to minimize the cognition load and fatigue level.

C.2.5 Subjects' optimum features

According to the findings by Pfurtscheller *et al.* (1997), MI of hand movement results in a decrement followed by an increment in the spectral power of sensorimotor rhythms. The former is known as event related desynchronization (ERD) whereas the latter is called event related synchronization (ERS). According to the results of the same study, for the majority of cases these phenomena occur in the contralateral sensorimotor area within the α (8–13 Hz) and β (16–26 Hz) frequency bands. However, in some occasions, ERD and ERS may occur bilaterally. To extract the relevant features of MI as early as possible during the online sessions, only ERDs were considered. Among the eight subjects that proceeded to the online session, six subjects generated only contralateral ERDs, whereas the other two exhibited bilateral ERDs.

C.2.6 Feedback provision

Every 24 ms either the position of the cursor on the monitor (IVF feedback) or the angle of the orthosis (PDVF feedback) was updated according to the classifier outputs. Feedback modality of the first run was randomly selected and then was alternated for the subsequent runs. To ensure availability of a sufficient amount of data for comparison, the minimum number of runs set to be four. If subjects were not exhausted, the number of runs could rise to eight.

C.2.7 Online training session

All participants took part in an online training session no later than two weeks after their screening sessions. The online session included 4-8 runs of MI of right/left hand four-finger flexion. Each run comprised 15 randomly presented trials with 8/7 left or right hand MIs and 7/8 relaxations. Trials started with auditory commands of "left/right" or "relax" that cued participants to start MI or relaxation according to the command. Then, feedback provision section started after two seconds of trial onset and became updated every 24 ms for 2.5 seconds. Finally, an auditory "beep" signal,

cued the end of the trial. The following trial was initiated after a four-second-long break.

C.2.8 Power spectrum estimation

EEG signals become blurred because of the heterogeneity of the tissues of the cortex and the scalp. A large Laplacian filter, which is an effective method for reduction of data blurring (Hjorth 1991), was applied, to enhance the spatial resolution of the EEG signals. The maximum entropy method (MEM) (Marple 1987) was adopted, to define an autoregressive (AR) model of the EEG data. It was chosen over fast Fourier transform (FFT) due to its capability of robust power spectrum estimation for short time series (Marple 1987). The spectral power of the most recent 500 ms was progressively estimated every 24 ms at the predefined frequencies and electrode positions.

C.2.9 Classification

A linear regression algorithm was used to classify the extracted feature of the EEG data every 24 ms (the duration of each sample block) due to its simple procedure and fast processing time. The classification results showed whether the subject's performance during the most recent 500 ms conforms to the requested task (either left/right hand MI or relaxation). Finally, the classification result was transferred to the application module to provide either IVF or PDVF.

C.2.10 Performance measures

Two measures were used, to compare the effects of different feedback modalities on the BCI performance. First, the conventional measure of the percentage of the trials that ended with a hit in each run as an index of accuracy was applied. As a second metric, the information transfer rate (ITR) that simultaneously appreciates the accuracy and speed of data transfer (McFarland and Krusienski 2012) was used. To calculate the ITR in bits per minute, Equation C.1 was adopted (McFarland and Krusienski 2012)

$$\text{ITR} = \log_2 N + P \log_2 P + (1 - P) \log_2 \left(\frac{1 - P}{N - 1} \right) \left(\frac{60}{8.5} \right) \quad (\text{C.1})$$

C.3 Results and discussion

where N is the number of classes, which is two in this study, P is the classification accuracy of each run, and 8.5 is the duration of each trial in seconds.

C.2.11 Statistical analysis

Since the resultant values of the aforementioned metrics did not have a normal distribution, the two-sided unpaired Wilcoxon rank-sum test (Wilcoxon 1945) was used. Due to the application of two comparison measures, Bonferroni correction for multiple comparisons was applied.

C.3 Results and discussion

Task performance was quantified using accuracy (hit rate percentage) and the ITR. Fig. C.1-A compares the hit rate percentage distribution between PDVF and IVF. It shows that PDVF with an average accuracy of 83% outperforms that of IVF by 11% ($p = 0.0015$). Fig. C.1-B indicates the comparison between the ITR distribution out of PDVF and IVF setups. The figure depicts that using PDVF results in the average ITR of 2.81 bits/min which is greater than two times of the average ITR of IVF (1.32 bits/min) ($p = 0.001$).

The main finding of our study is that the adoption of PDVF in MI-BCI systems significantly improves the accuracy and ITR of the BCI setup. While PDVF only improves the average accuracy by almost 10%, it resulted in enhancing the ITR by more than two times due to the logarithmic relationship between the ITR and accuracy. In other words, application of PDVF enables subjects to communicate more than two times faster than IVF.

Our results are in agreement with the findings of Gomez-Rodriguez *et al.* (2011), who showed that supplying proprioceptive feedback in parallel with IVF enhances the accuracy of MI performance compared to that with only IVF. However, they only studied the effect of adding proprioceptive feedback to the IVF. Thus, prior to our study, it remained unclear whether and to what extent PDVF (the regular feedback for motor learning) outperforms IVF (the most used feedback with MI-BCIs).

According to the Kahneman's attention theory (Magill 2014), attention resources of the human brain are limited. In other words, it is difficult for human agents to focus

on many different tasks concurrently. Thus, it makes it cumbersome to fully concentrate on both MI task and realizing IVF, simultaneously. In contrast, when PDVF is received during MI performance, the intrinsic visual and proprioceptive sensory feedback mechanisms are perceived quite similar to feedback perception in motor learning. Therefore, it may be concluded that receiving PDVF improves the MI performance whereas, receiving IVF may even distract subjects from MI performance.

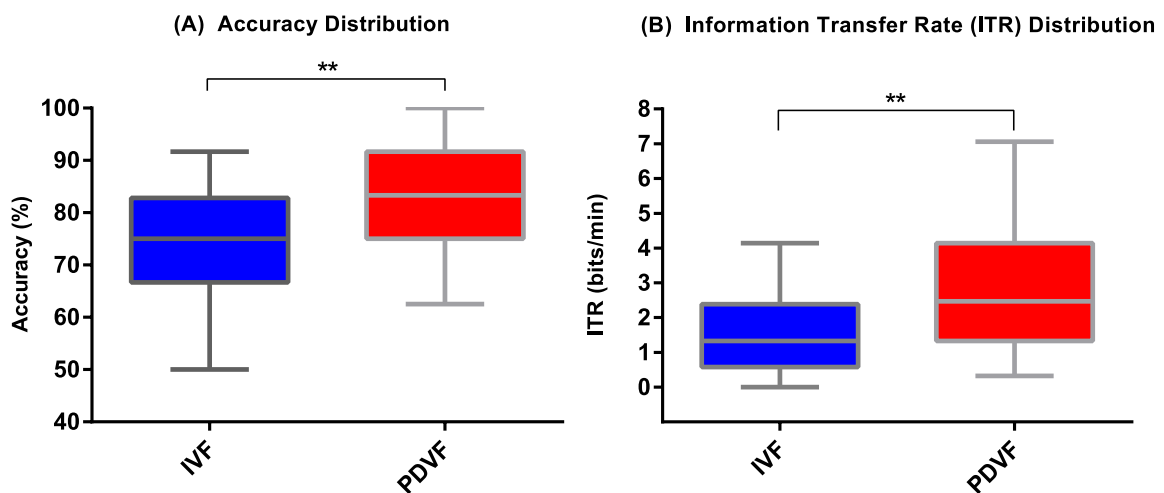


Figure C.1. Accuracy and information transfer rate (ITR) comparison for visual and proprioceptive feedback. Comparing the accuracy and ITR between two equal MI-BCI setups where either PDVF or IVF feedback provided. The edges of the boxes are the 25th and 75th percentiles, the horizontal line in each box is the median, and the whiskers extend to the minima and maxima (**: $p < 0.01$).

C.4 Conclusion

In the current study, the feature extraction and classification procedure used for both PDVF and IVF feedback were entirely equivalent. Thus, the improvement of the adopted metrics is expected to be due to more discriminant features elicited from PDVF. Specifically, receiving PDVF enables subjects to produce MIs that are easier to differentiate from relaxation compared to those with IVF. These high quality MIs in turn, lead to improved control over the BCI task and results in higher accuracy and faster communication. Thus, provision of PDVF feedback in MI-BCI may be used to render MI-BCI communication faster and more accurate.

Appendix D

Reaction Time Test Predicts Brain-Computer Interface Performance

BRAIN computer interfaces (BCIs) enable human brains to interact directly with machines. Motor imagery based BCI (MI-BCI) encodes the motor intentions of human agents and provides feedback accordingly. However, 15–30% of people are not able to perform vivid motor imagery. To save time and monetary resources, a number of predictors have been proposed to screen for users with low BCI aptitude. While the proposed predictors provide some level of correlation with MI-BCI performance, simple, objective and accurate predictors are currently not available. Thus, in this study we have examined the utility of a simple reaction time (SRT) test for predicting MI-BCI performance. We enrolled ten subjects and measured their motor imagery performance with either visual or proprioceptive feedback. Their reaction time was also measured using an SRT test. The results show a significant negative correlation ($r \approx -0.67$) between the SRT and MI-BCI performance. Therefore the SRT may be used as a simple and reliable predictor of MI-BCI performance.

D.1 Introduction

Brain-computer interfaces (BCI) provide a modality for the human brain to directly control robots and machines. A motor imagery based BCI (MI-BCI) is a particular type of BCI that encodes motor imagination of a specific part of the body. It may use functional magnetic resonance imaging (fMRI), near infrared spectroscopy (NIRS), magnetoencephalography (MEG) or electroencephalography (EEG) to record motor intentions. In this study EEG was used to record motor imagery signals. The EEG based MI-BCI decodes spectral power changes within sensorimotor rhythms (Pfurtscheller *et al.* 1997) originating from motor imagery performance. According to the decoded motor intention, feedback is supplied to the user, providing knowledge of performance.

It is believed that 15–30% of people are BCI-illiterate (Blankertz *et al.* 2010), i.e., they are not able to produce vivid motor imagery. Prediction of MI-BCI performance not only eliminates user's frustration after a long training time with no success, but it also saves time and monetary resources of research projects. In addition, it may help revealing the underlying reasons of BCI illiteracy. To this end, some neurophysiological and psychological predictors have been proposed.

Blankertz *et al.* (2010) proposed a neurophysiological predictor that is calculated from a 2-minute EEG recording, where subjects are relaxed with eyes open. The proposed measure showed a correlation of $r = 0.53$ with MI-BCI performance in a study involving 80 subjects. Halder *et al.* (2013) used structural integrity and myelination quality of deep white matter structures of the brain with a correlation of up to $r = 0.63$ in a study of 20 subjects. Ahn *et al.* (2013) also showed that high θ and low α band powers were noticeable only among users with low MI-BCI aptitude. The suggested index showed to be correlated with BCI performance with $r = 0.59$ in a study of 62 subjects. Bamdadian *et al.* (2014) revealed that modulation of high frontal theta and lower posterior α prior to motor imagery performance is correlated with high BCI accuracy with $r = 0.53$ in a study involving 17 subjects. Fazli *et al.* (2012) also showed that near-infrared spectroscopy (NIRS) activity prior to MI performance is correlated with BCI performance fluctuations in nine out of their 14 studied subjects. Grosse-Wentrup *et al.* (2011) demonstrated that modulation of the sensorimotor rhythms, induced by motor imagery, is positively correlated with the power of frontal and occipital γ oscillations. They also showed that it is negatively correlated with the power of centro-parietal γ oscillations.

Appendix D Reaction Time Test Predicts Brain-Computer Interface Performance

Regarding psychological predictors, Vuckovic and Osuagwu (2013) used kinaesthetic and visual imagery questionnaires. They suggested that the kinaesthetic imagery questionnaire can be a useful predictor of MI-BCI performance. Hammer *et al.* (2012) used the Two-Hand Coordination Test and Attitude Towards Work Test on 83 subjects and observed a moderate correlation with MI-BCI performance.

All measures reviewed above show some level of correlation with the MI performance quality. However, the neurophysiological measures require EEG, MEG, fMRI, or NIRS to be recorded with specific equipment. The psychological measures appear to suffer from inaccuracy, subjectivity and low resolution (e.g. questionnaires). Thus, the need for novel MI predictors that are simple, objective and accurate with no need for specific equipment remains desirable.

Online visual or proprioceptive feedback has been shown to improve MI-BCI performance (Gomez-Rodriguez *et al.* 2011, Neuper *et al.* 1999). Such real time feedback provides knowledge of performance and enables their recipients to adjust their motor imagery accordingly. Thus, we hypothesized that participants, who are quicker in feedback realization and subsequent motor imagery adjustment can benefit more from online sensory feedback than their slower counterparts and perform MI more accurately. To test this hypothesis, we compared the accuracy of BCI performance of ten participants with their simple reaction time (SRT) test (Meyer *et al.* 1988). To appreciate the effect of feedback modality on the BCI performance (Vukelić and Gharabaghi 2015a), motor imagery performance with either visual or proprioceptive feedback was measured separately.

The study in this appendix has been published in the *Proceedings of 37th Annual International Conference of the IEEE Engineering in Medicine and Biology Society* (Darvishi *et al.* 2015a).

D.2 Methods

D.2.1 Subjects

Ten able-bodied participants (six males), 20.8 ± 2.2 years old, were recruited among the undergraduate students of the University of Adelaide. The study was approved by the local Ethics Committee, and all participants provided their written consent to take part in the study.

D.2 Methods

D.2.2 Hardware and software

We used a 64 channel Waveguard EEG cap with a 72 channel Refa TMSi EXG amplifier to record EEG signals. The recorded data were sent to a PC after amplification through a 10-metre-long fiber optic cable. The BCI2000 (Schalk *et al.* 2004) was used as the software platform. We customized the source module of the BCI2000 to record data in real time and also modified its application modules to communicate with orthoses that provided proprioceptive feedback.

D.2.3 Screening session

The proposed imagery task for the online session was designed to be either right hand motor imagery versus rest or left hand motor imagery versus rest. As a common practice, a screening session was held prior to the online training session, in which EEG data were recorded from the bilateral hand representation (FC3, FC4, CP3, CP4, C3, C4). During the screening session, three runs of right/left hand motor imagery were recorded. Each run contained ten right and ten left hand motor imagery trials that were performed in a random order. Subsequently, the screening session data were analysed for each subject and the EEG channel and frequency within 8–30 Hz that maximized the coefficient of determination (r^2) were selected. The optimal task combination (left hand motor imagery vs. rest or right hand motor imagery vs. rest) was also chosen for each participant according to their (r^2). Fig. D.1 illustrates the time course of the screening session.

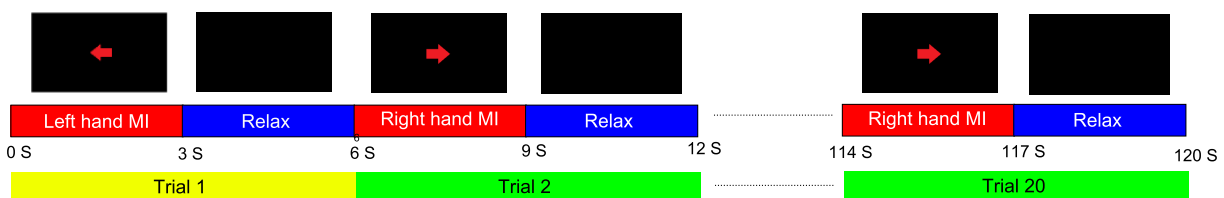


Figure D.1. Screening session time course. Fig. D.1 illustrates the timing procedure of the screening session.

D.2.4 Online training session

Every participant attended two online training sessions with proprioceptive and visual feedback, respectively. The sessions were held in different, days and the feedback

Appendix D Reaction Time Test Predicts Brain-Computer Interface Performance

update rate in both sessions was set to be 16 ms as the fastest technically possible feedback update rate. Each training session included eight runs of 20 trials each (10 hand motor imageries, ten rest), where consecutive runs had two minutes of break in between.

- **Data recording and pre-processing:** During the online session data were recorded from five channels: the selected channel (according to the screening session) and its four closest medial, central, anterior, and posterior channels. The sampling frequency was set to 1000 Hz, and signals passed through a 50 Hz notch filter (3rd order Chebyshev) followed by a band pass filter (1st order Butterworth) with corner frequencies set to 0.1 and 40 Hz. Finally, the central channel was subjected to spatial filtering (small Laplacian).
- **Feature extraction and classification:** In this study feedback was updated every 16 ms. Thus, the features were extracted with a method that made the least possible group delay (Marple 1987). Maximum entropy method (MEM), which is based on autoregressive modelling provides higher temporal resolutions and therefore lowers the group delay compared to Fourier transform (Marple 1987). Accordingly, a 20th order autoregressive (AR) model was built, to extract spectral features. The coefficients of the AR model were employed to estimate the spectral power of the most recent 500 ms time window of motor imagery. Considering the real time constraints of the adopted BCI design, the extracted features were classified using logistic regression. The classification result was updated every 16 ms according to the spectral power of most recent 500 ms time window.
- **Feedback provision:** In this study two different feedback modalities were provided within two separate training sessions. While a proprioceptive feedback was given through an orthosis during the first session, visual feedback through cursor position update on a monitor was provided during the second session.

In the runs with visual feedback, at the start of each trial, a “start” auditory command initiated the preparation phase. After 2 s either a “relax” or “right/left” auditory command was provided. Simultaneously, a rectangular target was presented at either the lower or upper right side of a monitor. After another 2 s the feedback period started by presenting a circle in the middle left side of the

D.2 Methods

screen. Then for 2.5 s, while the circle was moving from left to right with a constant speed, its vertical position was updated every 16 ms according to the classifier result that decoded participant's intention. When the circle finally reached the right edge of the screen if it hit the target, the circle and target's colour turned to yellow and then disappeared after 1 s. The next trial was initiated, after a 3 s inter-trial interval.

In the runs with proprioceptive feedback, the timing of trials matched to trials with visual feedback. In these trials, proprioceptive feedback was provided through flexion of the target hand's four fingers by an orthosis. At the start of each trial, a "start" auditory command cued the trial onset. Two seconds later either a "right/left" or a "relax" auditory command instructed the participant to perform either motor imagery of the target hand's four finger flexion or relaxation. After another 2 s, if the participant's intention (reflected in the classifier output) was congruent with the instructed command, the orthosis flexed the target hand for 0.4 degree and this procedure was repeated every 16 ms for 2.5 s (156 times). In case of the "relax" command, the redundant orthosis with no hand involvement was flexed similarly to provide knowledge of performance.

D.2.5 SRT Measurement

To measure the reaction time of participants, a simple reaction time (SRT) test was carried out, using the CANTAB battery test of Cambridge Cognition. To perform the SRT test, participants sat on a chair and were asked to concentrate on a tablet computer placed on a desk in front of them and to press the button on a press pad as soon as they saw a square on the screen. Each participant performed the task 30 times to obtain the average latency (reaction time), which was used as their SRT index.

D.2.6 Performance measures

To calculate the accuracy of motor imagery performance, the traditional measure of hit/miss percentage was used. Note that, while with proprioceptive feedback it was not clear for the participant if the trial ended with hit or miss, the final result was available to the instructor. For each participant only the average value of each session accuracy was considered. Thus each participant's performance was assessed with

Appendix D Reaction Time Test Predicts Brain-Computer Interface Performance

Table D.1. BCI accuracies and reaction time results. MI-BCI performance of 10 participants with either visual or proprioceptive feedback and their simple reaction time test result.

Participants	BCI accuracy (visual) (visual)	BCI accuracy (proprioceptive) (proprioceptive)	SRT (ms)
P1	65%	53%	244
P2	89%	86%	206
P3	75%	84%	214
P4	58%	59%	230
P5	62%	67%	245
P6	98%	97%	214
P7	56%	56%	221
P8	76%	64%	219
P9	89%	89%	221
P10	86%	83%	208

three indices: BCI accuracy with visual feedback, BCI accuracy with proprioceptive feedback, and the SRT index (Table D.1).

D.3 Results

To investigate the relationship among the aforementioned measures, a correlation analysis between the SRT and both BCI accuracy indices was run. The Pearson correlation coefficient between the SRT and BCI accuracy with visual feedback was $r = -0.6712$ ($p = 0.0336$) while its value between the SRT and BCI accuracy with proprioceptive feedback was $r = 0.6684$ ($p = 0.0346$). However, due to the small sample size of 10, the calculated Pearson correlation coefficients may be biased. Thus, we calculated Pearson correlation coefficients of 100,000 bootstrapped data samples and then calculated their mean value (r' , estimated correlation coefficient), its standard deviation and 95% confidence intervals (2.5th and 97.5th centiles of the 100,000 correlation coefficients). It resulted in $r' = -0.6835 \pm 0.1295$ (-0.4024 – -0.8988) between the SRT and accuracy with visual feedback and $r' = -0.6714 \pm 0.1403$ (-0.3702 – -0.8891) between the SRT and accuracy with proprioceptive feedback. Therefore, it reassures the reported significant correlation between the SRT and BCI accuracy with both visual and proprioceptive feedback at a 95% confidence interval.

D.4 Discussion

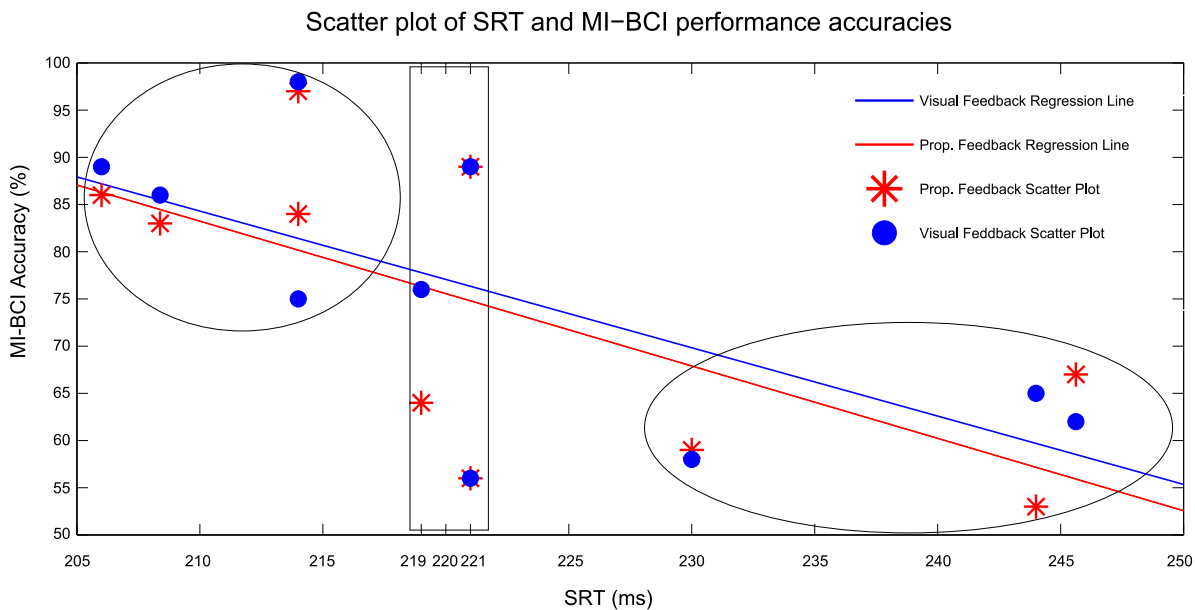


Figure D.2. Relationship between classification accuracies with visual and proprioceptive feedback and the SRT. Scatter plot of correlation between simple reaction time (SRT) and MI-BCI performance accuracy with visual and proprioceptive feedback (Prop: proprioceptive).

According to Fig. D.2, most participants with higher BCI accuracies have shorter reaction times, vice versa. However, there are three exceptions (P7–P9), which stay in the rectangular boundary area. Thus defining a threshold value of 220 ± 2 ms, allow the other seven participants to form two entirely distinctive clusters (elliptical shapes) with good margins from the boundary area. To sum up, it categorized correctly seven out of ten participants with a high level of certainty.

D.4 Discussion

The main finding of this study is a significant negative correlation ($r \approx -0.67$) between one's reaction time and their accuracy of motor imagery performance. The novel proposed measure shows a comparable (or slightly better) level of correlation compared with existing MI-BCI performance predictors. In the meantime, it is simple, fast, objective, and does not require specific equipment. Note that, while we measured the SRT using dedicated Cambridge Cognition equipment for higher reliability, any PC or tablet is able to compare users' reaction time through open source software.

Performing motor imagery within an MI-BCI setup involves motor planning, followed by feedback realization and re-adjustment of motor imagery. However, the provided

Appendix D Reaction Time Test Predicts Brain-Computer Interface Performance

continuous feedback can be beneficial only if the users are able to realize it in real time and potentially adjust their subsequent motor imagery. One application of the reaction time test is to show how a person interacts with the performance environment while preparing to produce a required action (Magill 2014) . Thus, it seems reasonable to assume that people with shorter reaction times are better able to adjust their motor imagery performance while receiving rapidly updated sensory feedback. This assumption may explain the reported negative correlation between the SRT and MI-BCI performance to some extent. Similarly, users with longer reaction time may not be able to realize fast sensory feedback in real time and therefore not benefit as much as their quicker counterparts from rapidly updated feedback. On the contrary, provision of quickly updated feedback may even deteriorate MI-BCI performance of those users. However, we did not study the MI-BCI performance of participants with longer reaction times in conjunction with receiving feedback at slower update rates.

To provide users with a fast feedback update rate, it was updated every 16 ms (\approx 62 Hz). Note that this parameter was set as 16 ms while realizing that frequencies of interest for MI-BCI occur within α and β frequency bands (8-30 Hz). Moreover, it is worth mentioning that the age range of the participants in this study was fairly narrow (19–26 years). Also we only tested the MI-BCI performance where feedback updated very quickly (every 16 ms) and thus required a high level of cognitive and processing resources. Thus, care must be taken when generalizing the reported relationship between the SRT and MI-BCI performance to the other age groups and slower feedback update rates.

D.5 Conclusion and further development

In this study we proposed the SRT as a novel index for prediction of MI-BCI performance. Our results show that it can be used as a simple, objective and moderately accurate measure for MI-BCI performance prediction. Future work will benefit from studying the effect of slower feedback update rate on BCI performance of subjects a with wider age range.

Appendix E

Specification of the Fabricated Orthosis

IN this appendix the specification of the custom-made orthosis that was designed, fabricated and program by the PhD candidate is provided.

E.1 Introduction

Since all studies reported in this thesis involve application of proprioceptive feedback, an application specific orthosis that can flex/extend four fingers in real-time was designed, fabricated, and programmed by the PhD candidate (Fig. E.1). In this appendix specification of the orthosis including its mechanical parts, controller, servomotors and the software is provided.

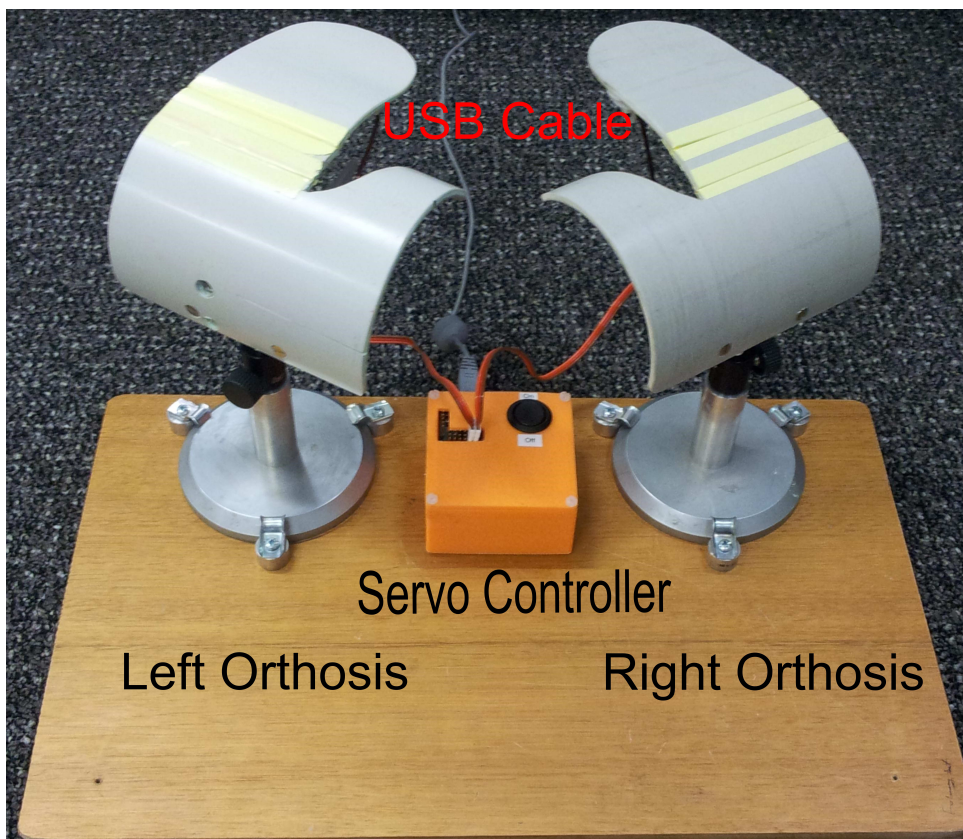


Figure E.1. Application specific orthosis. This figure illustrates the application specific orthosis that was designed, fabricated and programmed by the PhD candidate

E.2 Mechanical design

As it can be seen in Fig. E.1, two orthoses are mounted on a wooden board that is 30 cm wide and 50 cm long. Each orthosis comprises a mechanical body made of PVC that supports participants' hands in all assumed situations (from fully flexed fingers to fully extended fingers). The orthoses are attached to the wooden board using modular bases that allow adjustment of the orthoses angles (tilt and pan) in all directions.

E.3 Electrical design - servomotors and controllers

To flex/extend four fingers of each hand using the orthoses, two Blue Bird BMS-630 servomotors (one for each orthosis) were used to receive commands from a controller and adjust the angles of the orthoses, incrementally.

A Micro Maestro servo controller module that can control up to 6 servomotors was used to receive commands from BCI2000 software (Schalk *et al.* 2004) and translate them to a readable format for servomotors. The controller can read the current position of each servomotor and instruct it to a new position. For further details on the specifications of the controller see <https://www.pololu.com/product/1350>. Fig. E.2 depicts the used servomotors and controllers for the orthoses fabrication.

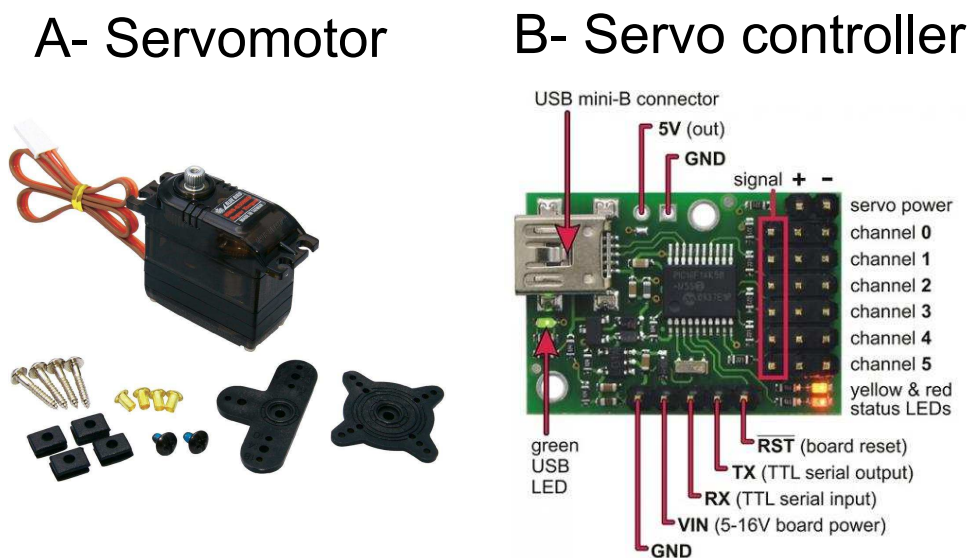


Figure E.2. Servomotors and the Micro Maestro controller. Panel A Shows the servomotor and Panel B shows the controller.

E.4 How the orthoses work

To update the flexion angle of the orthosis with proprioceptive feedback, for every feedback update the control signal of the BCI2000 software, that is a normalized value that represents current status of the oscillatory cortical signals, was used to determine whether ERD or ERS has occurred. The control signal was used as a binary value as a go/no go signal to change or not change the orthosis angle. With motor imagery

E.5 Software

trials, for instance, having a negative control signal (that represented ERD) flexed/extended the orthosis for a constant angle (go signal), while a positive control signal, that represented ERS, would lead to no movement (no go signal).

With visual feedback condition, the control signal has been used throughout this thesis as an analogue signal to update the vertical position of the cursor on a monitor. More specifically, with every feedback update the vertical position of the cursor was updated by addition of the previous vertical position and the control signal followed by a normalization procedure to not exceed the height of the monitor. Then, this procedure was repeated for 105 times (for an FUI of 24 ms) within the 2.5 s feedback period.

Note that if the control signal for proprioceptive feedback was used similar to visual feedback, the orthosis may have flexed to its maximum value just after few repetitions, instead of reacting along the whole feedback section. In that case, the participant would not have received continuous proprioceptive feedback of their motor imagery along the whole 2.5 s feedback period while with visual feedback they could have received feedback for the whole feedback section.

The intrinsic differences regarding the different feedback modalities necessitated the explained adjustment, however, the approach chosen here reflects the current state of the art in the field (Vukelić and Gharabaghi 2015a, Brauchle *et al.* 2015).

E.5 Software

The following script released by Pololu (<https://www.pololu.com>) was used to modify CursorTask class of BCI2000 software so as to make a RS-232 communication channel between BCI2000 application module and the controller and thereby control the angles of the orthoses:

```
// Uses POSIX functions to send and receive data from a Maestro.
// NOTE: The Maestro's serial mode must be set to "USB Dual Port".
// NOTE: You must change the 'const char * device' line below.

#include <fcntl.h>
#include <stdio.h>
#include <unistd.h>

#ifdef _WIN32
```

```
#define O_NOCTTY 0
#else
#include <termios.h>
#endif

// Gets the position of a Maestro channel.
// See the "Serial Servo Commands" section of the user's guide.
int maestroGetPosition(int fd, unsigned char channel)
{
    unsigned char command[] = {0x90, channel};
    if(write(fd, command, sizeof(command)) == -1)
    {
        perror("error writing");
        return -1;
    }

    unsigned char response[2];
    if(read(fd, response, 2) != 2)
    {
        perror("error reading");
        return -1;
    }

    return response[0] + 256*response[1];
}

// Sets the target of a Maestro channel.
// See the "Serial Servo Commands" section of the user's guide.
// The units of 'target' are quarter-microseconds.
int maestroSetTarget(int fd, unsigned char channel, unsigned short target)
{
    unsigned char command[] = {0x84, channel, target & 0x7F, target >> ...
        7 & 0x7F};
    if (write(fd, command, sizeof(command)) == -1)
    {
        perror("error writing");
        return -1;
    }
    return 0;
}

int main()
```

E.5 Software

```
{
    // Open the Maestro's virtual COM port.
    const char * device = "\\.\USBSER000"; // Windows, ...
        "\\.\COM6" also works
    //const char * device = "/dev/ttyACM0"; // Linux
    //const char * device = "/dev/cu.usbmodem00034567"; // Mac OS X
    int fd = open(device, O_RDWR | O_NOCTTY);
    if (fd == -1)
    {
        perror(device);
        return 1;
    }

    #ifdef _WIN32
    _setmode(fd, _O_BINARY);
    #else
    struct termios options;
    tcgetattr(fd, &options);
    options.c_iflag &= ~(INLCR | IGNCR | ICRNL | IXON | IXOFF);
    options.c_oflag &= ~(ONLCR | OCRNL);
    options.c_lflag &= ~(ECHO | ECHONL | ICANON | ISIG | IEXTEN);
    tcsetattr(fd, TCSANOW, &options);
    #endif

    int position = maestroGetPosition(fd, 0);
    printf("Current position is %d.\n", position);

    int target = (position < 6000) ? 7000 : 5000;
    printf("Setting target to %d (%d us).\n", target, target/4);
    maestroSetTarget(fd, 0, target);

    close(fd);
    return 0;
}
```


Bibliography

- AHN-M., CHO-H., AHN-S., AND JUN-S. C. (2013). High theta and low alpha powers may be indicative of BCI-illiteracy in motor imagery, *PLoS ONE*, **8**(11), art. no. e80886.
- ALLISON-B., FALLER-J., AND NEUPER-C. (2012). *BCIs that Use Steady-State Visual Evoked Potentials or Slow Cortical Potentials*, Oxford University Press, Oxford; New York, book section 14, pp. 241–250.
- ANG-K. K., AND GUAN-C. (2013). Brain-computer interface in stroke rehabilitation, *Journal of Computing Science and Engineering*, **7**(2), pp. 139–146.
- ANG-K. K., GUAN-C., CHUA-K. S. G., ANG-B. T., KUAH-C., WANG-C., PHUA-K. S., CHIN-Z. Y., AND ZHANG-H. (2009). A clinical study of motor imagery-based brain-computer interface for upper limb robotic rehabilitation, *Annual International Conference of the IEEE Engineering in Medicine and Biology Society, 2009. EMBC 2009.*, pp. 5981–5984.
- ANG-K. K., GUAN-C., CHUA-K. S. G., ANG-B. T., KUAH-C. W. K., WANG-C., PHUA-K. S., CHIN-Z. Y., AND ZHANG-H. (2011). A large clinical study on the ability of stroke patients to use an EEG-based motor imagery brain-computer interface, *Clinical EEG and Neuroscience*, **42**(4), pp. 253–258.
- BAI-O., HUANG-D., FEI-D. Y., AND KUNZ-R. (2014). Effect of real-time cortical feedback in motor imagery-based mental practice training, *NeuroRehabilitation*, **34**(2), pp. 355–363.
- BAI-O., LIN-P., VORBACH-S., FLOETER-M. K., HATTORI-N., AND HALLETT-M. (2008). A high performance sensorimotor beta rhythm-based brain-computer interface associated with human natural motor behavior, *J Neural Eng*, **5**(1), pp. 24–35.
- BAMDADIAN-A., GUAN-C., ANG-K. K., AND XU-J. (2014). The predictive role of pre-cue EEG rhythms on MI-based BCI classification performance, *J Neurosci Methods*, **235**, pp. 138–144.
- BASHASHATI-H., WARD-R. K., BIRCH-G. E., AND BASHASHATI-A. (2015). Comparing different classifiers in sensory motor brain computer interfaces, *PLoS One*, **10**(6), art. no. e0129435.
- BATTAGLIA-F., QUARTARONE-A., GHILARDI-M. F., DATTOLA-R., BAGNATO-S., RIZZO-V., MORGANTE-L., AND GIRLANDA-P. (2006). Unilateral cerebellar stroke disrupts movement preparation and motor imagery, *Clinical Neurophysiology*, **117**(5), pp. 1009–1016.
- BAUER-R., AND GHARABAGHI-A. (2015). Reinforcement learning for adaptive threshold control of restorative brain-computer interfaces: A Bayesian simulation, *Frontiers in Neuroscience*, **9**, doi:10.3389/fnins.2015.00036.
- BAUER-R., FELS-M., VUKELIC-M., ZIEMANN-U., AND GHARABAGHI-A. (2015). Bridging the gap between motor imagery and motor execution with a brain-robot interface, *Neuroimage*, **108**, pp. 319–327.
- BELLMAN-R. E. (1957). *Dynamic Programming*, Princeton University Press.

Bibliography

- BERGER-H. (1929). Über das Elektrenkephalogramm des Menschen, *Archiv für Psychiatrie und Nervenkrankheiten*, **87**(1), pp. 527–570.
- BIRBAUMER-N., GHANAYIM-N., HINTERBERGER-T., IVERSEN-I., KOTCHOUBEY-B., KUBLER-A., PERELMOUTER-J., TAUB-E., AND FLOR-H. (1999). A spelling device for the paralysed, *Nature*, **398**(6725), pp. 297–298.
- BIRBAUMER-N., MURGUIALDAY-A. R., AND COHEN-L. (2008). Brain-computer interface in paralysis, *Curr Opin Neurol*, **21**(6), pp. 634–638.
- BIRBAUMER-N., RUIZ-S., AND SITARAM-R. (2013). Learned regulation of brain metabolism, *Trends in cognitive sciences*, **17**(6), pp. 295–302.
- BLANKERTZ-B., SANNELLI-C., HALDER-S., HAMMER-E. M., KUBLER-A., MULLER-K. R., CURIO-G., AND DICKHAUS-T. (2010). Neurophysiological predictor of SMR-based BCI performance, *Neuroimage*, **51**(4), pp. 1303–1309.
- BOAS-D. A., DALE-A. M., AND FRANCESCHINI-M. A. (2004). Diffuse optical imaging of brain activation: Approaches to optimizing image sensitivity, resolution, and accuracy, *Neuroimage*, **23**, pp. 275–288.
- BOE-S., GIONFRIDDO-A., KRAEUTNER-S., TREMBLAY-A., LITTLE-G., AND BARDOUILLE-T. (2014). Laterality of brain activity during motor imagery is modulated by the provision of source level neurofeedback, *Neuroimage*, **101**, pp. 159–167.
- BOHANNON-R. W., AND SMITH-M. B. (1987). Interrater reliability of a modified ashworth scale of muscle spasticity, *Physical Therapy*, **67**(2), pp. 206–207.
- BOSTANOV-V., AND KOTCHOUBEY-B. (2006). The T-CWT: A new ERP detection and quantification method based on the continuous wavelet transform and Student's t-statistics, *Clin Neurophysiol*, **117**(12), pp. 2627–2644.
- BOULAY-C. B., SARNACKI-W. A., WOLPAW-J. R., AND MCFARLAND-D. J. (2011). Trained modulation of sensorimotor rhythms can affect reaction time, *Clin Neurophysiol*, **122**(9), pp. 1820–1826.
- BRAUCHLE-D., VUKELIC-M., BAUER-R., AND GHARABAGHI-A. (2015). Brain state-dependent robotic reaching movement with a multi-joint arm exoskeleton: combining brain-machine interfacing and robotic rehabilitation, *Front Hum Neurosci*, **9**, art. no. 564.
- BRITTAIN-J. S., SHAROTT-A., AND BROWN-P. (2014). The highs and lows of beta activity in cortico-basal ganglia loops, *Eur J Neurosci*, **39**(11), pp. 1951–1959
- BROUWER-B. J., AND SCHRYBURT-BROWN-K. (2006). Hand function and motor cortical output post-stroke: are they related?, *Arch Phys Med Rehabil*, **87**(5), pp. 627–634.
- BROWN-C. E., AMINOLTEJARI-K., ERB-H., WINSHIP-I. R., AND MURPHY-T. H. (2009). In vivo voltage-sensitive dye imaging in adult mice reveals that somatosensory maps lost to stroke are replaced over weeks by new structural and functional circuits with prolonged modes of activation within both the peri-infarct zone and distant sites, *The Journal of Neuroscience*, **29**(6), pp. 1719–1734.

- BUCH-E., WEBER-C., COHEN-L. G., BRAUN-C., DIMYAN-M. A., ARD-T., MELLINGER-J., CARIA-A., SOEKADAR-S., FOURKAS-A., AND BIRBAUMER-N. (2008). Think to move: A neuromagnetic brain-computer interface (BCI) system for chronic stroke, *Stroke*, **39**(3), pp. 910–917.
- CARIA-A., WEBER-C., BROTZ-D., RAMOS-A., TICINI-L. F., GHARABAGHI-A., BRAUN-C., AND BIRBAUMER-N. (2011). Chronic stroke recovery after combined BCI training and physiotherapy: A case report, *Psychophysiology*, **48**(4), pp. 578–582.
- CARMICHAEL-S. T. (2003). Plasticity of cortical projections after stroke, *The Neuroscientist*, **9**(1), pp. 64–75.
- CASTEL-LACANAL-E., MARQUE-P., TARDY-J., DE BOISSEZON-X., GUIRAUD-V., CHOLLET-F., LOUBINOUX-I., AND SIMONETTA-MOREAU-M. (2009). Induction of cortical plastic changes in wrist muscles by paired associative stimulation in the recovery phase of stroke patients, *Neurorehabilitation and Neural Repair*, **23**(4), pp. 366–372.
- CISOTTO-G. (2014). *Movement-Related Desynchronization in EEG-based Brain-Computer Interface Applications for Stroke Motor Rehabilitation*, PhD thesis, Information Science and Technology, University of Padova.
- COYLE-S. M., WARD-T. E., AND MARKHAM-C. M. (2007). Brain-computer interface using a simplified functional near-infrared spectroscopy system, *J Neural Eng*, **4**(3), pp. 219–226.
- DALY-I., PICHIORRI-F., FALLER-J., KAISER-V., KREILINGER-A., SCHERER-R., MÜLLER-PUTZ-G (2012). What does clean EEG look like?, *Annual International Conference of the IEEE Engineering in Medicine and Biology Society, EMBC 2012*, pp. 3963–3966.
- DALY-J. J., CHENG-R., ROGERS-J., LITINAS-K., HROVAT-K., AND DOHRING-M. (2009). Feasibility of a new application of noninvasive brain computer interface (BCI): a case study of training for recovery of volitional motor control after stroke, *Journal of Neurologic Physical Therapy*, **33**(4), pp. 203–211.
- DARVISHI-S., ABBOTT-D., AND BAUMERT-M. (2015a). Prediction of motor imagery based brain computer interface performance using a reaction time test, *Annual International Conference of the IEEE Engineering in Medicine and Biology Society, EMBC 2015*, pp. 2880–2883.
- DARVISHI-S., AND AL-ANI-A. (2007). Brain-computer interface analysis using continuous wavelet transform and adaptive neuro-fuzzy classifier, *Annual International Conference of the IEEE Engineering in Medicine and Biology Society, EMBC 2007*, pp. 3220–3223.
- DARVISHI-S., MORADI-M. H., BAUMERT-M., AND ABBOTT-D. (2012). Classification of motor imagery EEG signals using adaptive neuro-fuzzy inference system trained by particle swarm optimization, *Annual International Conference of the IEEE Engineering in Medicine and Biology Society, EMBC 2012, EMB-CAS-SMCS Workshop on Brain-Machine-Body Interfaces*, p. 4.
- DARVISHI-S., RIDDING-M. C., ABBOTT-D., AND BAUMERT-M. (2013a). Investigation of the trade-off between time window length, classifier update rate and classification accuracy for restorative brain-computer interfaces, *Conf Proc IEEE Eng Med Biol Soc*, 2013, pp. 1567–1570.
- DARVISHI-S., RIDDING-M. C., ABBOTT-D., AND BAUMERT-M. (2013b). Proposing a novel feedback provision paradigm for restorative brain-computer interfaces, *Proceedings of the Fifth International Brain-Computer Interface Meeting 2013*, doi:10.3217/978-4-83452-381-5/074.

Bibliography

- DARVISHI-S., RIDDING-M. C., ABBOTT-D., AND BAUMERT-M. (2015b). Does feedback modality affect performance of brain computer interfaces?, *7th International IEEE/EMBS Conference on Neural Engineering (NER), 2015*, pp. 232–235.
- DAVIS-N. J., TOMLINSON-S. P., AND MORGAN-H. M. (2012). The role of beta-frequency neural oscillations in motor control, *J Neurosci*, **32**(2), pp. 403–404.
- DAYAN-P., AND ABBOTT-L. F. (2001). *Theoretical neuroscience*, Vol. 806, Cambridge, MA: MIT Press.
- DECETY-J., JEANNEROD-M., AND PRABLANC-C. (1989). The timing of mentally represented actions, *Behavioural brain research*, **34**(1), pp. 35–42.
- DELL'ACQUA-M. L., LANDI-D., ZITO-G., ZAPPASODI-F., LUPOI-D., ROSSINI-P. M., FILIPPI-M. M., AND TECCHIO-F. (2010). Thalamocortical sensorimotor circuit in multiple sclerosis: an integrated structural and electrophysiological assessment, *Human Brain Mapping*, **31**(10), pp. 1588–1600.
- DELORME-A., AND MAKEIG-S. (2004). EEGLAB: An open source toolbox for analysis of single-trial EEG dynamics including independent component analysis, *J Neurosci Methods*, **134**(1), pp. 9–21.
- DE VRIES-S., AND MULDER-T. (2007). Motor imagery and stroke rehabilitation: A critical discussion, *Journal of Rehabilitation Medicine*, **39**(1), pp. 5–13.
- DIJKERMAN-H. C., IETSWAART-M., JOHNSTON-M., AND MACWALTER-R. S. (2004). Does motor imagery training improve hand function in chronic stroke patients? A pilot study, *Clinical Rehabilitation*, **18**(5), pp. 538–549.
- DIMYAN-M. A., AND COHEN-L. G. (2011). Neuroplasticity in the context of motor rehabilitation after stroke, *Nature Reviews Neurology*, **7**(2), pp. 76–85.
- DONCHIN-E., AND COLES-M. G. H. (1988). Is the P300 component a manifestation of context updating?, *Behavioral and Brain Sciences*, **11**(03), pp. 357–374.
- DONCHIN-E., SPENCER-K. M., AND WIJESINGHE-R. (2000). The mental prosthesis: Assessing the speed of a P300-based brain-computer interface, *IEEE Trans Rehabil Eng*, **8**(2), pp. 174–179.
- DONOGHUE-J. P., SANES-J. N., HATSOPOULOS-N. G., AND GAAL-G. (1998). Neural discharge and local field potential oscillations in primate motor cortex during voluntary movements, *J Neurophysiol*, **79**(1), pp. 159–173.
- DOYON-J., AND BENALI-H. (2005). Reorganization and plasticity in the adult brain during learning of motor skills, *Curr Opin Neurobiol*, **15**(2), pp. 161–167.
- DUDA-R. O., HART-P. E., AND STORK-D. G. (2012). *Pattern classification*, John Wiley & Sons.
- EDWARDSON-M., LUCAS-T., CAREY-J., AND FETZ-E. (2013). New modalities of brain stimulation for stroke rehabilitation, *Experimental Brain Research*, **224**(3), pp. 335–358.
- ENGELHARD-B., OZERI-N., ISRAEL-Z., BERGMAN-H., AND VAADIA-E. (2013). Inducing gamma oscillations and precise spike synchrony by operant conditioning via brain-machine interface, *Neuron*, **77**(2), pp. 361–375.
- FAZLI-S., J.-M., J.-S., AND BLANKERTZ-B. (2012). Using NIRS as a predictor for EEG-based BCI performance, *IEEE Eng Med Biol Soc. 2012*, pp. 4911–4914.

- FETZ-E. E. (1969). Operant conditioning of cortical unit activity, *Science*, **163**(3870), pp. 955–958.
- FETZ-E. E. (2007). Volitional control of neural activity: Implications for brain-computer interfaces, *J Physiol*, **579**(Pt 3), pp. 571–579.
- FETZ-E. E. (2013). Volitional control of cortical oscillations and synchrony, *Neuron*, **77**(2), pp. 216–218.
- FEURRA-M., BIANCO-G., SANTARNECCHI-E., DEL TESTA-M., ROSSI-A., AND ROSSI-S. (2011). Frequency-dependent tuning of the human motor system induced by transcranial oscillatory potentials, *The Journal of Neuroscience*, **31**(34), pp. 12165–12170.
- FINKE-A., LENHARDT-A., AND RITTER-H. (2009). The mindgame: A P300-based brain-computer interface game, *Neural Networks*, **22**(9), pp. 1329–1333.
- FLORIAN-R. V. (2007). Reinforcement learning through modulation of spike-timing-dependent synaptic plasticity, *Neural Computation*, **19**(6), pp. 1468–1502.
- FLORIN-E., BOCK-E., AND BAILLET-S. (2013). Targeted reinforcement of neural oscillatory activity with real-time neuroimaging feedback, *Neuroimage*, **88**, pp. 54–60.
- FOLSTEIN-M. F., FOLSTEIN-S. E., AND MCHUGH-P. R. (1975). Mini-Mental State: A practical method for grading the cognitive state of patients for the clinician, *Journal of Psychiatric Research*, **12**(3), pp. 189–198.
- FOX-P. T., MINTUN-M. A., RAICHLE-M. E., AND HERSCOVITCH-P. (1984). A noninvasive approach to quantitative functional brain mapping with $H_2^{15}O$ and positron emission tomography, *J Cereb Blood Flow Metab*, **4**(3), pp. 329–333.
- FRAK-V., PAULIGNAN-Y., AND JEANNEROD-M. (2001). Orientation of the opposition axis in mentally simulated grasping, *Experimental Brain Research*, **136**(1), pp. 120–127.
- GALLESE-V., AND GOLDMAN-A. (1998). Mirror neurons and the simulation theory of mind-reading, *Trends in Cognitive Sciences*, **2**(12), pp. 493–501.
- GANGULY-K., AND CARMENA-J. M. (2009). Emergence of a stable cortical map for neuroprosthetic control, *PLoS Biol*, **7**(7), art. no. e1000153.
- GAO-Q., DUAN-X., AND CHEN-H. (2011). Evaluation of effective connectivity of motor areas during motor imagery and execution using conditional Granger causality, *Neuroimage*, **54**(2), pp. 12801288.
- GAZZOLA-V., RIZZOLATTI-G., WICKER-B., AND KEYSERS-C. (2007). The anthropomorphic brain: the mirror neuron system responds to human and robotic actions, *Neuroimage*, **35**(4), pp. 1674–1684.
- GHARABAGHI-A., KRAUS-D., LEAO-M. T., SPULER-M., WALTER-A., BOGDAN-M., ROSENSTIEL-W., NAROS-G., AND ZIEMANN-U. (2014a). Coupling brain-machine interfaces with cortical stimulation for brain-state dependent stimulation: Enhancing motor cortex excitability for neurorehabilitation, *Front Hum Neurosci*, **8**(122), doi:10.3389/fnhum.2014.00122
- GHARABAGHI-A., NAROS-G., KHADEMI-F., JESSER-J., SPLER-M., WALTER-A., BOGDAN-M., ROSENSTIEL-W., AND BIRBAUMER-N. (2014b). Learned self-regulation of the lesioned brain with epidural electrocorticography, *Frontiers in Behavioral Neuroscience*, **8**, art. no. 429, doi:10.3389/fnbeh.2014.00429.

Bibliography

- GHARABAGHI-A., NAROS-G., WALTER-A., GRIMM-F., SCHUERMEYER-M., ROTH-A., BOGDAN-M., ROSENSTIEL-W., AND BIRBAUMER-N. (2014c). From assistance towards restoration with epidural brain-computer interfacing, *Restor Neurol Neurosci*, **32**(4), pp. 517–525.
- GHOMSHEH-V. S., SHOOREHDELI-M. A., AND TESHNEHLAB-M. (2007). Training ANFIS structure with modified PSO algorithm, *Mediterranean Conference on Control & Automation, 2007*, IEEE, doi:10.1109/MED.2007.4433927.
- GOMEZ-RODRIGUEZ-M., PETERS-J., HILL-J., SCHOLKOPF-B., GHARABAGHI-A., AND GROSSE-WENTRUP-M. (2011). Closing the sensorimotor loop: Haptic feedback facilitates decoding of motor imagery, *J Neural Eng*, **8**(3), art.no. 036005.
- GROSSE-WENTRUP-M., LIEFHOLD-C., GRAMANN-K., AND BUSS-M. (2009). Beamforming in noninvasive brain-computer interfaces, *IEEE Trans Biomed Eng*, **56**, pp. 1209–1219.
- GROSSE-WENTRUP-M., MATTIA-D., AND OWEISS-K. (2011). Using brain-computer interfaces to induce neural plasticity and restore function, *J Neural Eng*, **8**(2), art. no. 025004.
- GRUZELIER-J. H. (2014). Eeg-neurofeedback for optimising performance. iii: A review of methodological and theoretical considerations, *Neuroscience & Biobehavioral Reviews*, **44**, pp. 159–182.
- GUGER-C., EDLINGER-G., HARKAM-W., NIEDERMAYER-I., AND PFURTSCHELLER-G. (2003). How many people are able to operate an EEG-based brain-computer interface (BCI)?, *IEEE transactions on neural systems and rehabilitation engineering*, **11**(2), pp. 145–147.
- HALDER-S., VARKUTI-B., BOGDAN-M., KUBLER-A., ROSENSTIEL-W., SITARAM-R., AND BIRBAUMER-N. (2013). Prediction of brain-computer interface aptitude from individual brain structure, *Front Hum Neurosci*, **7**, art. no. 105.
- HALLETT-M. (1993). Movement-related cortical potentials., *Electromyography and Clinical Neurophysiology*, **34**(1), pp. 5–13.
- HALLIDAY-D. M., CONWAY-B. A., FARMER-S. F., AND ROSENBERG-J. R. (1998). Using electroencephalography to study functional coupling between cortical activity and electromyograms during voluntary contractions in humans, *Neurosci Lett*, **241**(1), pp. 5–8.
- HALSBAND-U., AND LANGE-R. K. (2006). Motor learning in man: A review of functional and clinical studies, *J Physiol Paris*, **99**(4-6), pp. 414–424.
- HAMMER-E. M., HALDER-S., BLANKERTZ-B., SANNELLI-C., DICKHAUS-T., KLEIH-S., MULLER-K. R., AND KUBLER-A. (2012). Psychological predictors of SMR-BCI performance, *Biol Psychol*, **89**(1), pp. 80–86.
- HAYES-M. H. (2009). *Statistical Digital Signal Processing and Modeling*, John Wiley & Sons.
- HAYKIN-S (1996). *Adaptive Filtering Theory*, Upper Saddle River, NJ, Prentice-Hall.
- HEBB-D. O. (2005). *The Organization of Behavior: A Neuropsychological Theory*, Psychology Press.
- HECKHAUSEN-J., AND HECKHAUSEN-H. (2008). *Motivation and Action*, Cambridge University Press.

- HERROJO RUIZ-M., BRUCKE-C., NIKULIN-V. V., SCHNEIDER-G. H., AND KUHN-A. A. (2014). Beta-band amplitude oscillations in the human internal globus pallidus support the encoding of sequence boundaries during initial sensorimotor sequence learning, *Neuroimage*, **85 Pt 2**, pp. 779–793.
- HESS-A., KUNESCH-E., CLASSEN-J., HOEPPNER-J., STEFAN-K., AND BENECKE-R. (1999). Task-specific afferent modulation of intracortical inhibition, *Experimental Brain Research*, **124**, pp. 321–330.
- HIREMATH-S. V., CHEN-W., WANG-W., FOLDES-S., YANG-Y., TYLER-KABARA-E. C., COLLINGER-J. L., AND BONINGER-M. L. (2015). Brain computer interface learning for systems based on electrocorticography and intracortical microelectrode arrays, *Front Integr Neurosci*, **9**, art. no. 40.
- HJORTH-B. (1991). Principles for transformation of scalp EEG from potential field into source distribution, *J Clin Neurophysiol*, **8(4)**, pp. 391–396.
- HUGGINS-J. E., GUGER-C., ALLISON-B., ANDERSON-C. W., BATISTA-A., BROUWER-A.-M., BRUNNER-C., CHAVARRIAGA-R., FRIED-OKEN-M., GUNDUZ-A., GUPTA-D., KBLER-A., LEEB-R., LOTTE-F., MILLER-L. E., MLLER-PUTZ-G., RUTKOWSKI-T., TANGERMANN-M., AND THOMPSON-D. E. (2014). Workshops of the fifth international brain-computer interface meeting: Defining the future, *Brain-Computer Interfaces*, **1(1)**, pp. 27–49.
- JAYARAM-G., AND STINEAR-J. W. (2008). Contralesional paired associative stimulation increases paretic lower limb motor excitability post-stroke, *Experimental brain research*, **185(4)**, pp. 563–570.
- JAYARAM-V., ALAMGIR-M., ALTUN-Y., SCHOLKOPF-B., AND GROSSE-WENTRUP-M. (2016). Transfer learning in brain-computer interfaces, *IEEE Computational Intelligence Magazine*, **11(1)**, pp. 20–31.
- JEANNEROD-M. (1994). The representing brain: Neural correlates of motor intention and imagery, *Behavioral and Brain Sciences*, **17(02)**, pp. 187–202.
- JEANNEROD-M. (1997). *The Cognitive Neuroscience of Action.*, Blackwell Publishing.
- JEANNEROD-M. (2001). Neural simulation of action: a unifying mechanism for motor cognition, *Neuroimage*, **14(1)**, pp. S103–S109.
- JEUNET-C., CELLARD-A., SUBRAMANIAN-S., HACHET-M., N’KAOUA-B., AND LOTTE-F. (2014). How well can we learn with standard BCI training approaches? A pilot study, *6th International Brain-Computer Interface Conference*, Graz, Austria, 2014, <https://hal.inria.fr/hal-01052692>.
- JEUNET-C., VI-C., SPELMEZAN-D., NKAOUA-B., LOTTE-F., AND SUBRAMANIAN-S. (2015). *Continuous Tactile Feedback for Motor-Imagery based Brain-Computer Interaction in a Multitasking Context*, Vol. 9296 of *Lecture Notes in Computer Science*, Springer International Publishing, book section 36, pp. 488–505.
- JOCHUMSEN-M. (2015). *Analysis of Movement-Related Cortical Potentials for Brain-Computer Interfacing in Stroke Rehabilitation*, PhD thesis, Videnbasen for Aalborg UniversitetVBN, Aalborg Universitet, Aalborg University, Det Sundhedsvidenskabelige Fakultet, The Faculty of Medicine.
- JURY-E. I. (1964). *Theory and Application of the z-Transform Method*, Wiley.

Bibliography

- KAISER-V., BAUERNFEIND-G., KREILINGER-A., KAUFMANN-T., KUBLER-A., NEUPER-C., AND MULLER-PUTZ-G. R. (2014). Cortical effects of user training in a motor imagery based brain-computer interface measured by fNIRS and EEG, *Neuroimage*, **85 Pt 1**, pp. 432–444.
- KAISER-V., KREILINGER-A., MÜLLER-PUTZ-G. R., AND NEUPER-C. (2011). First steps toward a motor imagery based stroke BCI: New strategy to set up a classifier, *Frontiers in Neuroscience*, **5(86)**, doi:10.3389/fnins.2011.00086
- KAPLAN-A. Y., BYEON-J.-G., LIM-J.-J., JIN-K.-S., PARK-B.-W., AND TARASOVA-S. U. (2005). Unconscious operant conditioning in the paradigm of brain-computer interface based on color perception, *International journal of neuroscience*, **5(86)**, doi:10.3389/fnins.2011.00086.
- KARABANOV-A., JIN-S.-H., JOUTSEN-A., POSTON-B., AIZEN-J., ELLENSTEIN-A., AND HALLETT-M. (2012). Timing-dependent modulation of the posterior parietal cortex–primary motor cortex pathway by sensorimotor training, *Journal of Neurophysiology*, **107(11)**, pp. 3190–3199.
- KASAI-T., KAWAI-S., KAWANISHI-M., AND YAHAGI-S. (1997). Evidence for facilitation of motor evoked potentials (MEPs) induced by motor imagery, *Brain Res*, **744(1)**, pp. 147–150.
- KASASHIMA-Y., FUJIWARA-T., MATSUSHIKA-Y., TSUJI-T., HASE-K., USHIYAMA-J., USHIBA-J., AND LIU-M. (2012). Modulation of event-related desynchronization during motor imagery with transcranial direct current stimulation (tdcs) in patients with chronic hemiparetic stroke, *Experimental Brain Research*, **221(3)**, pp. 263–268.
- KATTENSTROTH-J.-C., KALISCH-T., KOWALEWSKI-R., TEGENTHOFF-M., AND DINSE-H. R. (2013). Quantitative assessment of joint position sense recovery in subacute stroke patients: A pilot study, *Journal of Rehabilitation Medicine*, **45(10)**, pp. 1004–1009.
- KILAVIK-B. E., ZAEPFFEL-M., BROVELLI-A., MACKAY-W. A., AND RIEHLE-A. (2013). The ups and downs of beta oscillations in sensorimotor cortex, *Exp Neurol*, **245**, pp. 15–26.
- KILNER-J., AND LEMON-R. (2013). What we know currently about mirror neurons, *Current Biology*, **23(23)**, pp. R1057–R1062.
- KLEMMER-E. T. (1956). Time uncertainty in simple reaction time, *Journal of Experimental Psychology*, **51(3)**, pp. 179–184.
- KOBER-S. E., WITTE-M., NINAUS-M., NEUPER-C., AND WOOD-G. (2013). Learning to modulate ones own brain activity: the effect of spontaneous mental strategies, *Frontiers in Human Neuroscience*, **7**, doi:10.3389/fnhum.2013.00695.
- KOGANEMARU-S., MIMA-T., THABIT-M. N., IKKAKU-T., SHIMADA-K., KANEMATSU-M., TAKAHASHI-K., FAWI-G., TAKAHASHI-R., FUKUYAMA-H., AND DOMEN-K. (2010). Recovery of upper-limb function due to enhanced use-dependent plasticity in chronic stroke patients, *Brain*, **133(11)**, pp. 3373–3384.
- KRAUS-D., NAROS-G., BAUER-R., LEÃO-M. T., ZIEMANN-U., AND GHARABAGHI-A. (2016). Brain-robot interface driven plasticity: Distributed modulation of corticospinal excitability, *NeuroImage*, **125**, pp. 522–532.

- KRUSIENSKI-D., AND JENKINS-W. (2005). Design and performance of adaptive systems based on structured stochastic optimization strategies, *Circuits and Systems Magazine, IEEE*, 5(1), pp. 8–20.
- KRUSIENSKI-D., MCFARLAND-D. J., AND J.C.-P. (2012). *BCI Signal Processing: Feature Extraction*, Oxford University Press, Oxford; New York, book section 7, pp. 123–146.
- KUBLER-A., NEUMANN-N., KAISER-J., KOTCHOUBEY-B., HINTERBERGER-T., AND BIRBAUMER-N. P. (2001). Brain-computer communication: Self-regulation of slow cortical potentials for verbal communication, *Arch Phys Med Rehabil*, 82(11), pp. 1533–1539.
- KWAKKEL-G., KOLLEN-B. J., AND WAGENAAR-R. C. (1999). Therapy impact on functional recovery in stroke rehabilitation: A critical review of the literature, *Physiotherapy*, 85(7), pp. 377–391.
- LEEB-R., LEE-F., KEINRATH-C., SCHERER-R., BISCHOF-H., AND PFURTSCHELLER-G. (2007). Brain-computer communication: motivation, aim, and impact of exploring a virtual apartment, *IEEE Transactions on Neural Systems and Rehabilitation Engineering*, 15(4), pp. 473–482.
- LEMON-R. (1979). Short-latency peripheral inputs to the motor cortex in conscious monkeys, *Brain Research*, 161(1), pp. 150–155.
- LEOCANI-L., AND COMI-G. (2006). Movement-related event-related desynchronization in neuropsychiatric disorders, *Progress in Brain Research*, 159, pp. 351–366.
- LEON-M. I., AND SHADLEN-M. N. (1999). Effect of expected reward magnitude on the response of neurons in the dorsolateral prefrontal cortex of the macaque, *Neuron*, 24(2), pp. 415–425.
- LICHTENWALNER-R. J., AND PARENT-J. M. (2006). Adult neurogenesis and the ischemic forebrain, *Journal of Cerebral Blood Flow & Metabolism*, 26(1), pp. 1–20.
- LIN-C.-T., CHEN-Y.-C., HUANG-T.-Y., CHIU-T.-T., KO-L.-W., LIANG-S.-F., HSIEH-H.-Y., HSU-S.-H., AND DUANN-J.-R. (2008). Development of wireless brain computer interface with embedded multitask scheduling and its application on real-time driver's drowsiness detection and warning, *IEEE Transactions on Biomedical Engineering*, 55(5), pp. 1582–1591.
- LLOYD-JONES-D., ADAMS-R., CARNETHON-M., DE SIMONE-G., FERGUSON-T. B., FLEGAL-K., FORD-E., FURIE-K., GO-A., GREENLUND-K ETXXXXX AL.. (2009). Heart disease and stroke statistics 2009 update a report from the american heart association statistics committee and stroke statistics subcommittee, *Circulation*, 119(3), pp. e21–e181.
- LOPEZ-LARRAZ-E., ANTELIS-J. M., MONTESANO-L., GIL-AGUDO-A., AND MINGUEZ-J. (2012). Continuous decoding of motor attempt and motor imagery from EEG activity in spinal cord injury patients, *Engineering in Medicine and Biology Society (EMBC), 2012 Annual International Conference of the IEEE, IEEE*, pp. 1798–1801.
- LORENZ-R., PASCUAL-J., BLANKERTZ-B., AND VIDAURRE-C. (2014). Towards a holistic assessment of the user experience with hybrid BCIs, *J Neural Eng*, 11(3), art. no. 035007.
- LOTTE-F., AND JEUNET-C. (2015). Towards improved BCI based on human learning principles, *3rd International Winter Conference on Brain-Computer Interface (BCI), 2015, IEEE*, doi:10.1109/IWW-BCI.2015.7073024.

Bibliography

- LOTTE-F., CONGEDO-M., LECUYER-A., LAMARCHE-F., AND ARNALDI-B. (2007). A review of classification algorithms for EEG-based brain-computer interfaces, *J Neural Eng*, **4**(2), pp. R1–r13.
- LOTTE-F., LARRUE-F., AND MÜHL-C. (2013). Flaws in current human training protocols for spontaneous brain-computer interfaces: Lessons learned from instructional design, *Frontiers in Human Neuroscience*, **7**: 568, doi:10.3389/fnhum.2013.00568.
- LYLE-R. C. (1981). A performance test for assessment of upper limb function in physical rehabilitation treatment and research, *International Journal of Rehabilitation Research*, **4**(4), pp. 483–492.
- MACKAY-J., MENSAH-G. A., MENDIS-H., AND GREENLUND-K. (2004). *The Atlas of Heart Disease and Stroke*, World Health Organization, Geneva.
- MAK-J. N., AND WOLPAW-J. R. (2009). Clinical applications of brain-computer interfaces: current state and future prospects, *IEEE Reviews in Biomedical Engineering*, **2**, p. 187.
- MAKEIG-S., KOTHE-C., MULLEN-T., BIGDELY-SHAMLO-N., ZHANG-Z., AND KREUTZ-DELGADO-K. (2012). Evolving signal processing for brain-computer interfaces, *Proceedings of the IEEE*, **100**(Special Centennial Issue), pp. 1567–1584.
- MARPLE-S. (1987). *Digital Spectral Analysis with Applications*, Englewood Cliffs, NJ, Prentice-Hall, Inc.
- MCCRIMMON-C. M., KING-C. E., WANG-P. T., CRAMER-S. C., NENADIC-Z., AND DO-A. H. (2014). Brain-controlled functional electrical stimulation for lower-limb motor recovery in stroke survivors, *Engineering in Medicine and Biology Society (EMBC), 2014 36th Annual International Conference of the IEEE, IEEE*, pp. 1247–1250.
- MC FARLAND-D., AND KRUSIENSKI-D. (2012). *BCI Signal Processing: Feature Translation*, Oxford University Press, Oxford; New York, book section 8, pp. 147–163.
- MC FARLAND-D. J., MINER-L. A., VAUGHAN-T. M., AND WOLPAW-J. R. (2000). Mu and beta rhythm topographies during motor imagery and actual movements, *Brain Topogr*, **12**(3), pp. 177–186.
- MELDRUM-D., CAHALANE-E., CONROY-R., FITZGERALD-D., AND HARDIMAN-O. (2007). Maximum voluntary isometric contraction: Reference values and clinical application, *Amyotrophic Lateral Sclerosis*, **8**(1), pp. 47–55.
- MEYER-D. E., OSMAN-A. M., IRWIN-D. E., AND YANTIS-S. (1988). Modern mental chronometry, *Biol Psychol*, **26**(1-3), pp. 3–67.
- MILLER-K. J., SCHALK-G., FETZ-E. E., DEN NIJS-M., OJEMANN-J. G., AND RAO-R. P. (2010). Cortical activity during motor execution, motor imagery, and imagery-based online feedback, *Proc Natl Acad Sci USA*, **107**(9), pp. 4430–4435.
- MILLER-L., AND HATSOPOULOS-N. (2012). *Neuronal activity in motor cortex and related areas*, Oxford University Press, Oxford; New York, book section 2, pp. 15–46.
- MIMA-T., MATSUOKA-T., AND HALLETT-M. (2001a). Information flow from the sensorimotor cortex to muscle in humans, *Clin Neurophysiol*, **112**(1), pp. 122–126.

- MIMA-T., TOMA-K., KOSHY-B., AND HALLETT-M. (2001b). Coherence between cortical and muscular activities after subcortical stroke, *Stroke*, **32**(11), pp. 2597–2601.
- MOHAPP-A., SCHERER-R., KEINRATH-C., GRIESHOFFER-P., PFURTSCHELLER-G., AND NEUPER-C. (2006). Single-trial EEG classification of executed and imagined hand movements in hemiparetic stroke patients, *Proceedings of the 3rd Brain-Computer Interface in Stroke Rehabilitation Workshop and Training Course*, Graz, Austria, 2006.
- MOORE-M. M. (2003). Real-world applications for brain-computer interface technology, *IEEE Transactions on Neural Systems and Rehabilitation Engineering*, **11**(2), pp. 162–165.
- MOTTAZ-A., SOLCA-M., MAGNIN-C., CORBET-T., SCHNIDER-A., AND GUGGISBERG-A. G. (2015). Neurofeedback training of alpha-band coherence enhances motor performance, *Clin Neurophysiol*, **126**(9), pp. 1754–1760.
- MRACHACZ-KERSTING-N., KRISTENSEN-S. R., NIAZI-I. K., AND FARINA-D. (2012). Precise temporal association between cortical potentials evoked by motor imagination and afference induces cortical plasticity, *J Physiol*, **590**(Pt 7), pp. 1669–1682.
- MÜLLER-K.-R., ANDERSON-C. W., AND BIRCH-G. E. (2003). IEEE Transactions on Linear and nonlinear methods for brain-computer interfaces, *Neural Systems and Rehabilitation Engineering*, **11**(2), pp. 165–169.
- MULLER-PUTZ-G. R., ZIMMERMANN-D., GRAIMANN-B., NESTINGER-K., KORISEK-G., AND PFURTSCHELLER-G. (2007). Event-related beta EEG-changes during passive and attempted foot movements in paraplegic patients, *Brain Res*, **1137**(1), pp. 84–91.
- MURPHY-T. H., AND CORBETT-D. (2009). Plasticity during stroke recovery: From synapse to behaviour, *Nature Reviews Neuroscience*, **10**(12), pp. 861–872.
- NAROS-G., AND GHARABAGHI-A. (2015). Reinforcement learning of self-regulated beta-oscillations for motor restoration in chronic stroke, *Front Hum Neurosci*, **9**, art. no. 391.
- NAROS-G., NAROS-I., GRIMM-F., ZIEMANN-U., AND GHARABAGHI-A. (2016). Reinforcement learning of self-regulated sensorimotor β -oscillations improves motor performance, *NeuroImage*, **134**, pp. 142–152.
- NEUPER-C., AND PFURTSCHELLER-G. (2001). Event-related dynamics of cortical rhythms: frequency-specific features and functional correlates, *International Journal of Psychophysiology*, **43**(1), pp. 41–58.
- NEUPER-C., SCHLOGL-A., AND PFURTSCHELLER-G. (1999). Enhancement of left-right sensorimotor EEG differences during feedback-regulated motor imagery, *J Clin Neurophysiol*, **16**(4), pp. 373–382.
- NIAZI-I. K., MRACHACZ-KERSTING-N., JIANG-N., DREMSTRUP-K., AND FARINA-D. (2012). Peripheral electrical stimulation triggered by self-paced detection of motor intention enhances motor evoked potentials, *IEEE Trans Neural Syst Rehabil Eng*, **20**(4), pp. 595–604.

Bibliography

- NICOLO-P., RIZK-S., MAGNIN-C., PIETRO-M. D., SCHNIDER-A., AND GUGGISBERG-A. G. (2015). Coherent neural oscillations predict future motor and language improvement after stroke, *Brain*, **138**(Pt 10), pp. 3048–3060.
- NIJBOER-F., FURDEA-A., GUNST-I., MELLINGER-J., MCFARLAND-D. J., BIRBAUMER-N., AND KUBLER-A. (2008). An auditory brain-computer interface (BCI), *J Neurosci Methods*, **167**(1), pp. 43–50.
- NOCK-M. K., MICHEL-B. D., PHOTOS-V. I., MCKAY-D (2007). *Single-Case Research Designs, Handbook of Research Methods in Abnormal and Clinical Psychology*, Sage Publications., chapter 22, pp. 337–350.
- OGAWA-S., LEE-T.-M., KAY-A. R., AND TANK-D. W. (1990). Brain magnetic resonance imaging with contrast dependent on blood oxygenation, *Proceedings of the National Academy of Sciences*, **87**(24), pp. 9868–9872.
- OUJAMAA-L., RELAVE-I., FROGER-J., MOTTET-D., AND PELISSIER-J. Y. (2009). Rehabilitation of arm function after stroke. literature review, *Ann Phys Rehabil Med*, **52**(3), pp. 269–293.
- PARRA-L. C., SPENCE-C. D., GERSON-A. D., AND SAJDA-P. (2005). Recipes for the linear analysis of EEG, *Neuroimage*, **28**(2), pp. 326–341.
- PASCUAL-LEONE-A., GRAFMAN-J., HALLETT-M (1994). Modulation of cortical motor output maps during development of implicit and explicit knowledge, *Science*, **263**(5151), pp. 1287–1289.
- PERDIKIS-S., LEEB-R., AND DEL R MILLAN-J. (2014). Subject-oriented training for motor imagery brain-computer interfaces, *36th Annual International Conference of the IEEE Engineering in Medicine and Biology Society (EMBC 2014)*, pp. 1259–1262.
- PFURTSCHELLER-G. (2001). Functional brain imaging based on ERD/ERS, *Vision Res*, **41**(10-11), pp. 1257–1260.
- PFURTSCHELLER-G., AND ARANIBAR-A. (1979). Evaluation of event-related desynchronization (ERD) preceding and following voluntary self-paced movement, *Electroencephalography and Clinical Neurophysiology*, **46**(2), pp. 138–146.
- PFURTSCHELLER-G., AND LOPES DA SILVA-F. H. (1999). Event-related EEG/MEG synchronization and desynchronization: Basic principles, *Clin Neurophysiol*, **110**(11), pp. 1842–1857.
- PFURTSCHELLER-G., AND MCFARLAND-D. J. (2012). *BCIs that Use Sensorimotor Rhythms*, Oxford University Press, Oxford; New York, book section 13, pp. 227–240.
- PFURTSCHELLER-G., NEUPER-C., FLOTZINGER-D., AND PREGENZER-M. (1997). EEG-based discrimination between imagination of right and left hand movement, *Electroencephalogr Clin Neurophysiol*, **103**(6), pp. 642–651.
- PFURTSCHELLER-G., NEUPER-C., GUGER-C., HARKAM-W., RAMOSER-H., SCHLOGL-A., OBERMAIER-B., AND PREGENZER-M. (2000). Current trends in Graz brain-computer interface (BCI) research, *IEEE Trans Rehabil Eng*, **8**(2), pp. 216–219.
- PFURTSCHELLER-G., NEUPER-C., RAMOSER-H., AND MULLER-GERKING-J. (1999). Visually guided motor imagery activates sensorimotor areas in humans, *Neurosci Lett*, **269**(3), pp. 153–156.

- PFURTSCHELLER-G., WOERTZ-M., MULLER-G., WRIESSNEGGER-S., AND PFURTSCHELLER-K. (2002). Contrasting behavior of beta event-related synchronization and somatosensory evoked potential after median nerve stimulation during finger manipulation in man, *Neurosci Lett*, **323**(2), pp. 113–116.
- PHILIP-P., TAILLARD-J., QUERA-SALVA-M., BIOULAC-B., AND ÅKERSTEDT-T. (1999). Simple reaction time, duration of driving and sleep deprivation in young versus old automobile drivers, *Journal of Sleep Research*, **8**(1), pp. 9–14.
- PICHIORRI-F., FALLANI-F. D. V., CINCOTTI-F., BABILONI-F., MOLINARI-M., KLEIH-S., NEUPER-C., KÜBLER-A., AND MATTIA-D. (2011). Sensorimotor rhythm-based brain–computer interface training: the impact on motor cortical responsiveness, *Journal of Neural Engineering*, **8**(2), art. no. 025020.
- PICHIORRI-F., MORONE-G., PETTI-M., TOPPI-J., PISOTTA-I., MOLINARI-M., PAOLUCCI-S., INGHILLERI-M., ASTOLFI-L., CINCOTTI-F. (2015). Brain–computer interface boosts motor imagery practice during stroke recovery, *Annals of Neurology*, **77**(5), pp. 851–865.
- PLATZ-T., KIM-I., PINTSCHOVIVUS-H., WINTER-T., KIESELBACH-A., VILLRINGER-K., KURTH-R., AND MAURITZ-K.-H. (2000). Multimodal EEG analysis in man suggests impairment-specific changes in movement-related electric brain activity after stroke, *Brain*, **123**(12), pp. 2475–2490.
- POLLOK-B., LATZ-D., KRAUSE-V., BUTZ-M., AND SCHNITZLER-A. (2014). Changes of motor-cortical oscillations associated with motor learning, *Neuroscience*, **275**, pp. 47–53.
- PRADEEP-S., MATTHIAS-K., BENJAMIN-B., RAJESH-P. N. R., AND KLAUS-ROBERT-M. (2006). Towards adaptive classification for BCI, *Journal of Neural Engineering*, **3**(1), p. R13.
- PRASAD-G., HERMAN-P., COYLE-D., MCDONOUGH-S., AND CROSBIE-J. (2010). Applying a brain–computer interface to support motor imagery practice in people with stroke for upper limb recovery: A feasibility study, *Journal of NeuroEngineering and Rehabilitation*, **7**(1), pp. 1–17.
- PRESS-W. H. (2007). *Numerical Recipes: The Art of Scientific Computing*, third edn, Cambridge University Press.
- RAMOS-MURGUIALDAY-A., BROETZ-D., REA-M., LAER-L., YILMAZ-O., BRASIL-F. L., LIBERATI-G., CURADO-M. R., GARCIA-COSSIO-E., VYZIOTIS-A., CHO-W., AGOSTINI-M., SOARES-E., SOEKADAR-S., CARIA-A., COHEN-L. G., AND BIRBAUMER-N. (2013). Brain-machine interface in chronic stroke rehabilitation: A controlled study, *Ann Neurol*, **74**(1), pp. 100–108.
- RAMOS-MURGUIALDAY-A., SCHURHOLZ-M., CAGGIANO-V., WILDGRUBER-M., CARIA-A., HAMMER-E. M., HALDER-S., AND BIRBAUMER-N. (2012). Proprioceptive feedback and brain computer interface (BCI) based neuroprostheses, *PLoS One*, **7**(10), art. no. e47048.
- RAMSEY-N. F. (2012). *Signals Reflecting Brain Metabolic Activity*, Oxford University Press, Oxford; New York, book section 4, pp. 65–80.
- REYNOLDS-C., OSUAGWU-B. A., AND VUCKOVIC-A. (2015). Influence of motor imagination on cortical activation during functional electrical stimulation, *Clin Neurophysiol*, **126**(7), pp. 1360–1369.

Bibliography

- MAGILL-R., AND ANDERSON-D. (2014). *Motor Learning and Control: Concepts and Applications*, tenth edn, McGraw-Hill Education.
- RIDDING-M., AND ROTHWELL-J. (1999). Afferent input and cortical organisation: a study with magnetic stimulation, *Experimental Brain Research*, **126**(4), pp. 536–544.
- RIDDING-M., AND TAYLOR-J. (2001). Mechanisms of motor-evoked potential facilitation following prolonged dual peripheral and central stimulation in humans, *The Journal of Physiology*, **537**(2), pp. 623–631.
- RIDDING-M. C., AND ROTHWELL-J. C. (2007). Is there a future for therapeutic use of transcranial magnetic stimulation?, *Nature Reviews Neuroscience*, **8**(7), pp. 559–567.
- RIDDLE-C. N., AND BAKER-S. N. (2005). Manipulation of peripheral neural feedback loops alters human corticomuscular coherence, *J Physiol*, **566**(Pt 2), pp. 625–639.
- RIZZO-V., SIEBNER-H., MORGANTE-F., MASTROENI-C., GIRLANDA-P., AND QUARTARONE-A. (2009). Paired associative stimulation of left and right human motor cortex shapes interhemispheric motor inhibition based on a hebbian mechanism, *Cerebral Cortex*, **19**(4), pp. 907–915.
- ROSSI-S., HALLETT-M., ROSSINI-P. M., PASCUAL-LEONE-A., OF TMS CONSENSUS GROUP (2009). Safety, ethical considerations, and application guidelines for the use of transcranial magnetic stimulation in clinical practice and research, *Clinical Neurophysiology*, **120**(12), pp. 2008–2039.
- ROSSITER-H. E., BOUDRIAS-M. H., AND WARD-N. S. (2014). Do movement-related beta oscillations change after stroke?, *J Neurophysiol*, **112**(9), pp. 2053–2058.
- RUSHTON-D. (1997). Functional electrical stimulation, *Physiological measurement*, **18**(4), p. 241.
- SALENIUS-S., SCHNITZLER-A., SALMELIN-R., JOUSMAKI-V., AND HARI-R. (1997). Modulation of human cortical Rolandic rhythms during natural sensorimotor tasks, *Neuroimage*, **5**(3), pp. 221–228.
- SAMII-A., LUCIANO-C. A., DAMBROSIA-J. M., AND HALLETT-M. (1998). Central motor conduction time: Reproducibility and discomfort of different methods, *Muscle & Nerve*, **21**(11), pp. 1445–1450.
- SANO-A., AND BAKARDJIAN-H. (2009). Movement-related cortical evoked potentials using four-limb imagery, *International Journal of Neuroscience*, **119**(5), pp. 639–663.
- SAVAGE-L. M., AND RAMOS-R. L. (2009). Reward expectation alters learning and memory: The impact of the amygdala on appetitive-driven behaviors, *Behavioural Brain Research*, **198**(1), pp. 1–12.
- SCHALK-G., MCFARLAND-D. J., HINTERBERGER-T., BIRBAUMER-N., AND WOLPAW-J. R. (2004). BCI2000: A general-purpose brain-computer interface (BCI) system, *IEEE Trans Biomed Eng*, **51**(6), pp. 1034–1043.
- SCHULZ-H., UBELACKER-T., KEIL-J., MULLER-N., AND WEISZ-N. (2014). Now I am ready—now I am not: The influence of pre-TMS oscillations and corticomuscular coherence on motor-evoked potentials, *Cereb Cortex*, **24**(7), pp. 1708–1719.
- SHARMA-N., POMEROY-V. M., AND BARON-J.-C. (2006). Motor imagery a backdoor to the motor system after stroke?, *Stroke*, **37**(7), pp. 1941–1952.

-
- SHIBASAKI-H., AND HALLETT-M. (2006). What is the Bereitschaftspotential?, *Clinical neurophysiology*, **117**(11), pp. 2341–2356.
- SHINDO-K., KAWASHIMA-K., USHIBA-J., OTA-N., ITO-M., OTA-T., KIMURA-A., AND LIU-M. (2011). Effects of neurofeedback training with an electroencephalogram-based brain-computer interface for hand paralysis in patients with chronic stroke: A preliminary case series study, *J Rehabil Med*, **43**(10), pp. 951957.
- SIRIGU-A., COHEN-L., DUHAMEL-J., PILLON-B., DUBOIS-B., AGID-Y., AND PIERROT-DESEILLIGNY-C. (1995). Congruent unilateral impairments for real and imagined hand movements., *Neuroreport*, **6**(7), pp. 997–1001.
- SOEKADAR-S., BIRBAUMER-N., AND COHEN-L. (2011). *Brain-Computer Interfaces in the Rehabilitation of Stroke and Neurotrauma*, Springer Japan, book section 1, pp. 3–18.
- SRINIVASAN-R. (2012). *Acquiring Brain Signals from Outside the Brain*, Oxford University Press, Oxford; New York, book section 6, pp. 105–122.
- STEFAN-K., KUNESCH-E., COHEN-L. G., BENECKE-R., AND CLASSEN-J. (2000). Induction of plasticity in the human motor cortex by paired associative stimulation, *Brain*, **123**(3), pp. 572–584.
- STAPIEN-M., CONRADI-J., WATERSTRAAT-G., HOHLEFELD-F. U., CURIO-G., AND NIKULIN-V. V. (2011). Event-related desynchronization of sensorimotor EEG rhythms in hemiparetic patients with acute stroke, *Neuroscience Letters*, **488**(1), pp. 17–21.
- STREHL-U. (2014). What learning theories can teach us in designing neurofeedback treatments, *Front. Hum. Neurosci*, **8**(894), pp. 10–3389.
- STROOBANT-N., AND VINGERHOETS-G. (2000). Transcranial doppler ultrasonography monitoring of cerebral hemodynamics during performance of cognitive tasks: A review, *Neuropsychology review*, **10**(4), pp. 213–231.
- SZAMEITAT-A. J., SHEN-S., CONFORTO-A., AND STERR-A. (2012). Cortical activation during executed, imagined, observed, and passive wrist movements in healthy volunteers and stroke patients, *Neuroimage*, **62**(1), pp. 266–280.
- TAI-Y. F., SCHERFLER-C., BROOKS-D. J., SAWAMOTO-N., AND CASTIELLO-U. (2004). The human premotor cortex is 'mirror' only for biological actions, *Current Biology*, **14**(2), pp. 117–120.
- TAKEMI-M., MASAKADO-Y., LIU-M., AND USHIBA-J. (2013a). Event-related desynchronization reflects downregulation of intracortical inhibition in human primary motor cortex, *J Neurophysiol*, **110**(5), pp. 1158–1166.
- TAKEMI-M., MASAKADO-Y., LIU-M., AND USHIBA-J. (2013b). Is event-related desynchronization a biomarker representing corticospinal excitability?, *Conf Proc IEEE Eng Med Biol Soc*, 2013, pp. 281284.
- TAUB-E., MILLER-N., NOVACK-T., COOK 3RD-E., FLEMING-W., NEPOMUCENO-C., CONNELL-J., AND CRAGO-J. (1993). Technique to improve chronic motor deficit after stroke., *Archives of Physical Medicine and Rehabilitation*, **74**(4), pp. 347–354.
-

Bibliography

- THEODORIDIS-S., AND KOUTROUMBAS-K. (2006a). Chapter 2 - classifiers based on bayes decision theory, in S. Theodoridis., and K. Koutroumbas. (eds.), *Pattern Recognition (Third Edition)*, Academic Press, San Diego, pp. 13 – 67.
- THEODORIDIS-S., AND KOUTROUMBAS-K. (2006b). Chapter 3 - linear classifiers, in S. Theodoridis., and K. Koutroumbas. (eds.), *Pattern Recognition (Third Edition)*, Academic Press, San Diego, pp. 69 – 120.
- THORPE-D. E., AND VALVANO-J. (2002). The effects of knowledge of performance and cognitive strategies on motor skill learning in children with cerebral palsy, *Pediatr Phys Ther*, **14**(1), pp. 2–15.
- TOHYAMA-T., FUJIWARA-T., MATSUMOTO-J., HONAGA-K., USHIBA-J., TSUJI-T., HASE-K., AND LIU-M. (2011). Modulation of event-related desynchronization during motor imagery with transcranial direct current stimulation in a patient with severe hemiparetic stroke: A case report, *The Keio Journal of Medicine*, **60**(4), pp. 114–118.
- TURRIGIANO-G. G., AND NELSON-S. B. (2004). Homeostatic plasticity in the developing nervous system, *Nature Reviews Neuroscience*, **5**(2), pp. 97–107.
- VAN VLIET-P. M., AND WULF-G. (2006). Extrinsic feedback for motor learning after stroke: what is the evidence?, *Disabil Rehabil*, **28**(13-14), pp. 831–840.
- VAUGHAN-T., AND WOLPAW-J. (2006). The third international meeting on brain-computer interface technology: Making a difference, *IEEE Transactions on Neural Systems and Rehabilitation Engineering*, **14**(2), pp. 126–127.
- VIDAL-J.-J. (1973). Toward direct brain-computer communication, *Annual Review of Biophysics and Bioengineering*, **2**(1), pp. 157–180.
- VILLRINGER-A., PLANCK-J., HOCK-C., SCHLEINKOFER-L., AND DIRNAGL-U. (1993). Near infrared spectroscopy (NIRS): A new tool to study hemodynamic changes during activation of brain function in human adults, *Neuroscience Letters*, **154**(1), pp. 101–104.
- VOLOSYAK-I., VALBUENA-D., MALECHKA-T., PEUSCHER-J., AND GRASER-A. (2010). Brain-computer interface using water-based electrodes, *J Neural Eng*, **7**(6), art. no. 066007.
- VUCKOVIC-A., AND OSUAGWU-B. A. (2013). Using a motor imagery questionnaire to estimate the performance of a brain-computer interface based on object oriented motor imagery, *Clin Neurophysiol*, **124**(8), pp. 1586–1595.
- VUCKOVIC-A., WALLACE-L., AND ALLAN-D. B. (2015). Hybrid brain-computer interface and functional electrical stimulation for sensorimotor training in participants with tetraplegia: a proof-of-concept study, *Journal of Neurologic Physical Therapy*, **39**(1), pp. 3–14.
- VUKELIĆ-M., AND GHARABAGHI-A. (2015a). Oscillatory entrainment of the motor cortical network during motor imagery is modulated by the feedback modality, *NeuroImage*, **111**, doi:10.1016/j.neuroimage.2015.01.058.
- VUKELIC-M., AND GHARABAGHI-A. (2015b). Self-regulation of circumscribed brain activity modulates spatially selective and frequency specific connectivity of distributed resting state networks, *Front Behav Neurosci*, **9**: 181, doi:10.3389/fnbeh.2015.00181.

- VUKELIC-M., BAUER-R., NAROS-G., NAROS-I., BRAUN-C., AND GHARABAGHI-A. (2014). Lateralized alpha-band cortical networks regulate volitional modulation of beta-band sensorimotor oscillations, *Neuroimage*, **87**, pp. 147–153.
- WANG-P., LU-J., ZHANG-B., AND TANG-Z. (2015). A review on transfer learning for brain-computer interface classification, *2015 5th International Conference on Information Science and Technology (ICIST)*, IEEE, pp. 315–322.
- WEISKOPF-N., MATHIAK-K., BOCK-S. W., SCHARNOWSKI-F., VEIT-R., GRODD-W., GOEBEL-R., AND BIRBAUMER-N. (2004). Principles of a brain-computer interface (BCI) based on real-time functional magnetic resonance imaging (fMRI), *IEEE Trans Biomed Eng*, **51**(6), pp. 966–970.
- WELCH-P. D. (1967). The use of fast Fourier transform for the estimation of power spectra: A method based on time averaging over short, modified periodograms, *IEEE Transactions on Audio and Electroacoustics*, **15**(2), pp. 70–73.
- WILCOXON-F. (1945). Individual comparisons by ranking methods, *Biometrics Bulletin*, **1**(6), pp. 80–83.
- WILSON-J., GUGER-C., AND SCHALK-G. (2012). *BCI Hardware and Software*, Oxford University Press, Oxford; New York, book section 9, pp. 165–188.
- WITHAM-C. L., RIDDLE-C. N., BAKER-M. R., AND BAKER-S. N. (2011). Contributions of descending and ascending pathways to corticomuscular coherence in humans, *J Physiol*, **589**(Pt 15), pp. 3789–3800.
- WOLPAW-J. R., AND MCFARLAND-D. J. (2004). Control of a two-dimensional movement signal by a noninvasive brain-computer interface in humans, *Proceedings of the National Academy of Sciences of the United States of America*, **101**(51), pp. 17849–17854.
- WOLPAW-J. R., BIRBAUMER-N., HEETDERKS-W. J., MCFARLAND-D. J., PECKHAM-P. H., SCHALK-G., DONCHIN-E., QUATRANO-L. A., ROBINSON-C. J., VAUGHAN-T. M (2000). Brain-computer interface technology: A review of the first international meeting, *IEEE Transactions on Rehabilitation Engineering*, **8**(2), pp. 164–173.
- WOLPOW-J., AND WOLPOW-E. (2012a). *Brain-Computer Interfaces: Something New Under the Sun*, Oxford University Press New York, USA, Oxford; New York, book section 1, pp. 3–12.
- WOLPOW-J., AND WOLPOW-E. (2012b). *The Future of BCIs: Meeting the Expectations*, Oxford University Press, Oxford; New York, book section 25, pp. 387–392.
- XU-R., JIANG-N., MRACHACZ-KERSTING-N., LIN-C., ASIN PRIETO-G., MORENO-J. C., PONS-J. L., DREMSTRUP-K., AND FARINA-D. (2014). A closed-loop brain-computer interface triggering an active ankle-foot orthosis for inducing cortical neural plasticity, *IEEE Trans Biomed Eng*, **61**(7), pp. 20922101.
- YOUNG-B. M., NIGOGOSYAN-Z., NAIR-V. A., WALTON-L. M., SONG-J., TYLER-M. E., EDWARDS-D. F., CALDERA-K., SATTIN-J. A., WILLIAMS-J. C ET. AL. (2015). Case report: post-stroke interventional BCI rehabilitation in an individual with preexisting sensorineural disability, *Interaction of BCI with the Underlying Neurological Conditions in Patients: Pros and Cons*, **7**, doi:10.3389/fneng.2014.00018.

-
- ZIMMERMANN-SCHLATTER-A., SCHUSTER-C., PUHAN-M. A., SIEKIERKA-E., AND STEURER-J. (2008). Efficacy of motor imagery in post-stroke rehabilitation: a systematic review, *Journal of Neuroengineering and Rehabilitation*, 5(1), doi:10.1186/1743-0003-5-8.
- ZOEFEL-B., HUSTER-R. J., AND HERRMANN-C. S. (2011). Neurofeedback training of the upper alpha frequency band in EEG improves cognitive performance, *Neuroimage*, 54(2), pp. 1427–1431.

List of Acronyms

Acc Accuracy

ANOVA Analysis of variance

ANFIS Adaptive neuro-fuzzy inference system

AR Autoregressive

ARAT Arm research action test

BCI Brain-computer interface

BRI Brain-robot interface

BOLD Blood oxygen level dependent

CSP Common spatial patterns

CAR Common average referencing

CWT Continuous wavelet transform

DWT Discrete wavelet transform

ECoG Electrocorticogram

EEG Electroencephalogram

EMG Electromyogram

ERD Event related desynchronization

ERS Event related synchronization

EOG Electrooculogram

FFT Fast Fourier transform

FIS Fuzzy inference system

FP False positive

List of Acronyms

FN False negative

fTCD Functional transcranial Doppler

fNIRS Functional near infrared spectroscopy

fMRI Functional magnetic resonance imaging

FMA Fugl-Meyer assessment of motor recovery after stroke

FUI Feedback update interval

ICA Independent component analysis

ITR Information transfer rate

IVF Indirect visual feedback

LDA Linear discriminant analysis

LFP Local field potential

LLP Large Laplacian

LMS Least mean squares

MEG Magnetoencephalogram

MEP Motor evoked potentials

MEM Maximum entropy method

MI Motor imagery

MRC Medical Research Council

MI-BCI Motor imagery-based brain-computer interface

PDVF Proprioceptive and direct visual feedback

PET Positron emission tomography

PSO Particle swarm optimization

PSD Power spectral density

PCA Principal component analysis

r^2 coefficient of determination

RBF Radial basis function

SVM Support vector machine

SLP Small Laplacian

SSVEP Steady state visual evoked potentials

SCP Slow cortical potentials

SRT Simple reaction time

TP True positive

TN True negative

Biography

Sam Darvishi was born in Sarbandar, Iran, in 1974. He passed the Iranian University Entrance Exam also known as the *Concours* with a ranking of 93 among more than 30,000 students in District 3, and entered Urmia University in 1992. He graduated with a Bachelor of Engineering Degree in Electronic Engineering in 1997. After working as an Electronic Engineer in a variety of industrial sectors for 7 years, he re-joined academia in 2006 and graduated with a Master of Engineering in Automation with *Merit* from the University of Sydney, Australia. Following his master studies, he worked as a part-time research assistant at Amirkabir University of Technology, Tehran, Iran where he pursued his research on brain-computer interfaces (BCI). In the meantime, he provided engineering consultancy services for projects related to real time locating systems (RTLS) and radio frequency identification (RFID).



In 2012, he was awarded an scholarship to pursue his PhD on restorative BCIs under A/Prof. Mathias Baumert, Prof. Michael C. Ridding, and Prof. Derek Abbott, in the School of Electrical & Electronic Engineering, The University of Adelaide. During his candidature, he attended five international conferences and presented his research outcomes through oral presentations or posters. He has received a number of International and local awards and scholarships including, Travel award by IEEE EMBS to attend BMBI workshop in San Diego, USA (2012), IEEE-SA travel award to attend 35th International EMBC Conference, Osaka, Japan (2013), Walter and Dorothy Duncan Trust award and a travel award by National Science Foundation (NSF) to attend 5th International BCI Meeting, Monterey, CA, USA (2013).

He has served as a reviewer for a number of recognised journals and conferences including PROCEEDINGS OF THE IEEE and PLOSONE. He also Collaborated with Scope TV (an educational TV show of Channel 11 produced for teenagers) to explain his research on BCI and its broadcast video can be found through the following link:

<https://www.youtube.com/watch?v=iFwWFGG5Htk&feature=youtu.be>


Biography

He is a graduate student member of the IEEE, and Engineering in Medicine and Biology Society (EMBS), and during his candidature he served as postgraduate students' representative at the school of Electrical & Electronic Engineering in 2014–2015.

He has won an Endeavour Fellowship to join Functional and Restorative Neurosurgery Department, University of Tuebingen, Germany, to pursue his research on restorative BCIs under supervision of Prof. Alireza Gharabaghi.

Sam Darvishi

Scientific Genealogy of Sam Darvishi

— Formalised supervisor relationship
 Mentoring relationship
 Nobel prize

"If I have seen further it is by standing on the shoulders of Giants."
Isaac Newton

